Microvascular Extracellular Vesicles: Novel Mediators of Endothelial Communication in Wound Healing and Inflammatory Regulation

Ramon Castellanos-Sanchez

Biomedical engineering department

University of Virginia

Abstract:

Microvascular endothelial cells, which form the innermost lining of the smallest blood vessels, play crucial roles in vascular homeostasis, inflammatory responses, and tissue repair. While extracellular vesicles (EVs) have emerged as important mediators of intercellular communication, those derived from microvascular endothelial cells remain poorly characterized despite their potential significance in regulating local vascular microenvironments. This dissertation addresses critical knowledge gaps through a systematic approach encompassing methodological optimization, comprehensive proteomic characterization, and functional validation.

First, an optimized low-serum culture system was developed for the HMEC-1 cell line and established a scalable isolation methodology combining ultracentrifugation with size exclusion chromatography, yielding high-purity EV preparations. Comprehensive proteomic analysis revealed 316 proteins, including 70 not previously documented in microvascular endothelial cell-derived EVs, with significant enrichment for proteins involved in wound healing, angiogenesis regulation, inflammatory response, and cell-cell adhesion.

Functional studies demonstrated that these EVs significantly enhance wound closure in both dermal fibroblasts and keratinocytes, with improvements of up to 45% compared to controls. Remarkably, these vesicles exhibited a previously undocumented dual effect on endothelial function—simultaneously upregulating inflammatory markers while enhancing junctional integrity, suggesting a specialized role in maintaining vascular barrier function during inflammatory responses.

These findings establish microvascular endothelial cell-derived EVs as complex mediators of intercellular communication capable of coordinating tissue responses during vascular remodeling. Their ability to promote wound healing while preserving barrier function suggests promising therapeutic applications in conditions characterized by impaired tissue repair or endothelial dysfunction. This work provides a foundation for future investigations into the physiological and pathological roles of these vesicles, with potential implications for developing novel approaches to vascular medicine.

Acknowledgments:

The work presented here was only possible because of the guidance and support of my PI Dr. Shayn Peirce-Cottler and the advice of my fantastic Ph.D. committee formed by:

Dr. Silvia Blemker (Committee chair)
Dr. Luca Musante
Dr. Uta Erdbrügger
Dr. Matthew J. Lazzara

Their feedback and believe in me was invaluable during the completion of this thesis. Each one of them brought an elemental piece of knowledge to my formation as a junior scientist.

A special recognition to the members of my lab for their help, the UVA biotechnology training grant program and to Dr. Thurl Harris for kindly lend me his 45Ti rotor.

Above all, a unique shutout to my family.

Table of contents:

List of figures and tables:

Figures

Tables

List of abbreviations:

ANXA1 - Annexin A1

ANXA2 - Annexin A2

ANXA5 - Annexin A5

ANG1 - Angiopoietin-1

ANG2 - Angiopoietin-2

ANGPT2 - Angiopoietin-2

ATCC - American Type Culture Collection

BBB - Blood-Brain Barrier

bFGF - Basic Fibroblast Growth Factor

BP - Biological Process (in GO analysis)

CC - Cellular Component (in GO analysis)

CD106 - Cluster of Differentiation 106 (VCAM-1)

CD144 - Cluster of Differentiation 144 (VE-cadherin)

CD9 - Cluster of Differentiation 9

cAMP - Cyclic Adenosine Monophosphate

CV - Coefficient of Variation

cryo-EM - Cryogenic Electron Microscopy

DAPI - 4′,6-diamidino-2-phenylindole (nuclear stain)

DSP - Desmoplakin

EIF3CL - Eukaryotic Translation Initiation Factor 3 Subunit C-Like

EPC - Endothelial Progenitor Cell

EV - Extracellular Vesicle

ECM - Extracellular Matrix

FDR - False Discovery Rate

FN1 - Fibronectin-1

FR1 - Fraction 1 (from SEC)

GAPDH - Glyceraldehyde 3-phosphate Dehydrogenase

GO - Gene Ontology

HBEC-5i - Human Brain Endothelial Cell Line 5i

HDFa - Human Dermal Fibroblast adult

HDMEC - Human Dermal Microvascular Endothelial Cell

HEKa - Human Epidermal Keratinocyte adult

HEPES - 4-(2-hydroxyethyl)-1-piperazineethanesulfonic acid

HMEC-1 - Human Microvascular Endothelial Cell Line 1

HMGB-1 - High-Mobility Group Box 1

HMGB-2 - High-Mobility Group Box 2

HSPA1B - Heat Shock Protein Family A Member 1B

HSPA8 - Heat Shock Protein Family A Member 8

HULEC-5a - Human Lung Endothelial Cell 5a

HUVEC - Human Umbilical Vein Endothelial Cell

IBMX - 3-Isobutyl-1-methylxanthine

IGF-1 LR3 - Insulin-like Growth Factor-1 Long R3

ITGAV - Integrin Subunit Alpha V

ITGB1 - Integrin Subunit Beta 1

KLF-2 - Krüppel-like Factor 2

LGALS3BP - Galectin-3-Binding Protein

LOXL2 - Lysyl Oxidase-Like 2

MCAM - Melanoma Cell Adhesion Molecule

MF - Molecular Function (in GO analysis)

miRNA - MicroRNA

MISEV - Minimal Information for Studies of Extracellular Vesicles

NTA - Nanoparticle Tracking Analysis

PBS - Phosphate-Buffered Saline

PECAM-1 - Platelet Endothelial Cell Adhesion Molecule 1 (CD31)

PLSCR1 - Phospholipid Scramblase 1

rhEGF - Recombinant Human Epidermal Growth Factor

ROI - Region of Interest

SEC - Size Exclusion Chromatography

THBS1 - Thrombospondin-1

TNF-α - Tumor Necrosis Factor alpha

TOP1 - DNA Topoisomerase 1

TSG101 - Tumor Susceptibility Gene 101

UC - Ultracentrifugation

UC+SEC - Ultracentrifugation followed by Size Exclusion Chromatography

UC Bulk - Ultracentrifugation Bulk preparation

UVA - University of Virginia

VCAM-1 - Vascular Cell Adhesion Molecule 1 (CD106)

VE-Cadherin - Vascular Endothelial Cadherin (CD144)

VEGF - Vascular Endothelial Growth Factor

VEGFA - Vascular Endothelial Growth Factor A

VSMC - Vascular Smooth Muscle Cell

Chapter 1: Introduction

1.1 Extracellular vesicles on vascular biology.

Extracellular vesicles (EVs) comprise distinct subpopulations including exosomes (30-150 nm) derived from multivesicular bodies and microvesicles (100-1000 nm) budding directly from the plasma membrane. These two distinct populations have different biogenesis pathways and molecular signatures [1], though isolation methods can often co-isolate them together. These membrane-bound particles carry a cargo of lipids, proteins, and genetic material that play crucial roles in intercellular communication and regulation of recipient cells [2].
In the particular context of vascular biology, a review of the current literature shows that EV-mediated regulation has been found to impact to mayor areas: endothelial cell-vascular smooth muscle cell communication and atherosclerosis development.

Aortic endothelial cells-derived EVs have been shown to promote inflammatory clues in vascular smooth muscle cells (VSMC), in particular the adhesion molecule VCAM-1 and promote subsequent leukocyte adhesion. An *in-vitro* proteomic screen on VSMC exposed to endothelial-derived EVs documented the upregulation of several pro-inflammatory proteins such as high-mobility group box 1 and 2 (HMGB-1 and HMGB-2) altering the recipient cell (VSMC) phenotype [3]. In addition, Perivascular Adipose Tissue (PVAT)-derived EVs was found to mediate vascular remodeling through the transfer of miR-221-3p to VSMCs and suppress contractile genes in the arterial walls [4].

In the context of atherosclerosis, a disease characterized by inflammation, *in-vitro* experiments have assessed the active role of EVs on the progression of the condition [5]. Low-density-lipoproteins induced endothelial cells-derived EVs showed to shift the balance in monocyte activation by shifting the monocytes/microphages balance from anti-inflammatory M2 to pro-inflammatory M1 phenotype [5]. In contrast, when endothelial cells were engineered to express KLF-2, the effect of endothelial cell-derived EVs was favored a shift in monocyte and macrophage phenotype to an anti-inflammatory state, indicating a new role for endothelial cell-derived EVs in impacting atherosclerosis [5]. Vascular shear stress also semes to play a fundamental role in the packaging of proteins into EVs cargo [6], as low atheroprone shear stress stimulates the uptake of potentially damage mitochondria and pro-oxidative proteins into endothelial cell-derived EVs which are transmitted to recipient cell via MCAM and PECAM-1. This effect was diminished when EVs were isolated from endothelial cells exposed to high shear stress conditions, which impacts directly atherosclerotic lesions, mainly form in arterial areas exposed to low shear stress [6].

In the *in-vivo* setting of atherosclerosis, stem cell-derived EVs have shown a therapeutic potential by playing an active role in improving vascular function. Specifically, they have been shown to improve the structure and function of the thoracic aorta and carotid artery [7]. Furthermore, EVs isolated from symptomatic atherosclerotic plaques obtained from human biopsies showed a pro-angiogenic potential compared with cells cell cultured from marginal plaque samples [8].

The vast majority of functional areas documented in the literature regarding the effect of EVs on vascular biology could be numbered as regulators of (1) vascular remodeling during inflammation (2) angiogenesis (3) Atherosclerosis plaque progression.

1.2 Current understanding of microvascular endothelial cells-derived EVs

Microvascular endothelial cells form the innermost lining of the smallest blood vessels and are pivotal regulators of vascular homeostasis at the tissue level. A review on the available literature reveals that while considerable research has focused on EVs derived from human umbilical vein endothelial cells (HUVECs) and endothelial progenitor cells (EPCs), studies specifically examining microvascular endothelial cell-derived EVs remain notably limited. This represents a significant gap in our understanding, as microvascular endothelial cells have distinct phenotypic and functional characteristics compared to larger vessel endothelial cells or endothelial progenitor populations.

1.2.1 Biogenesis and Characterization of Microvascular Endothelial Cell-Derived EVs

The relatively sparse literature specifically describing microvascular endothelial cell-derived EVs indicates that their release can be triggered by various stimuli relevant to microvascular pathophysiology, including inflammatory cytokines such as TNF-α, hypoxic conditions, and glycemic stress. De Jong demonstrated that microvascular endothelial cells cultured under hypoxic conditions released EVs with upregulated RNA genes related to pro-inflammation compared to those from normoxic cells, suggesting stress-specific cargo selection mechanisms [9].

1.2.2 Functional Roles in Microvascular Homeostasis

The few studies focused specifically on microvascular endothelial cell-derived EVs suggest they may have unique functions in regulating local microcirculation. Osawa et al. [10] demonstrated that EVs from brain microvascular endothelial cells contain fibronectin on their surface that mediates their internalization into oligodendrocyte precursor cells, promoting survival and proliferation. This suggests a specialized role for these EVs in neurovascular communication that may not be replicated by EVs from larger vessels.

1.2.3 Involvement in Microvascular Pathology

Blood-Brain Barrier Regulation

One of the few areas where microvascular endothelial cell-derived EVs have received specific attention is in cerebrovascular disorders. EVs released from the brain microcirculation may influence blood-brain barrier (BBB) function, as supported by studies showing that following mechanical injury brain microvascular endothelial cells release EVs containing tight junction proteins. According to Hosseini-Beheshti and Grau, these EVs can serve as biomarkers of BBB disruption, but their functional significance remains incompletely understood [11].

Diabetic Microangiopathy

In diabetic conditions, microvascular complications are predominant clinical concerns, yet studies specifically examining the role of microvascular endothelial cell-derived EVs in diabetic retinopathy, nephropathy, or neuropathy are limited. The few available reports suggest that high glucose levels alter the release and content of these EVs, potentially contributing to pericyte detachment and increased vascular permeability [11].

Inflammation in Microvascular Beds

Microvascular inflammation has distinct characteristics from larger vessel inflammation, particularly in terms of leukocyte recruitment and vascular permeability. While EVs from various endothelial sources have been implicated in modulating inflammation, studies specifically examining how microvascular endothelial cell-derived EVs regulate local inflammatory responses are scarce. The available evidence suggests these EVs may carry specific adhesion molecules and inflammatory mediators, but comprehensive analyses are lacking.

1.2.4 Technical Challenges in Microvascular EV Research

The limited research on microvascular endothelial cell-derived EVs partly stems from technical challenges. Isolating primary microvascular endothelial cells is more difficult than obtaining HUVECs, and their culture characteristics differ. Additionally, the documentation reviewed points that the yield of EVs from microvascular endothelial cells is typically lower than from other endothelial sources, making comprehensive characterization more challenging.

Another significant challenge is the heterogeneity of microvascular endothelial cells across different tissue beds. Brain microvascular endothelial cells, for instance, have different phenotypic characteristics compared to those from cardiac or renal microvasculature [3, 9, 10, 12-14]. This heterogeneity likely extends to the characteristics of the EVs derived from them, but comparative studies are largely absent from the literature.

1.3 Knowledge gaps and clinical/research significance.

Despite the growing recognition of extracellular vesicles (EVs) as critical mediators of intercellular communication, significant knowledge gaps persist in our understanding of microvascular endothelial cell-derived EVs. These gaps limit our ability to harness their potential in both research and clinical applications, particularly for pathologies affecting the microvasculature.

1.3.1 Limited characterization of microvascular endothelial cell-derived EVs

A critical examination of the literature reveals that while EVs from large vessel endothelial cells (particularly HUVECs) and endothelial progenitor cells have been extensively characterized, microvascular endothelial cell-derived EVs remain poorly understood. This represents a significant limitation since microvascular endothelial cells display tissue-specific phenotypes and functions that distinguish them from their larger vessel counterparts. As demonstrated by de Jong and colleagues, even basic stimuli such as hypoxia can dramatically alter the RNA content of microvascular endothelial cell-derived EVs, suggesting unique stress-responsive mechanisms that merit further investigation [9].

1.3.2 Technical challenges in isolation and purification

A significant factor limiting progress in this field are the numerous technical challenges associated with isolating and purifying microvascular endothelial cell-derived EVs. Current isolation techniques face several key limitations:

1. **Low yield**: Microvascular endothelial cells typically produce fewer EVs compared to other cell types, making isolation of sufficient quantities for comprehensive analysis challenging.

2. **Heterogeneity of isolation protocols**: The lack of standardized isolation methods leads to variable EV preparations, complicating cross-study comparisons and challenging.
3. **Co-isolation of contaminants**: Current techniques often fail to adequately separate true EVs from protein aggregates, lipoproteins, or cell debris, potentially confounding functional studies.
4. **Size-based limitations**: Many isolation protocols favor certain EV subpopulations based on size, potentially missing functionally important vesicle subsets.

Developing optimized isolation techniques specifically tailored for microvascular endothelial cell-derived EVs represents a critical research priority. Such techniques must balance the need for high yield and purity while preserving the functional integrity of these vesicles.

1.3.3 Incomplete proteomic characterization

While proteomics has revolutionized our understanding of EV biology, comprehensive proteomic characterization of microvascular endothelial cell-derived EVs is notably absent from the literature. The limited studies available suggest these EVs may carry cargo distinct from those of large vessel endothelium, including specialized adhesion molecules, junction proteins, and tissue-specific signaling factors.

For example, as noticed in the previous section, Osawa et al. [10] identified fibronectin on the surface of brain microvascular endothelial cell-derived EVs as a key mediator of their interaction with oligodendrocyte precursor cells. This finding highlights the potential for unique protein cargo that facilitates specific cell-cell communication pathways in the microvascular environment. However, such studies remain isolated examples rather than part of a systematic effort to characterize the proteome of these vesicles.

A comprehensive proteomic analysis would provide crucial insights into:

1. The core protein composition shared among microvascular endothelial cell-derived EVs.
2. Tissue-specific protein signatures that reflect the specialized functions of different microvascular beds.
3. Changes in protein cargo in response to pathophysiological stimuli relevant to microvascular disease.
4. Potential biomarkers for microvascular pathologies.
5. Candidate proteins mediating the biological effects of these EVs on recipient cells.

1.3.4 Limited functional characterization in the microvascular niche

Perhaps the most significant knowledge gap concerns the functional impacts of microvascular endothelial cell-derived EVs on cells within the microvascular niche. The microvasculature functions as an integrated unit comprising endothelial cells, pericytes, and tissue-specific fibroblasts. How EVs mediate communication within this niche remains poorly understood.

The work by Cantaluppi et al. [15] demonstrating that endothelial progenitor cell-derived EVs enhance angiogenesis of pancreatic islets suggests potential roles in microvascular remodeling. However, studies specifically examining how microvascular endothelial cell-derived EVs affect:

1. **Neighboring endothelial cells** (autocrine signaling)
2. **Pericytes** (critical regulators of microvascular stability and function)

3. **Tissue-specific fibroblasts** (which contribute to extracellular matrix composition and tissue homeostasis)

are largely absent from the literature. Before expanding research into other cellular targets or systemic effects, establishing the fundamental functional impacts of EVs within the microvascular niche itself is essential.

1.3.5 Clinical and research significance

The knowledge gaps identified above have significant implications for both basic research and clinical applications. From a research perspective, a more comprehensive understanding of microvascular endothelial cell-derived EVs would enhance our knowledge of:

1. **Microvascular homeostasis**: How EVs contribute to normal microvascular function and tissue-specific adaptations.
2. **Stress responses**: The role of these EVs in adapting to common stressors such as inflammation, and metabolic alterations.
3. **Intercellular communication**: The specific signaling pathways mediated by these EVs within the microvascular niche.

From a clinical perspective, addressing these knowledge gaps could lead to:

1. **Novel biomarkers**: Microvascular endothelial cell-derived EVs could serve as accessible biomarkers for diseases affecting the microvasculature, including diabetic complications, cerebrovascular disorders, and various organ-specific microvascular pathologies
2. **Therapeutic targets**: Understanding the mechanisms by which these EVs influence microvascular function could reveal new therapeutic targets for intervention
3. **Drug delivery vehicles**: Engineered microvascular endothelial cell-derived EVs could potentially serve as tissue-specific delivery vehicles for therapeutic molecules

1.4 Research questions and hypothesis.

The main research questions driving this Ph.D. dissertation are:

1. What is the optimal isolation method for microvascular endothelial cell-derived extracellular vesicles that maximizes both yield and purity?

2. What is the distinct proteomic signature of microvascular endothelial cell-derived EVs, and what insights can a comprehensive proteomic analysis reveal about vesicle biogenesis and functionality?

3. How do microvascular endothelial cell-derived extracellular vesicles regulate vascular remodeling processes within the microvascular niche?

By addressing these questions, we will address significant gaps in the literature identified in the previous sections. Question one directly addresses the technical challenge of developing more effective isolation methods beyond ultracentrifugation, currently considered the gold standard in the field [16]. Question two addresses the lack of comprehensive proteomic characterization of microvascular endothelial cell-derived EVs, which remains a critical knowledge gap. Question three

investigates the functional significance of these EVs in vascular remodeling - a dynamic process central to inflammation, angiogenesis, and vascular repair.

Each aim of this Ph.D. thesis corresponds to one of these research questions. Our first aim (Aim 1) focuses on a technical goal: developing an optimized isolation method that delivers both high purity and sufficient EV yield. We hypothesize that a combination approach incorporating ultracentrifugation with complementary techniques will yield an EV population exceeding 5×10^9 nanoparticles, which has been established as a minimum threshold for therapeutic EV applications [17].

For question two, we hypothesize that the proteomic cargo of microvascular endothelial cell-derived EVs contains a distinct signature of proteins involved in tissue-specific vascular processes including endothelial activation, barrier function, and angiogenesis. This signature likely reflects specialized functions of their parent cells [18] and may differ significantly from EVs derived from large vessel endothelium.

Finally, based on the expected proteomic profile and the pivotal role of endothelial cells during inflammation, we hypothesize that microvascular endothelial cell-derived EVs play a regulatory role in modulating endothelial cell function during inflammatory conditions. Specifically, we expect these EVs to modulate the expression of endothelial activation markers such as VCAM-1, E-selectin, and VE-cadherin. Furthermore, we anticipate these vesicles will actively regulate critical microvascular processes including angiogenesis and wound healing through paracrine signaling within the microvascular niche and neighboring fibroblasts.

By addressing these research questions, this investigation will fill critical knowledge gaps regarding microvascular endothelial cell-derived EVs, establishing a solid foundation for future studies on their diagnostic and therapeutic applications in microvascular pathologies.

1.5 Rationale for Aims: isolation, proteomic characterization, and functional studies.

The three aims proposed in this study have a logical sequence that builds upon each preceding step to form a comprehensive investigation of microvascular endothelial cell-derived EVs. Each aim addresses a critical knowledge gap identified in the literature while establishing the foundation for subsequent investigations.

In Aim 1, we focused on developing a robust isolation methodology for microvascular endothelial cell-derived EVs. This initial step was foundational, addressing several technical questions: selection of appropriate microvascular endothelial cell types, optimization of low-serum media formulation to minimize contamination from exogenous EVs, adaptation of published protocols to our laboratory infrastructure, and comprehensive characterization of final EV preparations according to MISEV 2018 guidelines [19]. The technical challenges of isolating EVs from microvascular endothelial cells—which typically yield fewer vesicles than other cell types—necessitated this methodical approach to ensure sufficient quantity and purity for downstream analyses.

With optimized EV preparations in hand, Aim 2 employed shotgun proteomics [20] to comprehensively analyze the protein cargo of these vesicles. This unbiased mass spectrometry approach enabled identification of the complete proteomic signature of microvascular endothelial cell-derived EVs rather than focusing on preselected candidate proteins. As hypothesized, this analysis revealed distinct groups of proteins documented in UNIPROT [21] to participate in vascular biology processes including angiogenesis, endothelial activation, coagulation, and wound healing. Beyond merely cataloging proteins, this proteomic characterization identified enriched biological pathways,

providing critical insights into the potential functional roles of these EVs in the microvascular environment.

Informed by the specific biological processes highlighted in our proteomic analysis, Aim 3 investigated the functional effects of microvascular endothelial cell-derived EVs in three key aspects of vascular biology:

(i) Modulation of endothelial cell activation during inflammation
(ii) Regulation of wound healing processes
(iii) Influence on angiogenic potential

Each functional assay required methodological optimization to address challenges including appropriate cell seeding density, determination of effective EV dosage, timing of administration, and selection of appropriate controls—all detailed in Chapter 4. These in vitro functional studies establish the biological relevance of the microvascular endothelial cell-derived EVs, demonstrating their regulatory capabilities in processes fundamental to microvascular homeostasis and pathology.

This stepwise approach provides a logical framework for investigating a previously understudied EV population. Without the optimized isolation methodology developed in Aim 1, the comprehensive proteomic analysis in Aim 2 would have been compromised by insufficient yield or contamination with non-EV components. Similarly, without the pathway insights gained through proteomic characterization, the functional studies in Aim 3 would have lacked clear biological targets, representing essentially untargeted explorations of potential EV functions.

The significance of this work extends beyond the methodological advances. Microvascular endothelial cell-derived EVs are abundant in the circulation, yet their specific contributions to vascular homeostasis remain poorly understood. By demonstrating their regulatory roles in inflammation, wound healing, and angiogenesis, this study establishes their importance in microvascular biology and lays the groundwork for future translational studies exploring their potential as biomarkers or therapeutic agents in microvascular pathologies.

This integrated approach represents an essential step toward addressing the significant knowledge gaps identified in sections 1.2 and 1.3, with implications for both basic vascular biology research and clinical applications in microvascular diseases.

Chapter 2: Microvascular endothelial cells-derived extracellular vesicles isolation.

This chapter directly addresses the first research question posed in Section 1.4: "What is the optimal isolation method for microvascular endothelial cell-derived EVs that maximizes both yield and purity?" As established in the previous chapter, there are significant technical challenges in the isolation and purification of EVs from microvascular endothelial cells. The current literature presents minimal documentation regarding microvascular endothelial cell-derived EVs isolation, with most cell culture protocols utilizing high serum supplementation—a critical source of EVs contamination [22, 23]. To address these challenges and develop a methodology that would support our research aims, I focused on three fundamental aspects:

1. Selection of a microvascular endothelial cell line model capable of growth in low-serum conditions and able to withstand multiple passages for repeated EVs collection.
2. Development of a low-serum media formulation that maintains the characteristic cobblestone morphology of endothelial cells at confluence while supporting cell population doubling times below 72 hours for rapid growth and efficient EVs collection.
3. Optimization of an isolation method combining multiple lipoprotein separation techniques to ensure EVs yields higher than 5E9 nanoparticles per isolation and guarantee preparations free of Albumin and Calnexin contamination.

The sequential order of these tasks was critical for success. First, selecting an endothelial cell model capable of surviving and adapting to minimal nutritional conditions was fundamental for developing low-serum formulation. Once the cell model was established and the media optimized for rapid growth with minimal bovine EVs contaminants, the selection of methods for EVs isolation proceeded efficiently, as the initial cell culture material contained fewer contaminants, reducing the necessary cleaning steps and allowing greater focus on engineering a combination method for optimal output.

2.1 Selection of an Endothelial Cell Line for the Collection of Extracellular Vesicles

When evaluating microvascular endothelial cell-line candidates to meet the specific demands of this research, two main criteria were prioritized:

1. Capacity to withstand numerous passages without losing endothelial cell morphology or experiencing decreased population doubling rates.
2. Demonstrated ability to grow in low-serum media conditions.

The ability to withstand multiple passages was essential, as extensive experimentation was anticipated during media development, EVs isolation protocol optimization, characterization, and functional studies. The capacity to proliferate in low-serum conditions was paramount to avoid serum contamination of EVs preparations, which could potentially confound experimental results, particularly in functionality studies [22].

After reviewing more than 15 commercially available options, three candidates were shortlisted based on their documented characteristics (Table 1). The requirement for numerous passages eliminated the possibility of selecting primary cell lines in favor of immortalized lines. Among the three candidates, only one had peer-reviewed literature supporting growth in low-serum conditions [24], with the authors even reporting the possibility of growth under serum-free conditions.

Commercial cell name	Tissue origin	Type	Capability for low-serum
HMEC-1	Dermis	Immortal cell line	Yes
HULEC-5a	Lung	Immortal cell line	No
HBEC-5i	Brain	Immortal cell line	No

Table 1: Top-3 microvascular cell candidates for the study of in-vitro EVs.

The selected cell line—Human microvascular endothelial cell line 1 (HMEC-1)—not only met our desired criteria but has also been demonstrated to express vascular characteristics such as the capacity to form vessel-like formations in 3D cultures and express endothelial markers, including Vascular Endothelial Cadherin (VE-Cadherin) and Platelet Endothelial Cell Adhesion Molecule 1 (PECAM-1)[24, 25]. Additionally, the HMEC-1 has extensive documentation showing responses to vascular stresses such as hypoxia [26] and inflammatory cues [25, 27] similar to primary cell lines and *in-vivo* microvasculature responses. These characteristics suggest that HMEC-1 cells would likely secrete an EV profile, similar to that of microvascular endothelial cells in human physiology, making it an excellent model for our studies.

2.2 Developing a low-serum media for the expansion of HMEC-1

After selecting the HMEC-1 cell line, the next objective was to develop a low-serum media formulation to reduce bovine-derived EVs and contaminants. As documented in the literature [22, 23, 28], serum-derived contaminants co-precipitate with EVs and can influence in vitro experimental outcomes—an effect we aimed to minimize.

The starting point was the ATCC-recommended media for HMEC-1, based on MCDB131 supplemented with 10 ng/mL of recombinant human epidermal growth factor (rhEGF) and 10 mM of L-glutamine. This formulation typically requires 10% serum supplementation for cell growth, maintaining a population doubling time of approximately 36-48 hours. Initial tests with this media at serum concentrations below 5% resulted in extended population doubling times (>120 hours) and detrimental morphological changes like cell elongation and visible membrane holes. Our goal was to culture the cells with less than 2.5% serum supplementation while maintaining endothelial morphology and population doubling times of 16-36 hours. To achieve this, a new media formulation was developed based on growth factors, vitamins, and chemical reagents reported to stimulate endothelial cell growth.

Based on a comprehensive review of the available literature, potential candidates for media formulation were identified and are listed in Table 2. It is important to note that most of the positive effects documented in Table 2 were observed under high-serum conditions and with primary cells, suggesting that their translation to a cell line under low-serum conditions might differ. Furthermore, most of the documented effects were observed over short periods (16-24 hours) rather than in long-term cultures.

2.2.1 Strategy for formulating media.

Table 2 contains over 23 candidates considered for the media formulation based on commercial medias for endothelial cells and peer-reviewed literature [29]. The strategy followed two main steps:

1. Development of a core formulation capable of supporting population doubling times of 48 hours and cell viability higher than 90% at 5% serum supplementation.
2. Development of a low-serum media capable of supporting population doubling times of 48 hours and cell viability higher than 90% at 1-2% serum supplementation.

The initial core formulation (Table 3) maintained cobblestone morphology at 5% serum supplementation but failed to maintain adequate cell viability at lower serum concentrations (2-4%). A series of formulation modifications were subsequently tested (Table 4), eventually leading to the development of a media capable of supporting HMEC-1 growth at 1-2% serum supplementation.

Growth Factors	Literature reference	Documented effect
rhEGF	[12, 24, 25, 30]	Increased cell viability
bFGF	[31, 32]	Increased cell viability
IGF-1 LR3	[31]	Increased cell viability
VEGF	[32, 33]	Increased cell viability
ANG1	[34]	Reduced apoptosis
ANG2	[35, 36]	Stress protection
Essential amino acids		
Glutamax	[37]	Increased cell viability
L-Glutamine	[38, 39]	Increased cell viability
L-Serine	[40, 41]	Cytoprotective
Redox buffers		
Hydrocortisone	[42, 43]	Increased cell viability
Ascorbic acid 2p	[44-46]	Antioxidant, cytoprotective
Albumin	[47, 48]	Apoptosis inhibitor
AlbuMAX	[49]	Increased cell viability
pH buffers		
HEPES	[50, 51]	Buffer pH
cAMP activators		
Dibutryl-cAMP	[30]	Preserve endothelial morphology
Hypoxanthine	[30, 52, 53]	Preserve endothelial morphology
IBMX	[54-56]	Preserve endothelial morphology
Thymidine	[57, 58]	Increased cell viability
Other supplements		
Insulin	[59, 60]	Increased cell viability
Transferrin	[61, 62]	Cellular chemical exchange
Selenium	[63, 64]	Increased cell viability
Heparin	[65, 66]	Increased cell viability
N-acetyl-L-cysteine	[67-69]	Increased cell viability

Table 2: Candidates factors for low-serum media formulation.

Growth Factors	Literature reference	Concentration
rhEGF	[12, 24, 25, 30]	10 ng/mL
bFGF	[31, 32]	10 ng/mL
VEGF	[32, 33]	5 ng/mL
Essential amino acids		
L-Glutamine	[38, 39]	2 mM
Redox buffers		
Hydrocortisone	[42, 43]	1 μg/mL
Ascorbic acid 2p	[44-46]	1 mM
cAMP activators		
Dibutryl-cAMP	[30]	40.7 μM
Hypoxanthine	[30, 52, 53]	27 μM
IBMX	[54-56]	0.33 μM
Other supplements		
Heparin	[65, 66]	25 μg/mL

Table 3: Basic formulation for low-serum media.

Formulation (F) # –type	Reagent	Concentration tested	Documented effect
F1 – Addition	Insulin, Transferrin, Selenium	500,225,0.335 (mg/L)	Increased viability
F2 – Substitution	L-Glutamine for Glutamax	10 mM	Increased viability
F3 – Addition	L-Serine	76.25 μg/mL	No effect
F4 – Titration	Glutamax	2 mM – 10 mM	Increased viability, reduced pH
F5 – Addition	HEPES	5 mM	Buffer pH to 7.1-7.3
F6 – Addition	Albumin	0.2 μg/mL	Increased cell growth
F7 – Substitution	IGF-1 LR3 for VEGF	5 ng/mL	No effect
F8 – Substitution	ANG1 for VEGF	5 ng/mL	Increased cell growth
F9 – Addition	ANG2	0.1 ng/mL	Increased cell growth
Serum reduction 5% to 2%			
F10 - Titration	ANG2	0.1 ng-5ng	Increased cell growth, improved morphology.
F11 – Addition	N-acetyl-L-cysteine	48.8 μg/mL	No effect
F12 – Titration	Hypoxanthine	0-27 μM	When removed improved cell growth, viability and pH
F13 – Titration	Ascorbic acid 2p	0-1 mM	At 0.1 mM improved cell growth
F14 – Substitution	AlbuMAX for Albumin	0.2 μg/mL	Increased cell growth
F15 – Titration	AlbuMAX	0.2-0.5 μg/mL	At 0.5 μg/mL Increased cell growth

Table 4: Formulation modification and their documented effects.

Several significant observations emerged during the media development process. The addition of angiopoietins ANG1 and ANG2 notably increased cell viability, improved morphology, and reduced population doubling times. Particularly noteworthy was the cytoprotective and mitotic effect of ANG2, which enhanced population doubling times at just 0.5 times the concentration of VEGF required for similar effects. This mitotic, stress-protective effect of ANG2 aligns with existing peer-reviewed literature [35, 36].

Another unexpected finding was the positive effect observed after eliminating hypoxanthine from the media by titration, and reducing ascorbic acid concentration. As shown in Figure 1A, removing hypoxanthine from the media resulted in a significant increase in cell growth and improved pH levels. This outcome contrasts with reports in the literature, which describe hypoxanthine as necessary in cell culture formulations for microvascular endothelial cells to maintain mosaic morphology at confluence [30, 53]. Similarly, reducing ascorbic acid concentration by 10-fold in formulation F13 (Figure 1A) resulted in improved cell growth and a slight increase in pH. Figure 1B compares cell morphology under brightfield microscopy of confluent cultures grown in formulations F10 versus F13. Figure 1B shows how the F10 formulation created in the culture visible areas of damaged cell membranes with small holes (indicated by red circles) suggesting inadequate media support, which was visibly improved after the modifications implemented in F13.

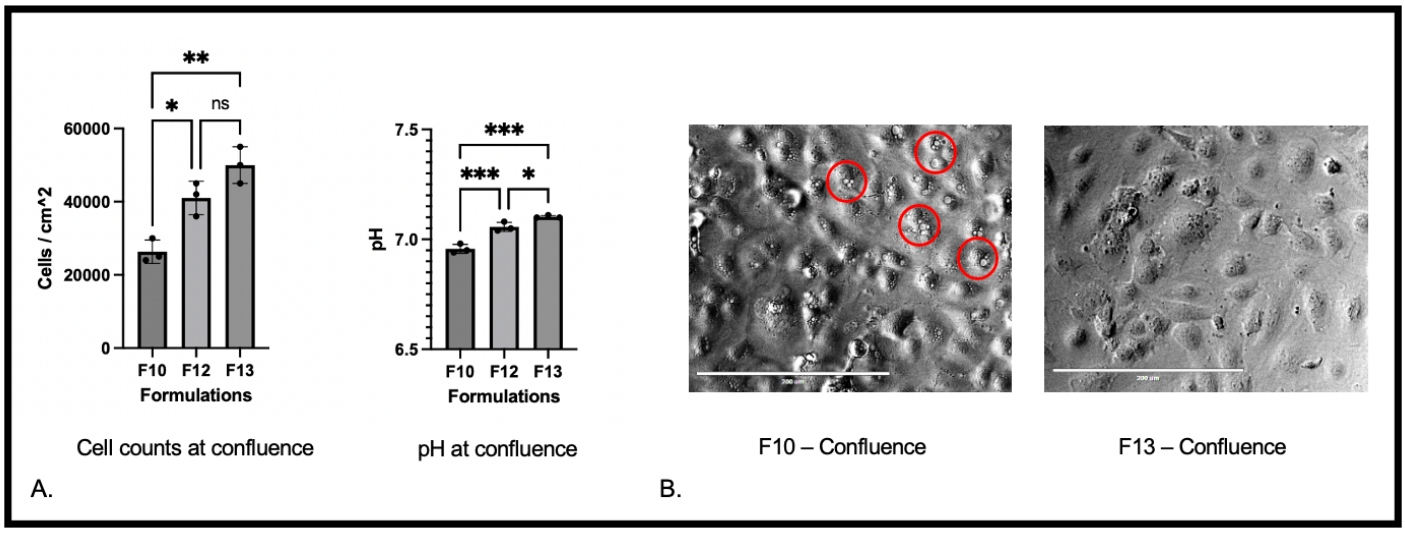

Figure 1: Basic formulation for low-serum media. (A) Cell counts and pH measurements comparing F10, F12 and F13 formulations. (B) Brightfield images of confluent cultures using formulation F10 vs. F13. Notice in the red circles the visible cell membrane damage indicating poor media support.

The final formulation, F15 (detailed in Table 5), was evaluated at various serum concentrations (0-5%), including an immunofluorescence study to assess expression of the endothelial cell marker VE-Cadherin (Figure 2). The media exceeded expectations, as MCDB131 F15 was able to sustain cell growth even under serum-free conditions, though with a noticeable decrease in growth rate when serum supplementation was below 2%. This was anticipated as the cells had been adapted for several passages to 2% serum concentration, and adaptation to lower concentrations typically requires 2-3 passages. The pH levels near confluency averaged 7.09, well within the target range of 7.05-7.25.

2.2.2 Limitation of the F15 supplemented medium

Although F15 media exceeded expectations in supporting HMEC-1 growth at low serum concentrations, one limitation was observed: when cell confluency exceeds 90-95%, there is a noticeable increase in floating cell debris compared to cells grown in the ATCC-recommended media with 10% serum supplementation. While this limitation does not significantly affect cell viability, pH levels, or population doubling times, it indicates potential for further media optimization.

A review of the existing literature suggests that increased floating cell debris likely results from a chemical imbalance in the media, which at high confluency may generate some degree of apoptosis [70] due to increased oxidative stress [71]. The maintenance of optimal pH ranges at confluency indicates that the issue is unlikely to stem from excess ammonia in the medium—a byproduct of cell metabolism that can be cytotoxic [72]. More likely, F15 at 2% serum supplementation still lacks optimal concentrations of key ingredients found at higher serum concentrations that mitigate oxidative stress. Interestingly, when Human Dermal Microvascular Endothelial Cells (HDMECs), a primary cell line typically more sensitive to oxidative stress, are cultured in F15, no significant cell debris is observed at high confluency. This suggests that the observed limitation may be specific to the HMEC-1 cell line.

Growth Factors	Literature reference	Concentration
rhEGF	[12, 24, 25, 30]	10 ng/mL
bFGF	[31, 32]	10 ng/mL
ANG1	[32, 33]	5 ng/mL
ANG2		
Essential amino acids		
Glutamax	[38, 39]	10 mM
Redox buffers		
Hydrocortisone	[42, 43]	1 μg/mL
Ascorbic acid 2p	[44-46]	0.1 mM
pH buffer		
HEPES	[50, 51]	5 mM
cAMP activators		
Dibutryl-cAMP	[30]	40.7 μM
IBMX	[54-56]	0.33 μM
Other supplements		
Heparin	[65, 66]	25 μg/mL
AlbuMAX	[49]	0.5 μg/mL
Insulin, Transferrin, Selenium	[59, 60] [61, 62] [63, 64]	500,225,0.335 (mg/L)

Table 5: Final formulation (F15) for low-serum media.

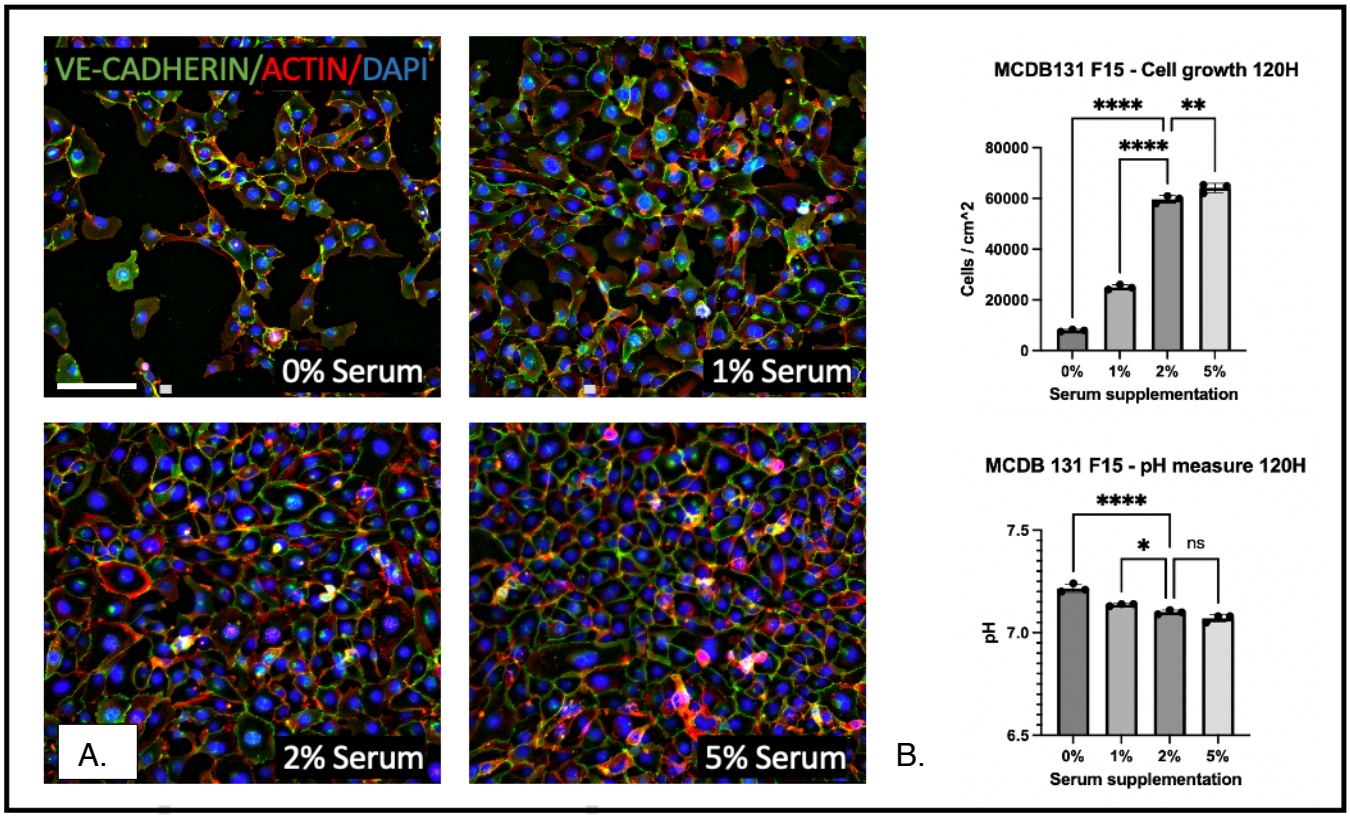

Figure 2: Characterization of HMEC-1 cells in MCDB131 F15 supplemented media (A) Immunofluorescence staining for VE-Cadherin (green) confirms maintenance of endothelial phenotype in all serum conditions. Nuclei are counterstained with DAPI (blue). (B) Cell growth measurements at various serum concentrations. (C) pH measurements across different serum concentrations. Scale 265 um.

2.2.3 Media formulation implications for EVs isolation optimization

The successful development of a low-serum media formulation for HMEC-1 cells represented a critical advancement in addressing the first research question posed in Section 1.4. By enabling the culture of microvascular endothelial cells in conditions with minimal serum contamination, this methodology lays the groundwork for obtaining pure EV preparations for subsequent proteomic and functional analyses.

The F15 formulation demonstrates several advantages over conventional high-serum culture methods:

1. It maintained endothelial cell phenotype as confirmed by morphological assessment and VE-Cadherin expression.
2. It supported robust cell growth with doubling times comparable to standard conditions.
3. It significantly reduced potential serum-derived EV contamination, addressing a major limitation in the field.

The unexpected findings regarding hypoxanthine and ascorbic acid effects on HMEC-1 growth highlight the importance of empirical optimization for specific cell lines, rather than relying solely on literature-based formulations. This observation underscores the heterogeneity among endothelial cell models and the need for tailored approaches to cell culture optimization.

With the establishment of this low-serum culture system, the next phase of research focused on optimizing EVs isolation methods.

2.3 Optimizing EVs isolation methods.

Once the cell line was selected and the media optimized for low-serum our next goal was optimize the process of microvascular cell isolation. As mentioned in section 1. 3. 1 the literature regarding the isolation of microvascular endothelial cells was limited [9, 10, 73, 74].

2.3.1 Ultracentrifugation as a foundational isolation method

Based on available resources and established principles in the field, we selected ultracentrifugation as our foundational method, adapting the protocol described by Xu et al. [73]. Since our laboratory was equipped with a Beckman 90Ti rotor rather than the SW32Ti rotor specified in the literature, we utilized the Intellifuge© Calculator from Beckman to translate the ultracentrifugation parameters appropriately, as illustrated in Figure 3. This conversion ensured equivalent g-force application despite the different rotor specifications, a critical consideration for reproducible EV isolation.

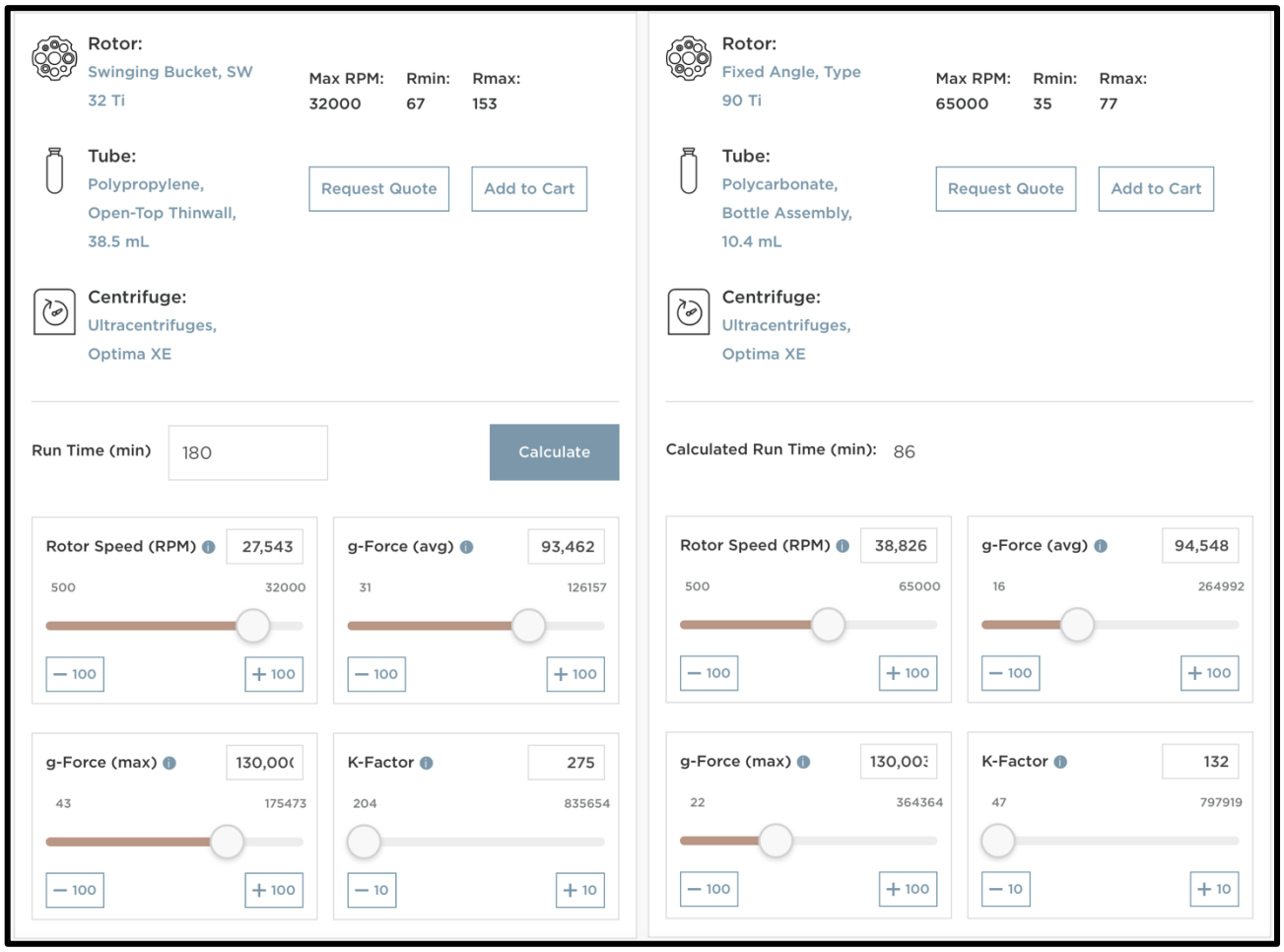

Figure 3: Intellifuge protocol transfer from SW32Ti rotor to 90Ti. The calculation ensures equal g-Force max between the two protocols, maintaining consistency in the separation principles despite different rotor types.

The ultracentrifugation protocol was based on the EV collection of two T175 confluent plates totaling 60 mL of media, the complete protocol is described below:

Ultracentrifugation: The collected conditioned media was centrifugated for 20 min at 2000 g-Force (max) in an Eppendorf R250 centrifuge. Pellet was discarded and the supernatant was filtered through a 0.45 μm VWR complete filtration unit (Cat# 10040) before a two-step differential ultracentrifugation process at 10,000 g-Force-max (10,800 rpm) for 30 minutes and 130,000 g-Force-max (38,800) for 85 minutes in a Beckman Coulter rotor 90Ti (k=132) using 10.4 mL bottle assembly polyacrylamide tubes (Cat# 355603). The final EV prep was resuspended in a 500 μL of 0.2 μm filtrated PBS. All centrifugation and ultracentrifugation steps were done at 4C.

This initial protocol gave us the chance to successfully isolate EVs and characterize them by nanoparticle tracking analysis (NTA) and also by immunoblotting by screening EVs marker Alix and TSG101. Our initial NTA documentation revealed that our cultures yield about 0.6-0.9E10 nanoparticles/mL in our half mL resuspension totaling about 0.3-0.45E10 nanoparticles per isolation which was below the range reported for EVs dosage for *in-vivo* functionality [75]. We also were aware that using only ultracentrifugation could lead potentially to dirty EVs preparations as reports start to come up highlighting the need for combining methods with ultracentrifugation for higher EVs purity [76].

In order to overcome the low EV yield for potential functionality studies and the need for a purer isolation method we developed a plan, we will first conduct a study comparing ultracentrifugation-only with two different isolation combo methods to assess purity and later up-scale our culture numbers to target an NTA range of 1-2E10 total nanoparticles per isolation.

The initial ultracentrifugation protocol was designed for EV collection from two T175 confluent plates yielding approximately 60 mL of conditioned media. The detailed protocol was as follows:

Ultracentrifugation Protocol: The collected conditioned media was centrifuged for 20 minutes at 2,000 g-Force (max) in an Eppendorf R250 centrifuge to remove cellular debris. The resulting pellet was discarded, and the supernatant was passed through a 0.45 μm VWR complete filtration unit (Cat# 10040) to eliminate larger vesicles and remaining debris. The filtered supernatant then underwent a two-step differential ultracentrifugation process: first at 10,000 g-Force-max (10,800 rpm) for 30 minutes to remove larger microvesicles and apoptotic bodies, followed by 130,000 g-Force-max (38,800 rpm) for 85 minutes to pellet the exosome-enriched fraction. This process was performed in a Beckman Coulter rotor 90Ti (k-factor=132) using 10.4 mL bottle assembly polyacrylamide tubes (Cat# 355603). The final EV pellet was resuspended in 500 μL of 0.2 μm filtered PBS. All centrifugation and ultracentrifugation steps were performed at 4°C to preserve EV integrity.

This protocol enabled successful isolation of EVs that were subsequently characterized using nanoparticle tracking analysis (NTA) and immunoblotting for established EV markers Alix and TSG101. Initial NTA results revealed that our cultures yielded approximately 0.6-0.9×10^10 nanoparticles/mL in our half-milliliter resuspension, totaling about 0.3-0.45×10^10 nanoparticles per isolation. This yield fell below the range of 1-2×10^10 nanoparticles typically reported as effective for EV dosage in in vivo functionality studies [75].

Additionally, recent literature has increasingly emphasized that ultracentrifugation alone may yield EV preparations contaminated with non-vesicular components such as protein aggregates and

lipoproteins [76]. Such contaminants can significantly confound downstream analyses, particularly proteomics and functional studies—both central to our research aims.

To address these dual challenges of insufficient yield and potential contamination, we developed a two-pronged approach: first, comparing ultracentrifugation-only with two different combination methods to assess purity, and subsequently scaling up our culture system to achieve the target yield of 1-2×10^10 total nanoparticles per isolation for functional studies.

2.3.1 Comparison of EVs isolation methods

To enhance the purity of our EV preparations while maintaining acceptable yields, we designed two methodological variants that integrated ultracentrifugation with complementary lipoprotein separation techniques, as illustrated in Figure 4. Each variant represented a distinct conceptual approach to the purification challenge:

The first variant (Variant A) introduced isolation steps prior to ultracentrifugation (Figure 4B), positioning filtration and density gradient centrifugation as initial purification methods to remove non-EV contaminants from the conditioned media. In this approach, the ultracentrifugation step served primarily as a final concentration method for the pre-purified EV fraction.

The second variant (Variant B) leveraged the concentrating power of ultracentrifugation as the initial step, followed by size exclusion chromatography for purification of the concentrated EV preparation (Figure 4C). This approach capitalized on the efficiency of ultracentrifugation for vesicle concentration while utilizing chromatography to separate EVs from co-pelleted contaminants.

Variant A — High filtration dialysis, density gradient concentration and ultracentrifugation

A significant technical challenge for Variant A was managing the large initial volume of conditioned media (60 mL) while maintaining efficient EV recovery. Based on recommendations from PhD committee member Dr. Luca Musante, we implemented a concentration step using a 100 kDa molecular weight cut-off dialysis membrane (Cole-Palmer Item # UX-02980-17) to reduce the volume while retaining the EV population.

Following concentration, we employed OptiPrep density gradient centrifugation (Sigma Cat#D1556), a method documented to effectively separate EVs from protein contaminants in various biofluids including cell culture supernatants, urine, and plasma [77-79]. The density gradient approach exploits the characteristic buoyant density of EVs to separate them from proteins and other non-vesicular components that distribute differently across the gradient.

The complete protocol for Variant A was as follows:

High filtration dialysis, density gradient concentration and ultracentrifugation protocol: The collected conditioned media was centrifuged for 20 minutes at 2,000 g-Force (max) in an Eppendorf R250 centrifuge. After discarding the pellet, the supernatant was filtered through a 0.45 µm VWR complete filtration unit (Cat# 10040). The filtered medium was then transferred into a 100 kDa dialysis membrane (Cole-Palmer Item # UX-02980-17) and allowed to concentrate by passive filtration. Once concentrated, 50 mL of PBS was added inside the membrane as a washing step to remove small molecular contaminants. When the internal PBS volume reduced to approximately 2-3 mL, this concentrate was carefully layered atop an OptiPrep (Sigma Cat#D1556) density gradient consisting of

six layers (60%, 50%, 40%, 30%, 20%, and 10% OptiPrep). The gradient was centrifuged in a Beckman Coulter rotor SW41 (k-factor=133) at 100,000 g-Force-max for 120 minutes. Following centrifugation, the interfaces between gradient layers (five interfaces from 10/20% to 50/60%) were collected, with each interface resuspended in 1 mL of PBS and further diluted 1:10. These diluted fractions were then subjected to a final ultracentrifugation step for 85 minutes in a Beckman Coulter rotor 90Ti (k-factor=132) using 10.4 mL bottle assembly polyacrylamide tubes (Cat# 355603) to pellet the purified EVs.

Variant B — Ultracentrifugation followed by size exclusion chromatography

Variant B took full advantage of the concentrating capabilities of ultracentrifugation as the initial step, producing a concentrated EV pellet that could be resuspended in a small volume (500 µL)—optimal for processing through size exclusion chromatography (SEC). SEC separates particles based on their hydrodynamic radius, with larger particles (including EVs) eluting earlier than smaller molecules such as proteins and lipoproteins.

For our SEC approach, we selected the IZON qEV 70nm second-generation column (Cat # ICO-70), specifically designed for high-resolution separation of EVs from smaller contaminants. The complete protocol for Variant B was as follows:

Ultracentrifugation and size exclusion chromatography protocol: The collected conditioned media underwent the standard ultracentrifugation protocol described in section 2.3.1, including initial centrifugation, filtration, and the two-step differential ultracentrifugation. The resulting EV pellet was resuspended in 500 µL of filtered PBS and loaded onto an IZON qEV 70nm second-generation column (Cat # ICO-70) mounted on an IZON automatic fraction collector. After loading the sample, a void volume of 2.90 mL was allowed to pass through the column (as per manufacturer recommendations), followed by collection of six 1 mL fractions containing the separated EVs. Between runs, the IZON columns were regenerated by washing with 8.5 mL of 0.5 M NaOH and stored at 4°C in 0.05% sodium azide to prevent microbial contamination.

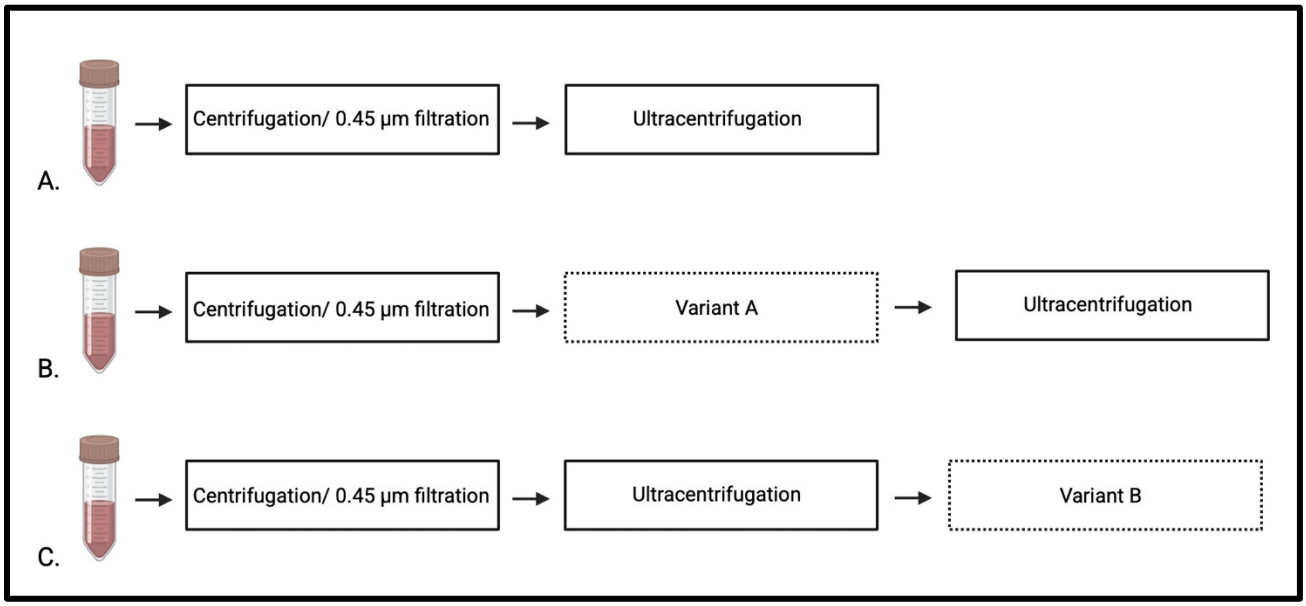

Figure 4: Combination of methods diagram. (A) Initial ultracentrifugation-only method. (B) Variant A method pre-ultracentrifugation step (B) Variant B method post-ultracentrifugation.

For a rigorous comparative evaluation of these methods, we focused on two primary parameters: quantitative nanoparticle yields as determined by NTA and qualitative assessment of EV purity through immunoblotting for established EV markers (Alix and TSG101) and potential contaminants (calnexin). We anticipated that introducing additional purification steps would inevitably reduce the absolute nanoparticle yield due to technical losses during processing, making it essential to balance purification efficiency against recovery.

Figure 5 presents the comprehensive results of our comparative analysis. Both variants demonstrated successful isolation of EVs as evidenced by positive immunoblotting for the EV markers Alix and TSG101 (Figure 5A). For Variant A, EV markers were most strongly detected in the 40/50% OptiPrep gradient interface, consistent with the expected buoyant density of small EVs. For Variant B, EV markers were predominantly detected in the first collected fraction (FR1) following the void volume, aligning with the established elution profile of EVs in size exclusion chromatography.

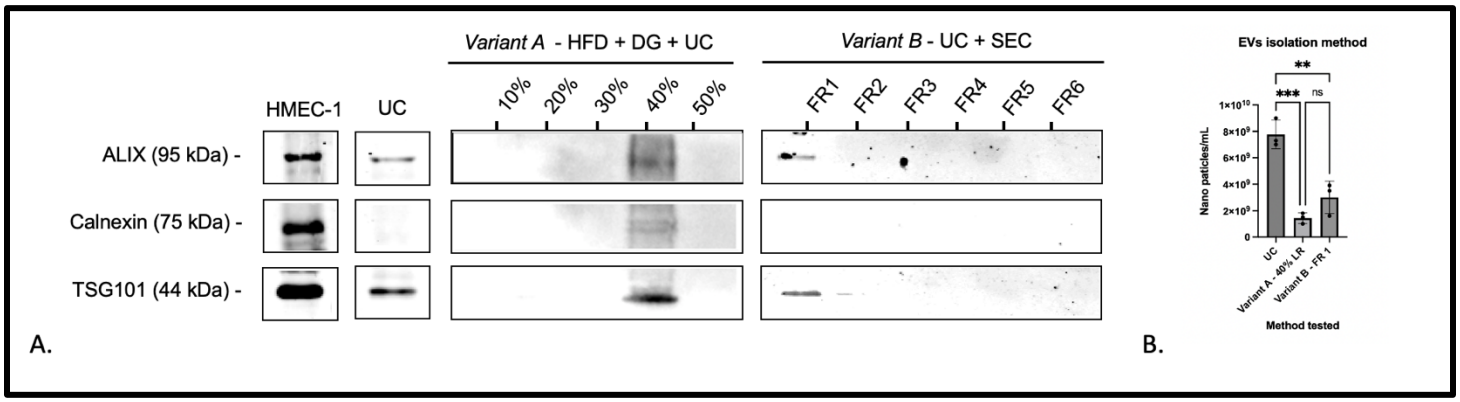

Figure 5: Comparative study of isolation methods variants. (A) Immunoblotting for positive EVs markers ALIX and TSG101 and negative marker Calnexin. Notice on Variant A the EVs fall in the 40%-50% intersection layer (LR) and for Variant B in Fraction 1 (B) Nanoparticle tracking analysis comparing all three-method tested.

Importantly, both variants demonstrated effective removal of calnexin (a cellular protein marker that should be absent in pure EV preparations), indicating successful purification from cellular contaminants. However, quantitative analysis of nanoparticle yield revealed significant differences between the methods (Figure 5B). While the statistical difference did not reach significance (likely due to variability between biological replicates), Variant B consistently demonstrated approximately twice the nanoparticle recovery compared to Variant A, with yields averaging 3.2×10^9 versus 1.6×10^9 nanoparticles per isolation, respectively.

Beyond yield and purity considerations, we evaluated the practical aspects of each methodology, including procedural complexity, time requirements, and scalability. Variant A required approximately 60-65 minutes of hands-on time, primarily for gradient preparation and fraction collection, with a total procedure duration of about 5 hours. In contrast, Variant B demanded only 30-40 minutes of hands-on time, mostly for chromatography column preparation and fraction collection, with a total duration of approximately 2 hours.

Furthermore, when considering the planned scale-up of our culture system, Variant B offered superior adaptability. The ultracentrifugation step could readily accommodate increased volumes by transitioning to larger-capacity rotors, while the SEC step, requiring only the concentrated EV pellet, would remain unchanged. In contrast, scaling Variant A would necessitate increasing the number of

dialysis membranes and density gradients proportionally, substantially increasing both hands-on time and procedural complexity.

2.3.3 Up-scaling EV production

Having established an optimized isolation methodology, our next objective was to scale up EV production to achieve the target yield of 1-2×10^10 nanoparticles per isolation required for comprehensive proteomic characterization and functional studies. This necessitated increasing both the cell culture surface area and adapting the ultracentrifugation parameters accordingly.

For scaling up ultracentrifugation, we transitioned from the Beckman Coulter 90Ti rotor to the higher-capacity Beckman Coulter 45Ti rotor and used the once more the Intellifuge© Calculator from Beckman to adjust the final protocol, which accommodates up to 400 mL of sample volume. This larger capacity aligned perfectly with the conditioned media volume generated from four T500 flasks, enabling efficient processing of increased culture volumes while maintaining the established protocol parameters.

The protocol for large volumes ultracentrifugation is as follows:

Ultracentrifugation: The collected conditioned media was centrifugated for 20 min at 2000 g-Force (max) in an Eppendorf R250 centrifuge. Pellet was discarded and the supernatant was filtered through a 0.45 μm VWR complete filtration unit (Cat# 10040) before a two-step differential ultracentrifugation process at 10,000 g-Force-max (9,266 rpm) for 30 minutes and 120,000 g-Force-max (32,097 rpm) for 144 minutes in a Beckman coulter rotor 45Ti (k=133) using 70 mL polyacrylamide tubes (Cat# 355622).

Table 5 summarizes the quantitative outcomes of our scale-up strategy, documenting the relationship between culture surface area, cell yield, and EV recovery at different scales of production.

Flask model	Total area cm^2	Avg. HMEC-1 cell counting	UC Bulk NTA	SEC FR1 NTA
2 x T175	350	17.5x10^10	0.8 x10^10	0.35-0.15 x10^10
1 x T500	500	25 x10^10	1-2.25 x10^10	0.5-1 x10^10
4 x T500	2000	100 x10^10	4-7.5 x10^10	2-4 x10^10
8 x T500	4000	200 x10^10	8-13 x10^10	4-8 x10^10

Table 6: Table 5: Scale-up of EV production with increasing culture surface area.

As demonstrated in Table 6, scaling up from two T175 flasks to four T500 flasks resulted in a nearly six-fold increase in cellular yield (from 17.5×10^6 to 100×10^6 cells) and, importantly, a proportional increase in EV recovery. The SEC-purified fraction 1 (FR1) consistently yielded approximately 50% of the bulk ultracentrifugation (UC) preparation, reflecting the loss of non-vesicular components during the purification process while maintaining a high recovery of genuine EVs.

Notably, with four T500 flasks, we consistently achieved our target yield of 2-4×10^10 nanoparticles in the purified FR1 fraction, exceeding our minimum threshold of 1×10^10 particles for downstream applications. This scale proved optimal for our research needs, balancing practical considerations of laboratory capacity with sufficient EV yield for comprehensive proteomic analysis and functional studies

2.4 Final remarks on EVs optimization.

The systematic approach described in this chapter successfully addresses the first research question posed in Section 1.4: "What is the optimal isolation method for microvascular endothelial cell-derived EVs that maximizes both yield and purity?" Through careful selection of an appropriate cell line, development of a specialized low-serum media formulation, and optimization of a two-stage isolation protocol combining ultracentrifugation with size exclusion chromatography, we have established a reproducible methodology for isolating microvascular endothelial cell-derived EVs with high yield and purity.

Several key achievements deserve emphasis:

1. Development of a low-serum culture system: The F15 media formulation enabled HMEC-1 culture with just 2% serum supplementation while maintaining endothelial phenotype and robust growth kinetics. This represents a significant advancement over conventional high-serum conditions, reducing potential serum-derived EV contamination—a critical consideration for downstream proteomic and functional analyses.
2. Optimization of isolation methodology: The combination of ultracentrifugation and size exclusion chromatography proved superior to alternative approaches, balancing high EV recovery with effective removal of potential contaminants. The optimized protocol consistently yielded EVs positive for established markers (Alix and TSG101) while eliminating cellular contaminants (calnexin).
3. Successful scale-up: The scalable nature of our methodology enabled production of highly purified EVs at yields exceeding 2×10^10 nanoparticles per isolation, meeting the requirements for comprehensive proteomic characterization and functional studies.

Throughout this optimization process, several unexpected findings emerged that contribute to the broader field of EV research. The observed effects of hypoxanthine and ascorbic acid on HMEC-1 growth highlight the importance of empirical optimization for specific cell lines, while the comparative analysis of isolation methodologies provides practical insights for researchers working with microvascular endothelial cell-derived EVs.

The methodologies established in this chapter lay the foundation for addressing our subsequent research questions regarding the proteomic signature and functional capabilities of microvascular endothelial cell-derived EVs. With a reliable and scalable system for producing highly purified EVs, we proceeded with confidence to the comprehensive proteomic characterization described in the following chapter.

Chapter 3: Microvascular endothelial cells-derived extracellular vesicles characterization.

Building upon our successful optimization of EV isolation methods in Chapter 2, this chapter focuses on comprehensive characterization of microvascular endothelial cell-derived EVs. Our previous work established a reliable protocol combining ultracentrifugation with size exclusion chromatography that yields high-purity EV preparations with minimal contaminants. Here, we extend this work by addressing two critical aims: (1) documenting vesicle morphology through cryo-electron microscopy to fulfill the MISEV characterization guidelines, and (2) performing shotgun proteomic analysis in biological triplicate to comprehensively identify and categorize the protein cargo of these EVs.

This characterization serves multiple purposes. First, it validates our isolation methodology by confirming the presence of vesicular structures with characteristic morphology. Second, the proteomic analysis provides insights into the biological cargo of these EVs, enabling us to predict their functional roles and plan targeted experiments to test these functions. Finally, by conducting this analysis on EVs isolated through both ultracentrifugation-only and our optimized ultracentrifugation with size exclusion chromatography method, we can evaluate how isolation methodology influences characterization results.

3.1 Documenting EVs morphology by cryo-electron microscopy

In order to comply MISEV vesicle morphology needed to be confirmed by electron microscopy. EVs preparations from ultracentrifugation-only and ultracentrifugation and size exclusion chromatography were submitted to cryo-electron microscopy at the UVA Electron microscopy core. The sample preparation protocol is described as follow:

In order to comply with MISEV guidelines [19], vesicle morphology needed to be confirmed through electron microscopy. We submitted EV preparations from both our ultracentrifugation-only method and our optimized ultracentrifugation with size exclusion chromatography protocol to cryo-electron microscopy at the UVA Electron Microscopy Core. This approach allows visualization of EVs in their native state without fixation artifacts that can occur in traditional transmission electron microscopy. The sample preparation protocol is described as follows:

Grid Preparation Using Vitrobot Mark IV

Quantifoil R2/2 holey carbon copper grids (200 mesh) were selected for this study based on their optimal hole size and distribution for extracellular vesicle (EV) imaging. Prior to sample application, the grids were glow-discharged for 45 seconds at 15 mA to render the carbon film hydrophilic, which improves sample spreading and reduces aggregation of EVs. Grids were used within 30 minutes of glow discharge to ensure optimal hydrophilicity.

The Vitrobot Mark IV (FEI/Thermo Fisher) was prepared by setting the climate chamber temperature to 4°C and humidity to 100% to prevent sample evaporation during the blotting process. The ethane cup was cooled to liquid temperature using liquid nitrogen in the surrounding container, taking care to maintain the ethane in a liquid state throughout the vitrification procedure. The liquid ethane was prepared by condensing ethane gas into the pre-cooled cup until it was approximately 75% full.

For sample vitrification, 3.5 µL of each EV preparation (either from ultracentrifugation or ultracentrifugation followed by size exclusion chromatography) was applied to the glow-discharged grid held in anti-capillary tweezers. The grid was then loaded into the Vitrobot and the vitrification process was initiated. Blotting parameters were optimized for the EV samples with a blot force of -2, blot time of 4 seconds, wait time of 0 seconds, and drain time of 0 seconds. These parameters were determined after several test preparations to ensure optimal ice thickness and particle distribution. The blotting was performed using filter paper (Whatman No. 1) applied from both sides of the grid simultaneously.

Immediately after blotting, the grid was rapidly plunged into the liquid ethane, resulting in vitrification of the sample. The vitrified grid was then transferred to a grid box under liquid nitrogen to maintain vitrification and prevent ice crystal formation. Grid boxes were stored in liquid nitrogen storage dewars until data collection. For each sample type (UC and UC+SEC FR1), at least three grids were prepared to ensure sufficient sampling and to account for potential variability in grid quality.

Data Acquisition on 300kV FEI Titan Krios

Cryo-EM data acquisition was performed using a 300kV FEI Titan Krios transmission electron microscope. Prior to specimen loading, the microscope was aligned according to standard procedures, including gun alignment, condenser aperture centering, and coma-free alignment. A cryo-specimen holder was pre-cooled with liquid nitrogen for at least 20 minutes before grid transfer. The specimen was loaded following the manufacturer's guidelines to minimize ice contamination, and the system was allowed to stabilize for approximately 1 hour after insertion to minimize stage drift during data collection.

Low-dose imaging procedures were implemented to minimize electron beam damage to the radiation-sensitive EV samples. A three-mode low-dose setup was configured with the following parameters: search mode with a dose rate of approximately 0.05 e-/Å²/s at 2,500× magnification; focus mode with a dose rate of 0.2 e-/Å²/s at 44,000× magnification; and exposure mode with a dose rate of 8-10 e-/Å²/s at 75,000× magnification. This configuration allowed for sample navigation and focusing with minimal pre-exposure of the acquisition area.

Data collection was performed using automated acquisition software (EPU, FEI/Thermo Fisher). Initially, a low-magnification atlas of the entire grid was acquired at 150× magnification to identify suitable grid squares with optimal ice thickness. From this atlas, grid squares showing consistent ice thickness and minimal contamination were selected for high-resolution data collection. Within each selected grid square, individual holes in the carbon film were targeted for acquisition.

Imaging was performed at a nominal magnification of 75,000×, resulting in a calibrated pixel size of 1.08 Å/pixel at the specimen level. The objective aperture (70 µm) and C2 aperture (50 µm) were selected to optimize contrast while maintaining high resolution. The beam diameter was set to approximately 1.2 µm to ensure illumination of the area of interest while minimizing unnecessary exposure of adjacent areas.

Exposure parameters were optimized for EV imaging with a frame rate of 7 frames per second over a total exposure time of 4 seconds, resulting in 28 total frames per micrograph. The total electron dose was limited to 32 e-/Å² to minimize radiation damage while maintaining sufficient signal-to-noise ratio for visualization of EV membranes. Images were collected across a defocus range from -1.0 to -3.0

µm in 0.5 µm increments to enhance phase contrast, particularly important for the visualization of small EVs with diameters below 100 nm.

Autofocus was performed every 10 µm or before each acquisition to maintain consistent imaging conditions throughout the data collection session. The targeting strategy involved collecting multiple images per hole (typically 4 images offset from the center) to maximize data collection efficiency and to sample different areas within each hole. Data collection proceeded until at least 300 high-quality micrographs were obtained for each sample type, requiring approximately 48-72 hours of microscope time per sample.

Throughout the acquisition, image quality was monitored in real-time by assessing drift, ice thickness, and defocus accuracy. Focus was adjusted as needed to maintain optimal imaging conditions, and areas showing excessive drift or contamination were avoided. The microscope alignment was verified and adjusted periodically during the multi-day data collection sessions to ensure consistent imaging quality.

For comparative analysis between the two isolation methods (UC and UC+SEC FR1), care was taken to maintain identical imaging conditions across all samples. Data collection strategies were designed to ensure representative sampling across multiple grids and grid areas to account for potential heterogeneity in the EV populations and to enable statistically robust comparisons between the two preparation methods.

Figure 6 shows representative cryo-EM images from both isolation methods. The images from the UC+SEC FR1 samples (Fig. 6B) exhibit noticeably reduced background debris compared to the UC-only samples (Fig. 6A), confirming the enhanced purity achieved through our size exclusion chromatography step. This observation aligns with our previous findings from Chapter 2, where we demonstrated that SEC effectively removes non-vesicular contaminants. The reduced number of vesicles visible in the UC+SEC FR1 samples also corresponds with the quantitative reduction in nanoparticle counts measured by NTA (Fig. 5B), further validating the consistency between our different characterization methods.

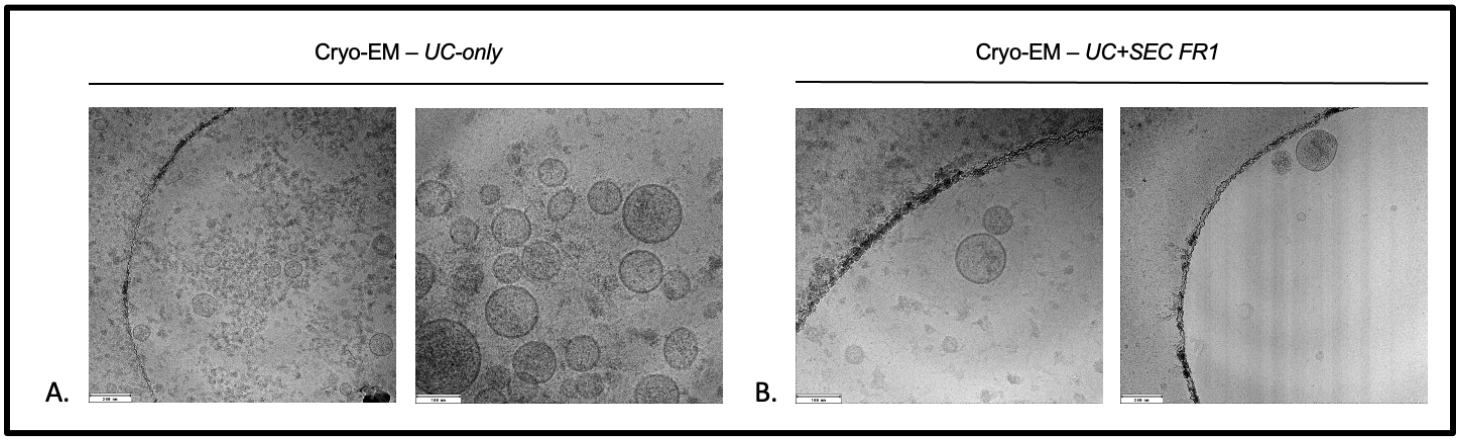

Figure 6: Cryo-EM images from UC-only vs UC+SEC FR1 (A) UC-only images (B) UC+SEC FR1. Notice the difference in non-EVs debris between methods.

Morphologically, EVs from both isolation methods exhibited the characteristic round, cup-shaped appearance typical of exosomes and small microvesicles. No multivesicular bodies were observed in any of the samples, suggesting effective elimination of cellular components during the isolation

process. The size distribution of visualized vesicles was consistent with our NTA measurements, with most vesicles ranging between 30-150 nm in diameter, corresponding to the exosome size range. This morphological confirmation represents a critical validation of our isolation methodology, demonstrating that our protocols yield vesicular structures with the expected physical characteristics of EVs.

Having confirmed the vesicular morphology of our preparations and thus completed all three major MISEV characterization requirements— (1) Nanoparticle tracking analysis, (2) Immunoblotting of EV markers, and (3) Vesicle morphology confirmation by electron microscopy—we proceeded to comprehensive proteomic analysis to characterize the molecular cargo of these EVs.

3.2 Shotgun proteomic analysis

Our next goal in the characterization process was to conduct a comprehensive shotgun proteomic analysis to identify the protein population in our EV preparations. While a previous study by de Jong et al. [9] reported proteomic analysis of HMEC-1-derived EVs, their focus was primarily on comparing protein populations between EVs from cells cultured under TNF-alpha stimulation versus hypoxia. Our analysis extends and complements this earlier work in three significant ways:

1. **EVs collected from low-serum conditions**: The previous study collected EVs from HMEC-1 cultured with the ATCC-recommended high-serum medium, which likely introduced bovine protein contamination that could confound mass spectrometry results due to the high similarity (>90%) between bovine and human protein spectral profiles [80] [81]. By utilizing our optimized low-serum culture conditions described in Chapter 2, we minimize this source of contamination.
2. **EVs collected from ultracentrifugation + size exclusion chromatography**: As demonstrated by our cryo-EM studies, SEC effectively removes non-vesicular debris from ultracentrifugation preparations. This enhanced purification allows for a more focused analysis of genuine EV cargo proteins rather than co-isolated contaminants.
3. **Bioinformatics analysis focused on EV cargo functionality**: Unlike the previous study, which effectively compared protein populations between different endothelial cell activation states, our analysis specifically targets potential functional domains where the identified proteins may have biological relevance. This approach provides direct insights into potential physiological roles of microvascular endothelial cell-derived EVs.

To ensure statistical robustness, all samples were prepared in biological triplicates. Recognizing that ultracentrifugation remains the gold standard isolation method in the field, we conducted parallel proteomic analyses on both UC-only (UC Bulk) and UC+SEC preparations to enable direct methodological comparisons. All cultures were grown in 4×T500 plates, maintaining consistent cell counts, pH values, and nanoparticle yields as documented in Table 6 of Chapter 2.

Total protein content in each sample was quantified using the Micro-BCA® Protein kit from Thermo (Cat#23235), and samples were normalized to 7-8 µg total protein before analysis. The tandem mass spectrometry analysis combining high-performance liquid chromatography and mass spectrometry was conducted at the Mass Spectrometry Core Facility at Georgetown University following a standardized protocol:

All samples were resuspended with 5%SDS buffer (containing 50 mM TEABC and 20 mM DTT) and heated for 10 min at 95 °C. After cooling down to room temperature, iodoacetamide in 5% SDS solution was added to a final concentration of 40 mM and incubated in the dark for 30 min. Undissolved matter was centrifuged for 8 min at 13,000 x g. The supernatant was saved and used for downstream processing using a S-Trap column (ProtiFi, LLC). Proteins were digested with sequencing-grade Lys-C/trypsin (Promega) by incubation at 37°C overnight. The resulting peptides were eluted and dried down with a SpeedVac (Fisher Scientific).

NanoUPLC-MS/MS: Peptides were analyzed with a nanoAcquity UPLC system (Waters) coupled with Orbitrap Fusion Lumos mass spectrometer (Thermo Fisher), as described previously (1). In brief, samples in 0.1% FA solution are loaded onto a C18 Trap column (Waters Acquity UPLC M-Class Trap, Symmetry C18, 100 Å, 5 µm, 180 µm x 20 mm) at 10 µL/min for 4 min. Peptides are then separated with an analytical column (Waters Acquity UPLC M-Class, peptide BEH C18 column, 300 Å, 1.7 µm, 75 µm x 150 mm) with the temperature controlled at 45°C. The flow rate is set as 350 nL/min. A 150-min gradient of buffer A (2% ACN, 0.1% formic acid) and buffer B (0.1% formic acid in ACN) is used for separation: 1% buffer B at 0 min, 5% buffer B at 1 min, 22% buffer B at 90 min, 50% buffer B at 100min, 98% buffer B at 120 min, 98% buffer B at 130 min, 1% buffer B at 130.1 min, and 1% buffer B at 150 min. Data were acquired with the Orbitrap Fusion Lumos mass spectrometer using an ion spray voltage of 2.2 kV and an ion transfer temperature of 275°C. Mass spectra were recorded with Xcalibur 4.0. MS parameter: OT MS: Detector Type: Orbitrap; Orbitrap Resolution: 60000; Scan Range (m/z): 380-1400; RF Lens (%): 30; AGC Target: Standard; Maximum Injection Time Mode: Auto; Microscans: 1. Charge state(s): 3-8; Exclusion duration (s): 40. Data Dependent Mode: Cycle Time; Time between Master Scans (sec): MS/MS parameter: ddMS² OT HCD: Isolation Mode: Quadrupole; Isolation Window (m/z): 1.6; Activation Type: HCD; HCD Collision Energy (%): 35; Detector Type: Orbitrap; Orbitrap; Resolution: 30000; Normalized AGC Target (%):200.

Data analysis: The MS data files were processed using the Proteome Discoverer platform (version 2.4, Thermo Scientific) with the Sequest HT algorithm. MS/MS data files were searched against the human proteome database with the following parameters: two missed cleavages allowed, minimum peptide length of seven amino acids, variable modifications set as oxidation (M), fixed modification as carbamidomethylation (C), and MS and MS/MS ion tolerances of 10 ppm and 0.02 Da, respectively. The false discovery rate (FDR) was estimated using fixed value PSM validation.

To ensure high confidence in our protein identifications, we based our comparative analysis on total unique peptide counts with a minimum threshold of three peptides required for protein inclusion. This criterion is more stringent than the common two-peptide threshold, enhancing the reliability of our results at the expense of potentially excluding some low-abundance proteins.

Our analysis yielded approximately 229 unique proteins per sample in the UC Bulk preparations and approximately 316 proteins in the UC+SEC preparations. This represents a noticeable reduction compared to the protein numbers reported by de Jong et al. [9], likely reflecting our use of low-serum conditions and improved isolation methods that minimize non-EV protein contamination.

The subsequent sections will detail our bioinformatic analysis of this proteomic dataset. Given the complexity of the data, we followed a systematic analytical approach:

1. First, we assessed the statistical strength of our results through correlation analysis between biological replicates within each method (UC Bulk and UC+SEC) and then compared results between methods.

2. Next, we benchmarked our findings against the Top-100 EV proteins database from Vesiclepedia to evaluate how our results align with established EV proteomes and to identify potentially novel proteins not previously documented in EVs.
3. We then performed gene ontology (GO) term analysis to group proteins by functional categories, with particular emphasis on microvascular-related functions relevant to our research focus.
4. Finally, we conducted pathway analysis to identify specific biological processes likely influenced by the protein cargo of microvascular endothelial cell-derived EVs.

This sequential analytical approach was designed not only to characterize the EV proteome comprehensively but also to identify the most promising biological processes for subsequent functional validation studies. By determining where and how these EVs might exert their biological effects, we can design targeted experimental approaches to test these predictions in our future functional studies.

3.2.1 Mass spectrometry correlation analysis

To establish the reliability of our proteomic data, we first performed correlation analysis across our biological triplicates for both isolation methods. This analysis is crucial for validating the reproducibility of our findings and ensuring that observed differences between methods reflect genuine biological or methodological variations rather than technical inconsistencies.

Correlation analysis was performed using the unique peptide counts for each identified protein across all replicates (Figure 7). The UC Bulk method demonstrated excellent reproducibility between technical replicates with correlation coefficients ranging from r = 0.91 to 0.93, indicating high consistency in protein identification and quantification. The UC+SEC method showed good but slightly lower correlation coefficients ranging from r = 0.75 to 0.84. This marginal reduction in technical reproducibility is likely attributable to the method's enhanced sensitivity in detecting low-abundance proteins, which inherently exhibit greater variability in detection between replicates.

Direct comparison between the two isolation methods (Figure 7A) revealed moderate to strong correlations (r = 0.70-0.79), confirming a substantial overlap in the proteins identified by both approaches. However, the correlation plots demonstrated a consistent pattern where UC+SEC identified more unique peptides per protein than UC Bulk across all replicates. This was evidenced by the majority of data points falling above the theoretical 1:1 diagonal line in the method comparison plots. Furthermore, numerous proteins were exclusively detected by UC+SEC, with zero or minimal peptides identified in the UC Bulk preparations.

The UC+SEC method identified approximately 316 proteins across all replicates compared to 229 proteins detected using the UC Bulk method (Figure 7B). This substantial difference in detection sensitivity is likely attributable to the additional purification step in the UC+SEC method, which effectively removes non-vesicular contaminants that might otherwise suppress ionization of low-abundance peptides during mass spectrometry analysis.

These findings confirmed that while UC+SEC exhibits marginally lower technical reproducibility, this trade-off comes with significant advantages in terms of detection sensitivity and protein sequence coverage. This observation aligns with our cryo-EM findings in Section 3.1, which demonstrated that SEC effectively removes non-vesicular debris, potentially allowing for enhanced detection of genuine EV cargo proteins. The high technical reproducibility of our proteomic data provides a solid foundation

for subsequent bioinformatic analyses aimed at identifying the biological functions of these EV proteins.

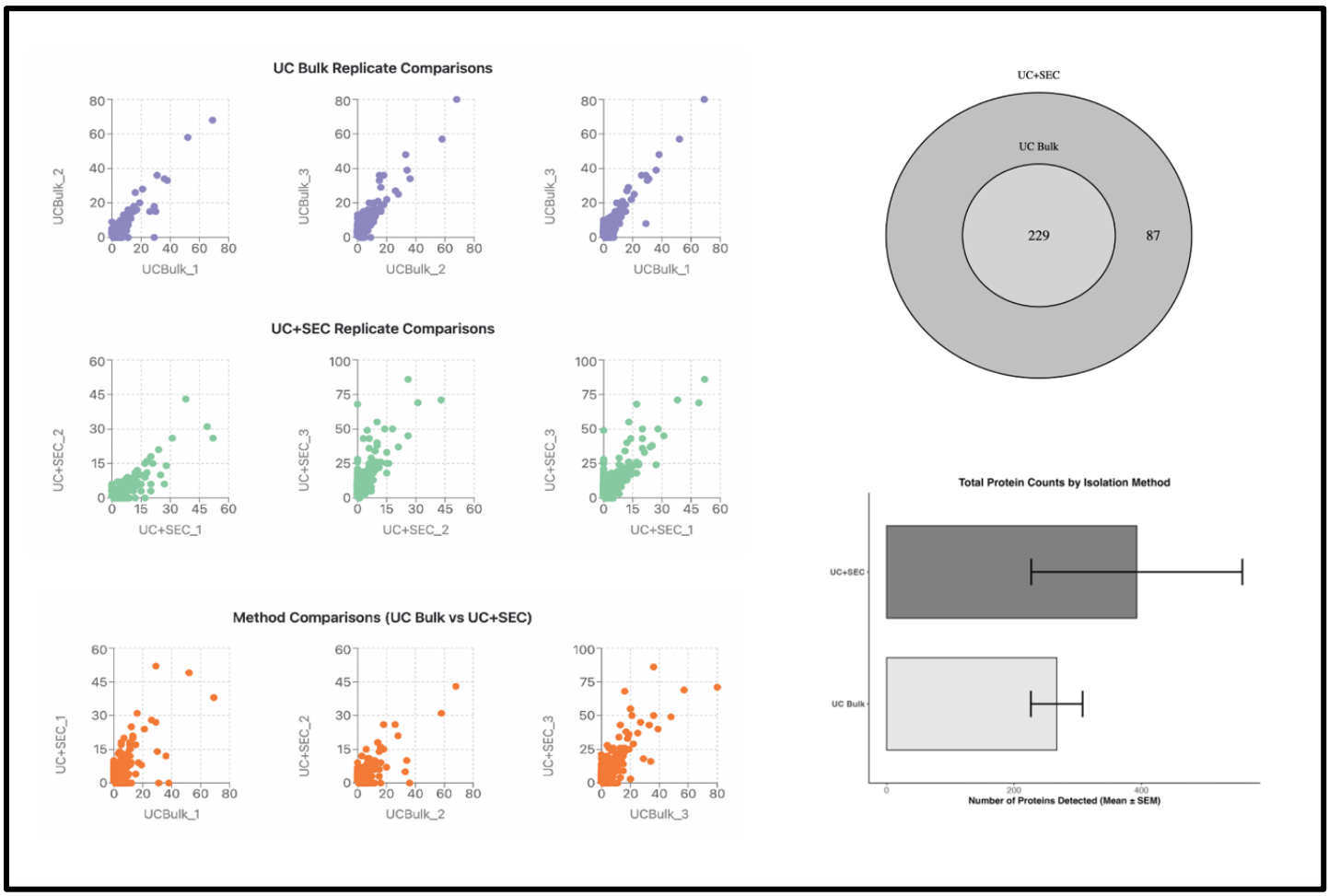

Figure 7: Mass spec correlation analysis (A) Sample replicate comparison (B) Two-way Venn diagram UC Bulk vs UC+SEC. Notice that all proteins detected in the UC Bulk analysis were also found on the UC+SEC (C) Bar graph total protein counts by isolation method.

The proteomic analysis of extracellular vesicles isolated by different methods revealed that the UC+SEC approach yielded substantially more identified proteins compared to UC Bulk, with mean counts of 392.7 ± 165.75 and 267 ± 40.63 proteins, respectively (Figure 7C). This represents a 47.1% increase in protein detection using the UC+SEC method. While both methods demonstrated variability across replicates, the UC+SEC method showed higher variability (CV: 73.1%) compared to UC Bulk (CV: 26.4%), suggesting that further optimization of the SEC protocol might improve reproducibility. The considerable increase in protein identification with UC+SEC indicates enhanced sensitivity of this approach for detecting the EV proteome, despite its greater technical variability.

3.2.2 Mass spectrometry comparison with previous studies

Once we confirmed the strong correlation of our study, we moved forward to compare our results with previous mass spectrometry studies available. In particular we focused on two targets: (1) The Top 100 EVs protein list from Vesiclepedia, a public web domain containing more than 500,000 protein entries from EVs proteomic analysis and (2) Comparing our results with the previously cited study by De Jong et al. [9] done in HMEC-1 cells. Our goal for each target is described below:

1. Confirm that our preparations contain a large number of cofounding proteins with the Top 100 EVs list from Vesiclepedia, which will serve as validation of an effective EVs preparation.

2. Compare if we had identified a new set of proteins not previously described by De Jong in HMEC-1 cells, which will indicate if the low-serum culture conditions and the size exclusion chromatography step cleaning power have been effective in clearing noise spectra to give room for novel proteomic.

Figure 8 shows the Venn diagram comparing the UC Bulk and UC+SEC studies with the Top 100 EVs protein list and the previous study by De Jong et al. [9].

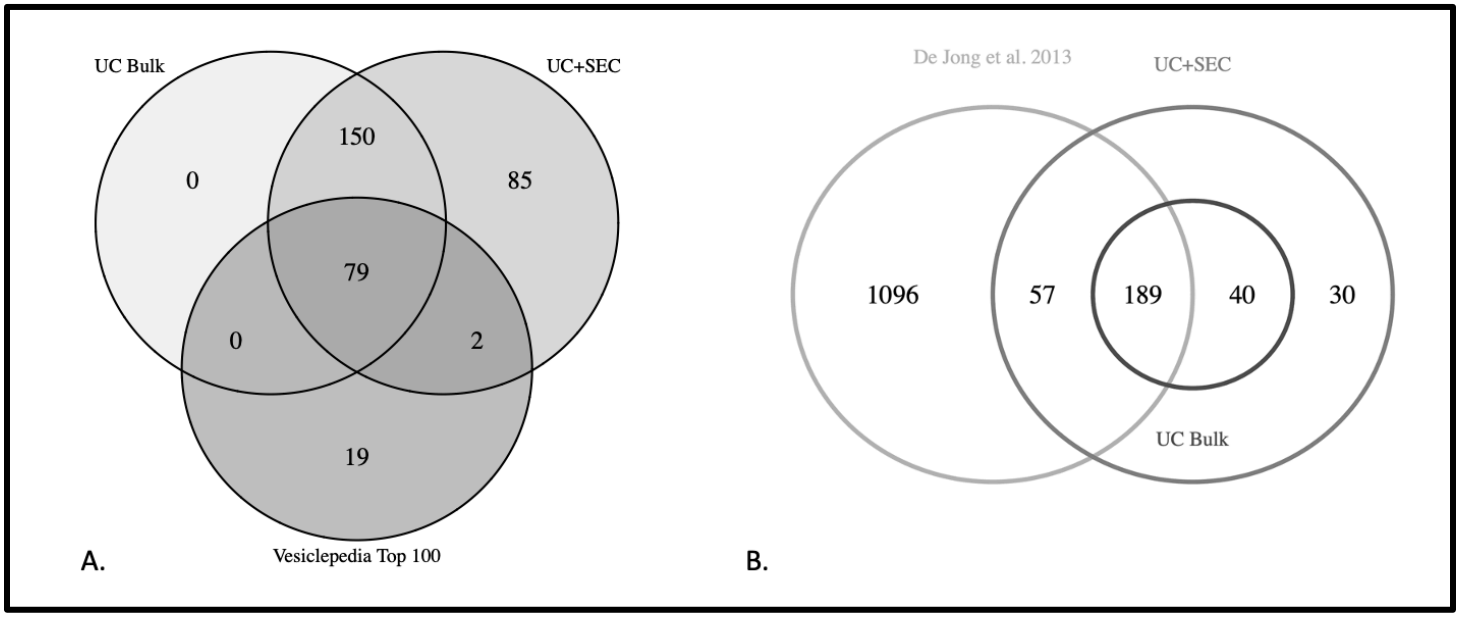

Figure 8: Venn diagram comparison between our mass spectrometry data and two EVs proteomic databases (A) Top 100 EVs protein list from Vesiclepedia (B) A previously cited study by De Jong et al. [9] done in HMEC-1 cells.

As previously mentioned, the Venn diagram analysis in Figure 8A revealed that UC+SEC identified 316 proteins compared to 229 proteins with UC Bulk, with all UC Bulk proteins also being detected in UC+SEC samples. Both isolation methods showed robust detection of established EV proteins, capturing 81 and 79 of the Vesiclepedia Top 100 proteins for UC+SEC and UC Bulk respectively. The complete overlap of UC Bulk proteins with UC+SEC proteins, along with the identification of additional proteins and slightly higher coverage of Vesiclepedia markers, suggests that UC+SEC offers enhanced sensitivity while maintaining the detection capabilities of the UC Bulk method. The high degree of overlap of both methods with the Vesiclepedia Top 100 proteins validated the efficiency of our isolation methods.

When comparing with the previous EVs proteomic study done in HMEC-1 (Figure 8B), the three-way Venn diagram illustrates the overlap between proteins identified in UC Bulk samples (n=229), UC+SEC samples (n=316), and those previously reported in the De Jong database (n=1342). Notably, our study uncovered 70 novel proteins not previously reported in the De Jong database using the UC+SEC method, with 40 of these also detected in UC Bulk preparations. This includes highly abundant proteins like Thrombospondin-1 (THBS1), Desmoplakin (DSP), and Galectin-3-binding protein (LGALS3BP), which have established roles in cell adhesion, wound healing, and angiogenesis. Perhaps most interesting are the 30 proteins exclusively identified in UC+SEC samples and absent from both UC Bulk and the De Jong database, including Phospholipid Scramblase 1

(PLSCR1), DNA Topoisomerase 1 (TOP1), and Eukaryotic translation initiation factor 3 subunit C-like (EIF3CL). These findings demonstrate that our optimized isolation methodology substantially enhances the detection of previously unreported EV proteins from microvascular endothelial cells, particularly those involved in cell-cell interactions and vascular functions, reinforcing the importance of isolation technique selection for comprehensive EV characterization.

The identification of these novel proteins with established roles in vascular biology provides intriguing insights into potential functional roles of microvascular endothelial cell-derived EVs. To systematically analyze these potential functions and identify biological processes that could be experimentally tested, we next performed comprehensive Gene Ontology (GO) analysis of our proteomic dataset. This analysis allowed us to group proteins by functional categories, with particular emphasis on processes related to vascular biology, cell-cell interactions, and wound healing—areas suggested by our initial examination of the novel proteins identified in this study.

3.2.3 Gene Ontology Analysis

To gain insights into the potential biological functions of proteins identified in our EV preparations, we performed Gene Ontology (GO) analysis using the clusterProfiler package. This approach allowed us to systematically categorize proteins based on their associated biological processes (BP), molecular functions (MF), and cellular components (CC). Our analysis compared proteins identified through both isolation methods (UC Bulk and UC+SEC) to determine whether methodological differences influenced the functional profiles of the detected proteomes.

General GO Term Analysis

Using Entrez gene IDs mapped from the UniProt accessions in our proteomic dataset, we performed enrichment analysis for each GO category. The UC+SEC method yielded 310 unique proteins that could be mapped to Entrez IDs, compared to 225 proteins from the UC Bulk method. This difference in protein numbers is consistent with our cryo-EM observations, which showed that the SEC step effectively removed non-vesicular contaminants while preserving genuine EV cargo.

For each GO category, we identified significantly enriched terms (adjusted p-value < 0.05) and compared the top terms between isolation methods. Figure 9 displays the top five enriched terms for each GO category, with significance represented as -log10 (adjusted p-value).

In the Biological Process category (Figure 9A), both isolation methods showed significant enrichment for vesicle-mediated transport, protein localization to membrane, and exocytosis-related processes. However, the UC+SEC method showed stronger enrichment (higher -log10(adjusted p-value)) for these processes, suggesting that the additional purification step may have enhanced the detection of genuine EV-associated proteins. The UC Bulk method showed relatively stronger enrichment for translation and protein metabolic processes, which could potentially indicate contamination from cellular debris or co-isolated non-vesicular material.

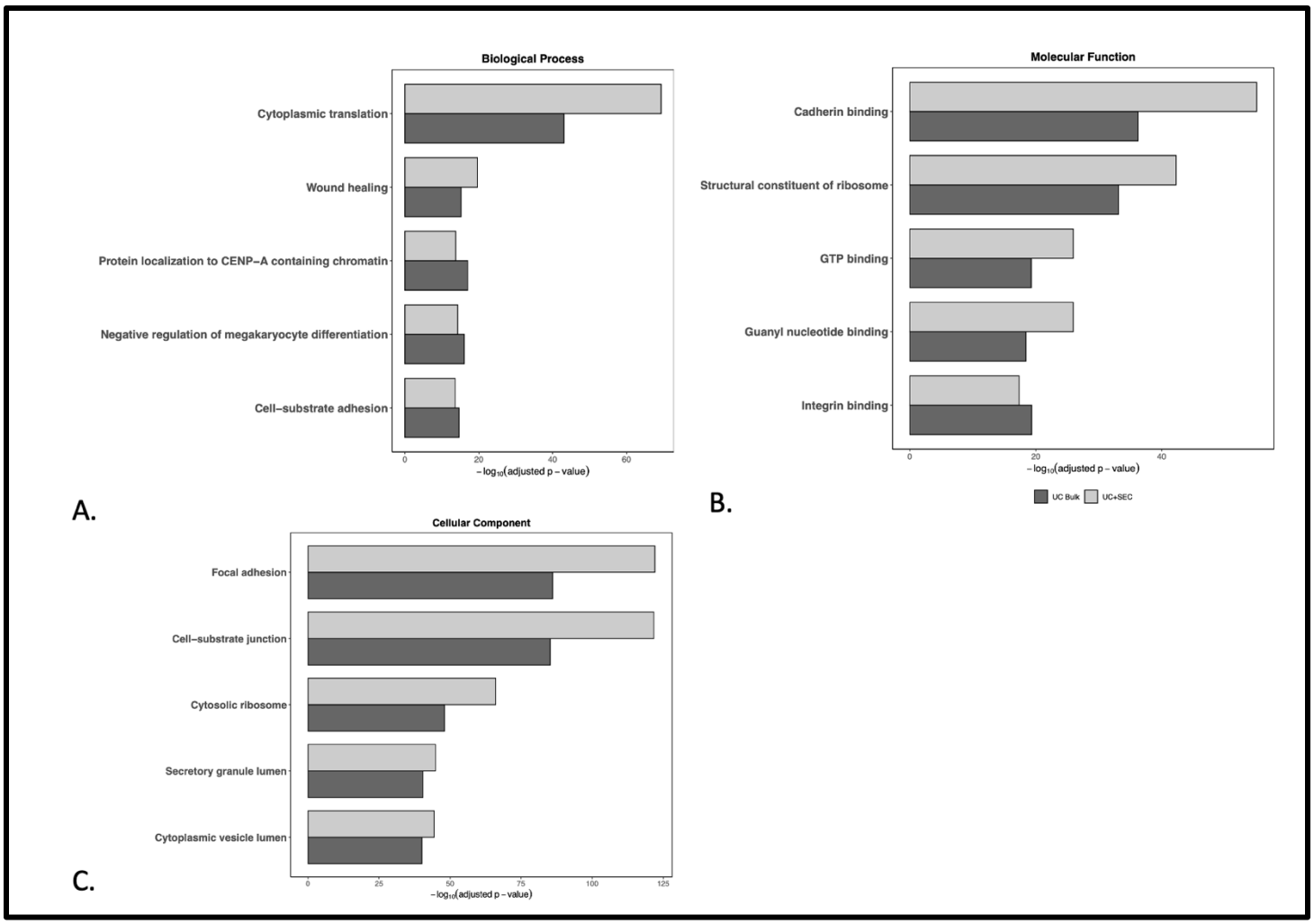

Figure 9: GO analysis (A) Biological process (B) Molecular function (C) Cellular component.

For Molecular Function Figure 9B, cadherin binding, protein binding involved in cell adhesion, and GTPase activity were among the top enriched terms for both methods. Both methods also showed strong enrichment for structural constituents of ribosomes, which aligns with previous findings on EV cargo from microvascular endothelial cells [9]. The similarity in MF profiles between methods suggests that despite differences in protein numbers, both isolation approaches captured essential functional aspects of the EV proteome.

The Cellular Component analysis (Figure 9C) provided particularly informative results, with both methods showing strong enrichment for extracellular exosome, membrane-bounded vesicle, and focal adhesion terms. Notably, the UC+SEC method showed stronger enrichment for vesicle lumen and melanosome components, while the UC Bulk method showed higher enrichment for ribosomal components. This pattern aligns with our hypothesis that the SEC step preferentially preserves vesicular components while reducing contamination from cellular debris.

While this general GO term analysis provided valuable insights into the broader functional landscape of our EV preparations, we found it insufficient for directing our subsequent functional studies. The enriched terms, while statistically significant, often represented broad biological categories with hundreds of associated proteins, making it challenging to translate these findings into focused experimental hypotheses.

Functional Category Analysis for Experimental Planning

To address this limitation, we narrowed our analysis to specific functional categories that have established experimental assays and are relevant to microvascular endothelial physiology. Based on literature review and our preliminary data, we selected five key functional categories for in-depth analysis:

1. Wound healing
2. Cell-cell adhesion (homotypic)
3. Regulation of angiogenesis
4. Hemostasis
5. Acute inflammatory response

Figure 10 shows the comparative enrichment of these functional categories between our isolation methods, with both the significance (-log10(adjusted p-value)) and the number of associated proteins indicated.

The wound healing category showed particularly strong enrichment in both isolation methods (adjusted p-value < 1 × 10^-22), with 74 associated proteins detected. This finding was especially relevant given the critical role of microvascular endothelial cells in tissue repair processes. The high protein count and strong statistical significance suggested that this would be a promising functional area for experimental validation.

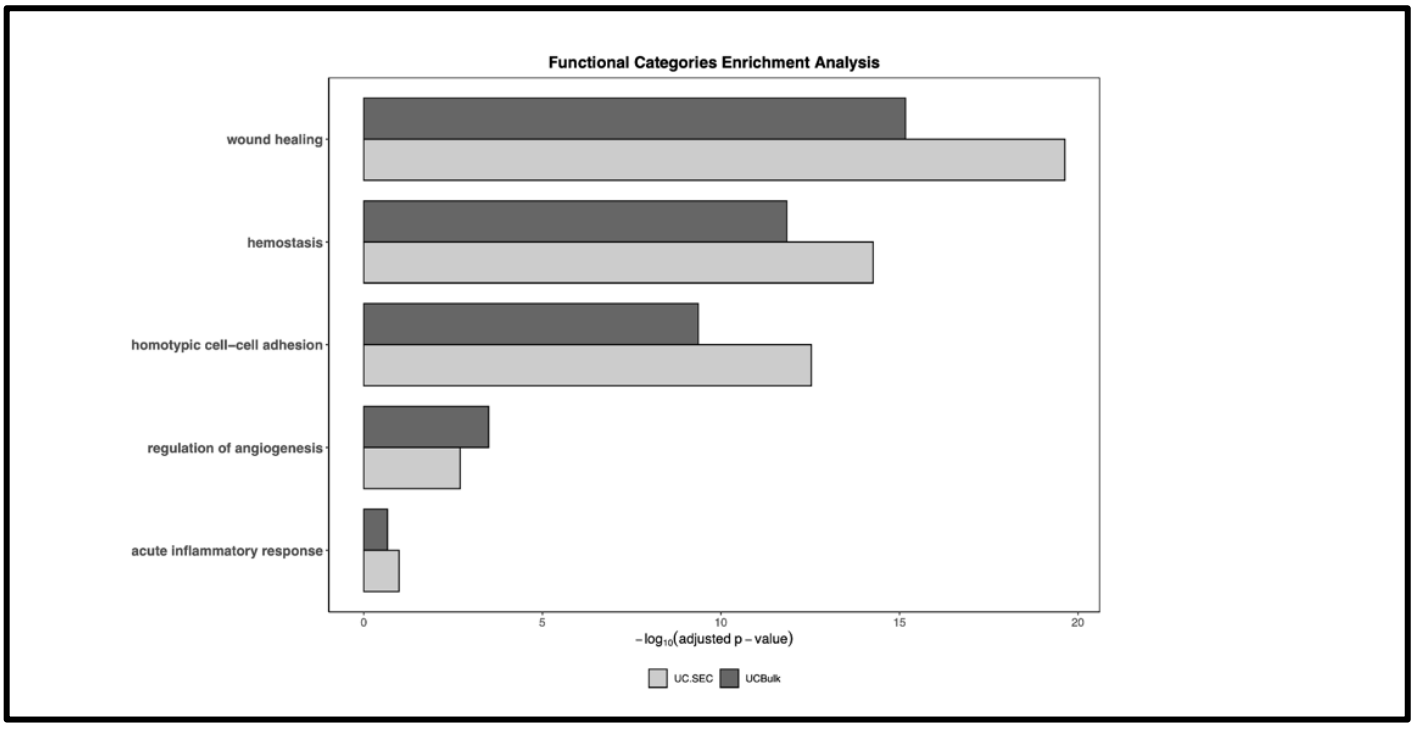

Figure 10. Functional GO analysis.

Hemostasis and blood coagulation processes also showed strong enrichment (adjusted p-value < 1 × 10^-16), with 47 and 46 associated proteins, respectively. This enrichment aligned with the known role of endothelial cells in regulating vascular hemostasis but our lab was not equipped with the

plasma supply or the tools to design a coagulation assay so we decided not to pursue this functional GO term.

Homotypic cell-cell adhesion (adjusted p-value < 1 × 10^-14, 28 proteins) and regulation of angiogenesis (adjusted p-value < 3 × 10^-4, 32 proteins) were also significantly enriched. These processes are central to endothelial cell function and can be readily tested through established experimental paradigms such as tube formation assays (angiogenesis) and cell aggregation assays (adhesion).

In order to further investigate the four functional GO terms that we could plan bench experiments to test in our laboratory (i.e., Wound healing, Homotypic cell-cell adhesion, angiogenesis and acute inflammatory response), we developed a bioinformatic analysis via heatmaps. For each protein, peptide counts were normalized to GAPDH expression levels to account for technical variations between samples, ensuring that observed differences reflected true biological variation rather than technical artifacts. Z-score transformation was then applied to the normalized data, converting expression values to standard deviations from the mean. This standardization allowed for effective visualization of relative protein enrichment patterns independent of absolute abundance levels.

The resulting heatmaps (Figure 11) display protein expression patterns across triplicate samples for both isolation methods (UC Bulk and UC+SEC), with red indicating higher expression and blue indicating lower expression relative to the mean. This visualization approach enabled identification of consistent expression patterns and method-specific enrichment.

The wound healing protein cluster (Figure 11A) demonstrates a consistent pattern of protein expression across both isolation methods. Most proteins show similar enrichment patterns between UC Bulk and UC+SEC preparations, with an overall fold-change ratio (SEC vs. Bulk) of 0.959. Importantly, we analyzed specific genes associated with this functional category to identify key proteins that might drive these processes. For wound healing, we identified proteins such as ANXA1, ANXA2, ANXA5, FN1, and ITGB1, which have well-documented roles in tissue repair. These findings suggest that microvascular endothelial EVs may contribute to wound healing processes, potentially by delivering these active proteins to injury sites.

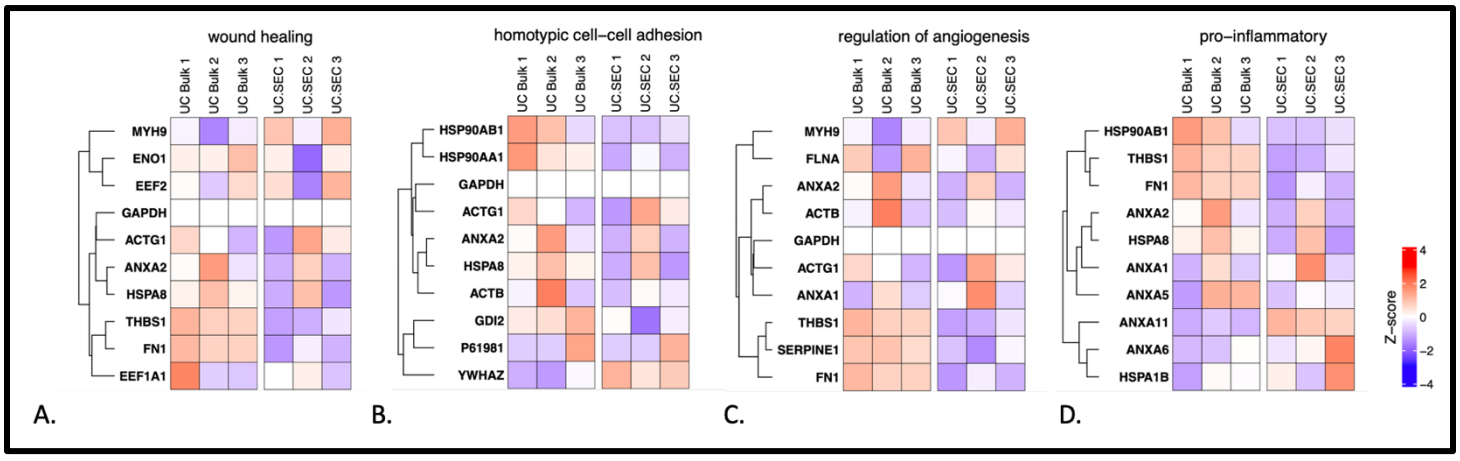

Figure 11: Top 10 proteins per functional GO analysis heatmaps (A) Wound healing (B) Homotypic cell-cell adhesion (C) Regulation of angiogenesis (D) Pro-inflammatory proteome. Notice the difference in upregulated protein population between methods.

The homotypic cell-cell adhesion cluster (Figure 11B) revealed proteins involved in cell-to-cell interactions and adhesion. The similarity between isolation methods (FC 0.927) suggests these proteins are genuine EV cargo rather than co-isolated contaminants. Prominently featured are integrin subunits, cadherins, and cellular junction proteins. The presence of these adhesion molecules suggests EVs could potentially modulate cell-cell interactions in recipient tissues, an important mechanism for endothelial function during angiogenesis.

Figure 11C displays proteins involved in the regulation of angiogenesis, a process critical to microvascular function. With a fold-change ratio of 0.943 between methods, the consistency of these findings strengthens their reliability. For angiogenesis regulation, proteins including VEGFA, THBS1, ITGAV, and ANGPT2 were identified. These specific protein identifications provided a more direct pathway from our proteomic data to experimental hypotheses. The identification of these proteins suggests that microvascular endothelial EVs may contribute to the regulation of new vessel formation, potentially allowing endothelial cells to influence angiogenic processes in their microenvironment.

While our initial GO term analysis identified "acute inflammatory response" as a category of interest (Figure 10, adjusted p-value < 0.057), the limited number of proteins (10) and modest statistical significance prompted us to conduct a more comprehensive investigation of inflammatory proteins in our EV samples. As shown in Figure 10, this category ranked below other enriched terms like wound healing and cell adhesion, but its biological relevance to endothelial function warranted deeper exploration. To address this limitation, we expanded our analysis beyond strict GO term classifications by incorporating literature-based functional annotations. This expanded approach allowed us to identify proteins with inflammatory functions that might have been missed by relying solely on GO term enrichment, which can be limited by incomplete or inconsistent annotations across protein databases.

The expanded inflammatory protein analysis is visualized in Figure 11D, which displays proteins identified through both GO term enrichment and our literature-based approach. To expand upon our initial findings, we conducted a comprehensive literature-based analysis to identify additional pro-inflammatory proteins that may have been missed by relying solely on GO term annotations. This approach combined pattern matching of gene names associated with inflammation (e.g., annexins, heat shock proteins, complement components) with manual curation of proteins known to be involved in inflammatory processes from recent literature. Through this expanded analysis, we identified an additional 28 proteins with established pro-inflammatory functions, bringing the total to 38 proteins (4.9% of the total proteome). These proteins spanned diverse functional categories including annexins (8 proteins), coagulation and complement system proteins (8 proteins), endothelial activation mediators (5 proteins), heat shock proteins (5 proteins), and ECM modulators (3 proteins). Notably, many of these proteins were significantly enriched in the UC+SEC fraction (57.9%), suggesting our optimized isolation method better preserves vesicles containing important inflammatory mediators. Among the most abundant were fibronectin (FN1), thrombospondin-1 (THBS1), annexin A2 (ANXA2), and heat shock proteins (HSPA8, HSPA1B), indicating a potentially significant role for these EVs in regulating inflammatory processes in recipient cells.

The proteomic analysis revealed GO term enrichments that align with known endothelial functions, particularly in wound healing, cell-cell adhesion, angiogenesis regulation, and inflammatory responses. The consistent identification of these functional protein clusters across both isolation methods strengthens confidence in these findings and suggests genuine biological roles for these EV-associated proteins.

Limitations of Standard GO Analysis for Experimental Planning

It is worth noting that standard GO enrichment analysis, while statistically robust, presented several limitations for experimental planning purposes:

1. **Broad term definitions**: Many of the most significantly enriched GO terms were extremely broad (e.g., "protein binding," "cytoplasm"), encompassing hundreds of proteins with diverse functions.
2. **Overlapping categories**: Substantial overlap between GO categories complicated interpretation, with many proteins appearing in multiple functional groupings.
3. **Statistical vs. biological significance**: Terms with high statistical significance did not always correspond to biologically testable functions.
4. **Lack of directionality**: Enrichment analysis identified associated functional categories but could not predict whether EVs would activate or inhibit these processes.

By complementing standard GO analysis with our targeted functional category approach, we overcame these limitations and established a clear path from proteomics to experimental validation. The specific proteins identified within each functional category provided mechanistic insights and potential targets for validation, effectively bridging the gap between bioinformatic analysis and bench experimentation.

In summary, our GO analysis revealed both broad functional patterns across the EV proteome and specific functional categories with experimental relevance. The identified categories—particularly wound healing, angiogenesis regulation, and inflammatory response—directly guided our subsequent functional studies, as detailed in Chapter 4.

3.3 Final remarks on EVs characterization.

This chapter has comprehensively addressed the second research question posed in Section 1.4: "What is the distinct proteomic signature of microvascular endothelial cell-derived EVs, and what insights can a comprehensive proteomic analysis reveal about vesicle biogenesis and functionality?" Through methodical characterization of EV morphology via cryo-electron microscopy and detailed proteomic analysis, we have established a clear proteomic signature of microvascular endothelial cell-derived EVs and gained significant insights into their potential functional roles.

Several key achievements deserve emphasis:

1. **Morphological validation**: Cryo-EM analysis confirmed the vesicular nature of our preparations, with both isolation methods yielding vesicles with characteristic morphology. Importantly, this analysis revealed the superior purity of UC+SEC preparations, with noticeably reduced non-vesicular debris compared to UC-only samples, validating our methodological improvements from Chapter 2.
2. **Comprehensive proteomic characterization**: Our shotgun proteomic approach identified 316 proteins in UC+SEC preparations and 229 proteins in UC Bulk samples, with high reproducibility across biological replicates. The substantial overlap with the Vesiclepedia Top 100 EV proteins (approximately 80%) confirms the authenticity of our EV preparations while highlighting the sensitivity of our methodological approach.
3. **Novel protein discoveries**: Perhaps most significantly, our optimized low-serum culture conditions and enhanced isolation methodology revealed 70 proteins not previously

documented in microvascular endothelial cell-derived EVs, including 30 proteins exclusively detected in UC+SEC preparations. These novel identifications include proteins with established roles in vascular biology, such as Thrombospondin-1, Desmoplakin, and Galectin-3-binding protein.

4. **Functional insights**: Gene Ontology analysis revealed significant enrichment for processes central to vascular biology, including wound healing, cell-cell adhesion, angiogenesis regulation, and inflammatory responses. The identification of specific proteins within these categories provides mechanistic insights and testable hypotheses regarding the functional roles of these EVs.

The systematic approach employed in this characterization has yielded several unexpected findings that contribute to the broader field of EV research. The enhanced protein detection achieved through our UC+SEC method suggests that many previous studies using ultracentrifugation alone may have underestimated the complexity of the EV proteome. Furthermore, the identification of novel proteins not previously documented in microvascular endothelial cell-derived EVs highlights the importance of optimized isolation methodologies and low-serum culture conditions for comprehensive EV characterization.

Our findings also have important implications for understanding the biological functions of these EVs. The enrichment for proteins involved in wound healing, angiogenesis, and inflammatory responses suggests that microvascular endothelial cell-derived EVs may play critical roles in coordinating vascular repair, remodeling, and inflammatory processes. These functional insights directly inform the design of our subsequent functional validation studies, as detailed in Chapter 4.

In conclusion, this comprehensive characterization of microvascular endothelial cell-derived EVs has established their distinct proteomic signature and provided valuable insights into their potential functional roles. By fulfilling all MISEV characterization requirements and employing rigorous statistical analysis, we have established a solid foundation for subsequent functional studies in the next chapter aimed at validating the biological significance of these findings.

Chapter 4: Microvascular endothelial cells-derived extracellular vesicles *in-vitro* functionality.

This chapter documents our *in-vitro* functional studies based on findings from previous investigations. In Chapter 2, we established optimized protocols for extracellular vesicle (EV) isolation and demonstrated the scalability of our collection methods. Chapter 3 provided comprehensive EV characterization, with particular emphasis on proteomic analysis that identified specific functional domains where microvascular cell-derived EVs might exert biological effects. As detailed in section 3.2.3, our Gene Ontology analysis highlighted four key functional domains amenable to experimental validation:

1. Wound healing
2. Regulation of angiogenesis
3. Acute inflammatory response
4. Cell-cell adhesion (homotypic)

The chapter is structured into three main sections, each exploring the experimental design, methodology, and results for these functional domains. Due to the physiological interconnection between inflammatory responses and cell-cell adhesion, we address these two domains within a single experimental paradigm.

Importantly, all functional domains investigated relate to the broader physiological process of wound healing and tissue regeneration—a complex multicellular response. During wound healing, fibroblasts respond rapidly upon activation by secreting cytokines and enhancing migration, thus signaling inflammation to the immune system. Concurrently, endothelial cells upregulate adhesion molecules to facilitate leukocyte recruitment to the inflamed site. Following immune system involvement, endothelial cells contribute to tissue regeneration by initiating angiogenesis to restore oxygen and nutrient supply to the healing tissue.

Microvascular endothelial cell-derived EVs likely play significant but previously undocumented roles in these processes, as these vesicles circulate abundantly in the bloodstream and directly interact with inflamed vasculature, immune cells, and vascular-adjacent cell populations such as fibroblasts. As outlined in Chapter 1, this role has been inadequately characterized in the literature. This chapter aims to establish a foundational understanding of these functions within controlled experimental settings.

For all *in vitro* assays described herein, EVs were isolated according to protocols detailed in Chapter 2 and resuspended in 0.2µm-filtered PBS. Based on the differential protein expression patterns observed between UC Bulk and UC+SEC preparations (Figure 11, Chapter 3), both preparation types were tested comparatively. All EV preparations were normalized by nanoparticle concentration using ZetaView NTA analysis as described in Chapter 2. As a negative control, we utilized pooled SEC fractions 2-6, which contained smaller EVs and non-EV contaminants that would normally be present alongside purified EVs in UC Bulk preparations. This approach not only provided a negative control but also allowed us to assess whether combinations of purified EVs with smaller vesicles and contaminants might exhibit synergistic effects not detectable after SEC separation. To maintain optimal biological activity, all EV preparations were used fresh within one week of isolation and stored at 4°C rather than frozen.

4.1 Wound healing assay

Our Gene Ontology analysis identified several proteins with well-documented roles in tissue repair, including ANXA1, ANXA2, ANXA5, FN1, and ITGB1 (Figure 12A). These findings suggested that microvascular endothelial cell-derived EVs might contribute to wound healing processes by delivering these bioactive proteins to injury sites. To test this hypothesis, we conducted wound healing assays using two cell types central to *in vivo* wound healing: dermal fibroblasts and dermal keratinocytes.

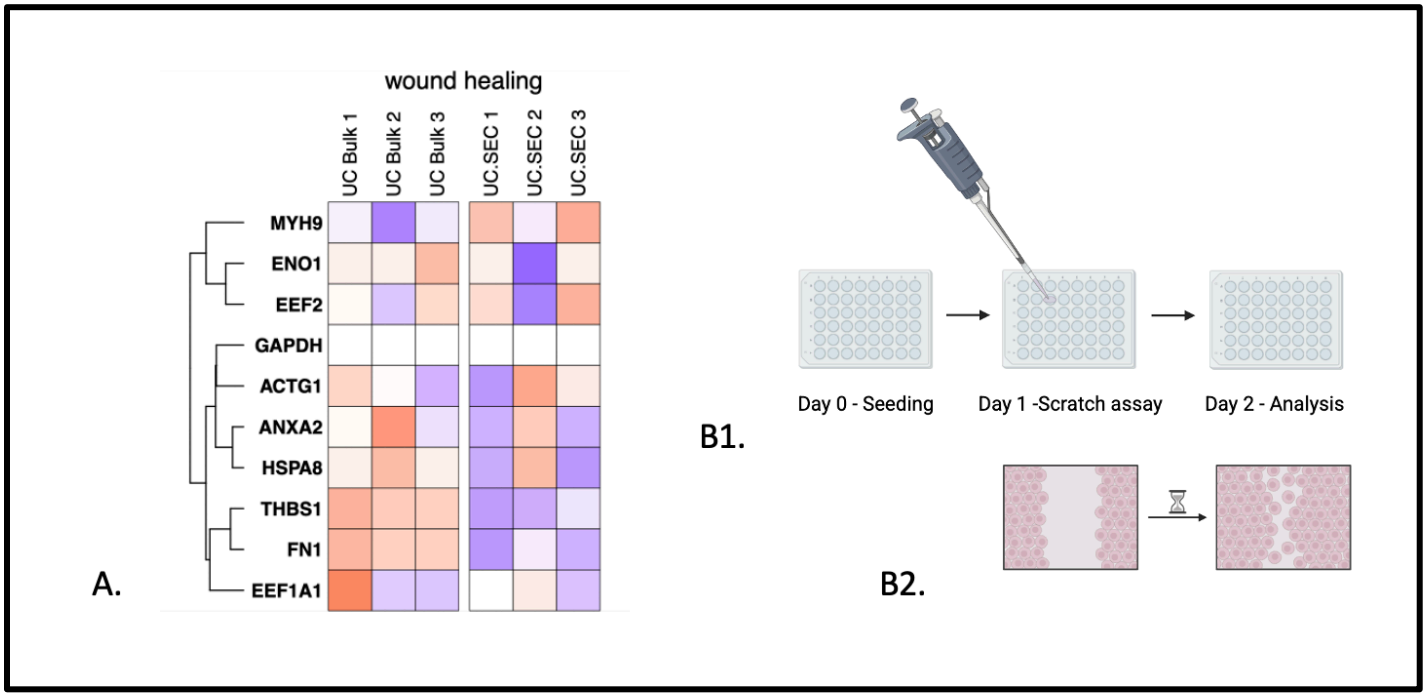

Figure 12: Wound healing assay. (A) Heatmap indicating the initial motivation for conducting the assay (B) Experimental design (B1) Timeline (B2) Wound healing imaging representation.

The experimental design and timeline for the wound healing assays are illustrated in Figure 12B1. For both cell types, we employed a standardized protocol that directly addressed our central research question regarding EV effects on wound closure:

Wound healing protocol: Cells were seeded in 48-well plates in biological triplicates and cultured until confluence. Once confluent, a standardized scratch was created using a 200µL pipette tip, and the culture medium was replaced with one of the following experimental conditions:

1. Control (PBS diluted 1:10 with cell-specific medium)
2. EVs Bulk (EV preparation diluted 1:10 with cell-specific medium)
3. EVs UC+SEC FR1 (EV preparation diluted 1:10 with cell-specific medium)
4. EVs UC+SEC FR2-6 pool (EV preparation diluted 1:10 with cell-specific medium)

Using the position-saving feature of our Leica Thunder microscope, we captured images of each well at 0 hours, centering the scratch in the field of view. Following overnight incubation (16 hours), cells were fixed with 4% paraformaldehyde, permeabilized with 0.1% Triton-X for 5 minutes, blocked with Li-Cor Odyssey blocking buffer in PBS for 1 hour, and stained with phalloidin for 1 hour. Although phalloidin staining is not commonly employed in wound healing assays, we found that it significantly improved wound recovery quantification by reducing background noise from cell debris.

Image processing and analysis: After phalloidin staining, we captured images at identical positions as the 0-hour timepoint to assess wound closure. Images were processed using ImageJ software following a standardized protocol. The initial wound area at 0 hours was quantified by selecting the region of interest (ROI) on each scratch image (Figure 13A). For the 16-hour timepoint, fluorescently-labeled phalloidin-stained images were converted to 8-bit format (Figure 13B), which provided a clear distinction between cell-covered areas (white) and remaining uncovered wound area (black) (Figure 13C). The dark background was measured as the final wound area. We calculated the percentage of wound closure using the following formula:

Wound closure (%) = (1 - (Final wound area / Initial wound area)) × 100

This standardized approach allowed for objective quantification of wound closure across all experimental conditions.

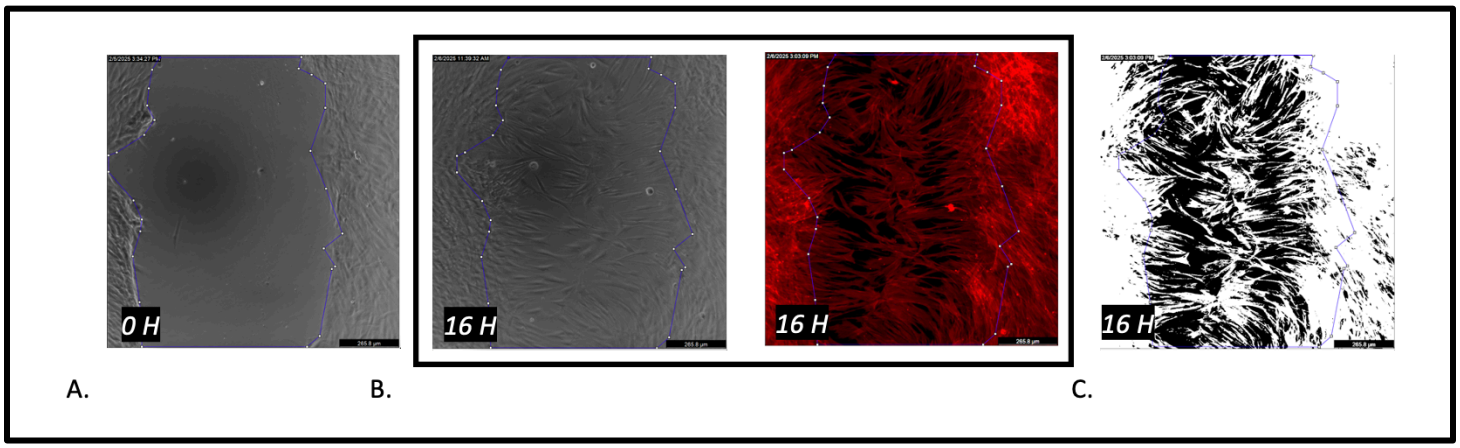

Figure 13: Wound healing assay image processing. (A) Brightfield imaged at 0H, notice the initial wound area marked by blue lines as ROI (B) 16H imaging, notice the difference between brightfield and phalloidin staining. (C) 8-bits conversion images, notice how easy the cells (white) and uncovered wound area (black) can be differentiated.

4.1.2 Dermal fibroblast wound healing closure

We first examined the effects of EVs on human dermal fibroblast adult (HDFa) cells obtained from ATCC (Cat# PCS-201-012). Cells were cultured in Fibroblast Basal Medium (Cat# PCS-201-030) supplemented with Low-serum growth kit (Cat# PCS-201-041). Following the protocol outlined in Figure 12, HDFa were seeded at a density of 100,000 cells per well in 48-well plates and cultured for 24 hours until confluence.

For EV treatment, we prepared a working dilution of 7×10^9 nanoparticles/mL by diluting the master EV preparation 1:10 with Fibroblast Basal Medium. Each well received 300µL of working solution, resulting in a total of 2.1×10^9 nanoparticles per condition and a ratio of 21×10^3 nanoparticles per cell.

The results, presented in Figure 14, demonstrate that microvascular endothelial cell-derived EVs significantly enhanced wound closure in dermal fibroblasts. Qualitative differences are evident in the timeline images (Figure 14A), while quantitative analysis (Figure 14B) revealed that control replicates achieved approximately 37% wound closure, compared to 79% for UC Bulk, 82% for UC+SEC FR1, and 64% for UC+SEC FR2-6 pool. Although statistical analysis did not detect significant differences

between the three EV treatment conditions, the 18% difference in wound closure between UC+SEC FR1 and UC+SEC FR2-6 pool suggests biologically relevant variation in their wound healing capacity.

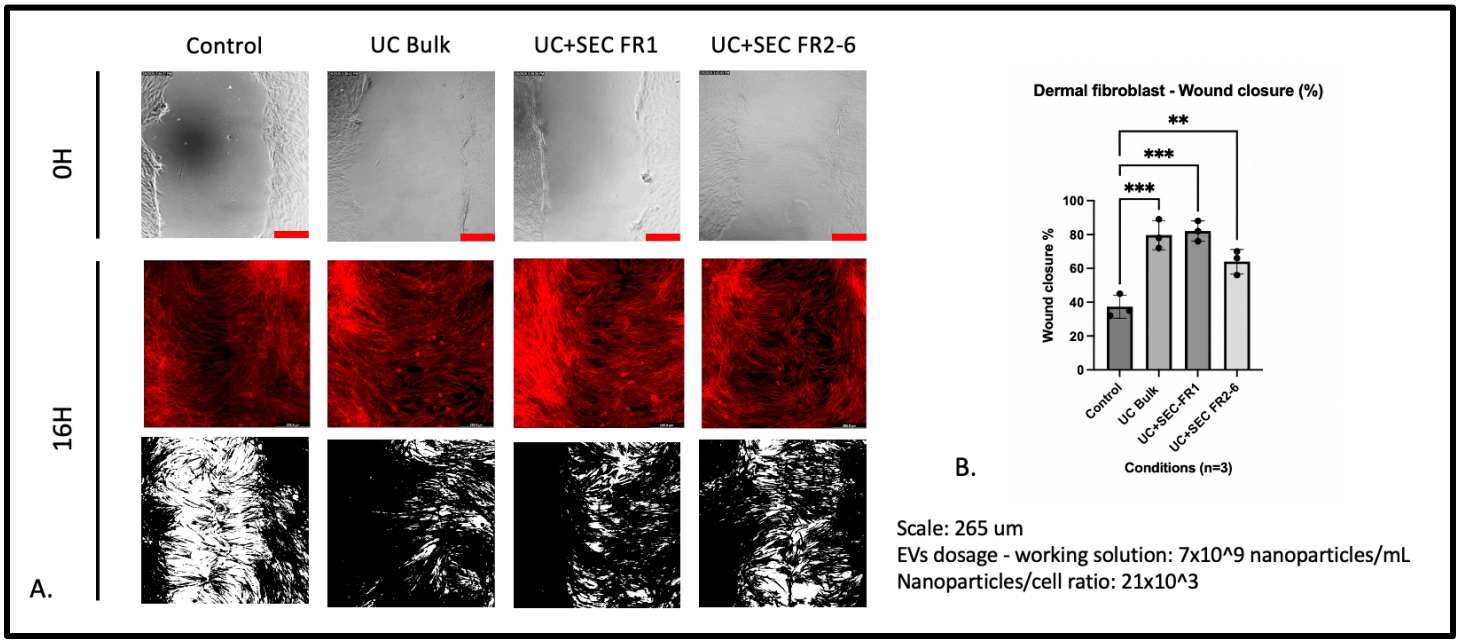

Figure 14: Dermal fibroblast wound healing assay (A) Timeline imaging for the scratch 0H vs. 16H. Notice how the EVs preparation stimulated wound closure (B) ANOVA quantification.

These promising results prompted us to validate our findings in a second cell type integral to the wound healing process.

4.1.2 Dermal keratinocytes wound healing closure

To further validate the wound healing effects observed in fibroblasts, we conducted parallel experiments using primary Human Epidermal Keratinocytes adult (HEKa) from ATCC (Cat# PCS-200-011). We choose Dermal keratinocytes have a similar key role in the process of wound healing as dermal fibroblast [82].

Cells were cultured in Dermal Basal Medium (Cat# PCS-200-030) supplemented with Keratinocyte Growth Kit (Cat# PCS-200-040). Following the established protocol (Figure 12), HEKa were seeded at 25,000 cells per well in 48-well plates and cultured for 72 hours until confluence. This lower seeding density was specifically chosen after we observed poor cell attachment and adaptation at higher densities.

For EV treatment, we prepared a working dilution of 9×10^9 nanoparticles/mL by diluting the master EV preparation 1:10 with Keratinocyte Basal Medium. Each well received 300µL of working solution, resulting in a total of 2.70×10^9 nanoparticles per condition and a ratio of 36×10^3 nanoparticles per cell.

The results of the keratinocyte wound healing assay (Figure 15) corroborate our findings in fibroblasts. All EV conditions significantly enhanced wound closure compared to control (Figure 15A). Quantitative analysis (Figure 15B) demonstrated that control replicates achieved approximately 57%

wound closure, compared to 86% for UC Bulk, 82% for UC+SEC FR1, and 82% for UC+SEC FR2-6 pool. The higher baseline wound closure in keratinocyte controls compared to fibroblasts (57% vs. 37%) may reflect their extended adaptation period (72 hours vs. 24 hours), potentially allowing for improved cellular attachment and migration capacity.

Unlike in fibroblasts, we observed no substantial differences between the three EV treatment conditions in keratinocytes. This suggests that wound healing-promoting factors are present in both the purified EV fraction (FR1) and the smaller EVs/non-EV contaminants (FR2-6 pull), with no apparent synergistic effect when combined (UC Bulk).

Collectively, these results confirm our proteomic findings and demonstrate that microvascular endothelial cell-derived EVs significantly enhance wound closure in two distinct cell types central to dermal wound healing. This functional validation supports our hypothesis that the wound healing-associated proteins identified in our proteomic analysis translate to measurable biological effects.

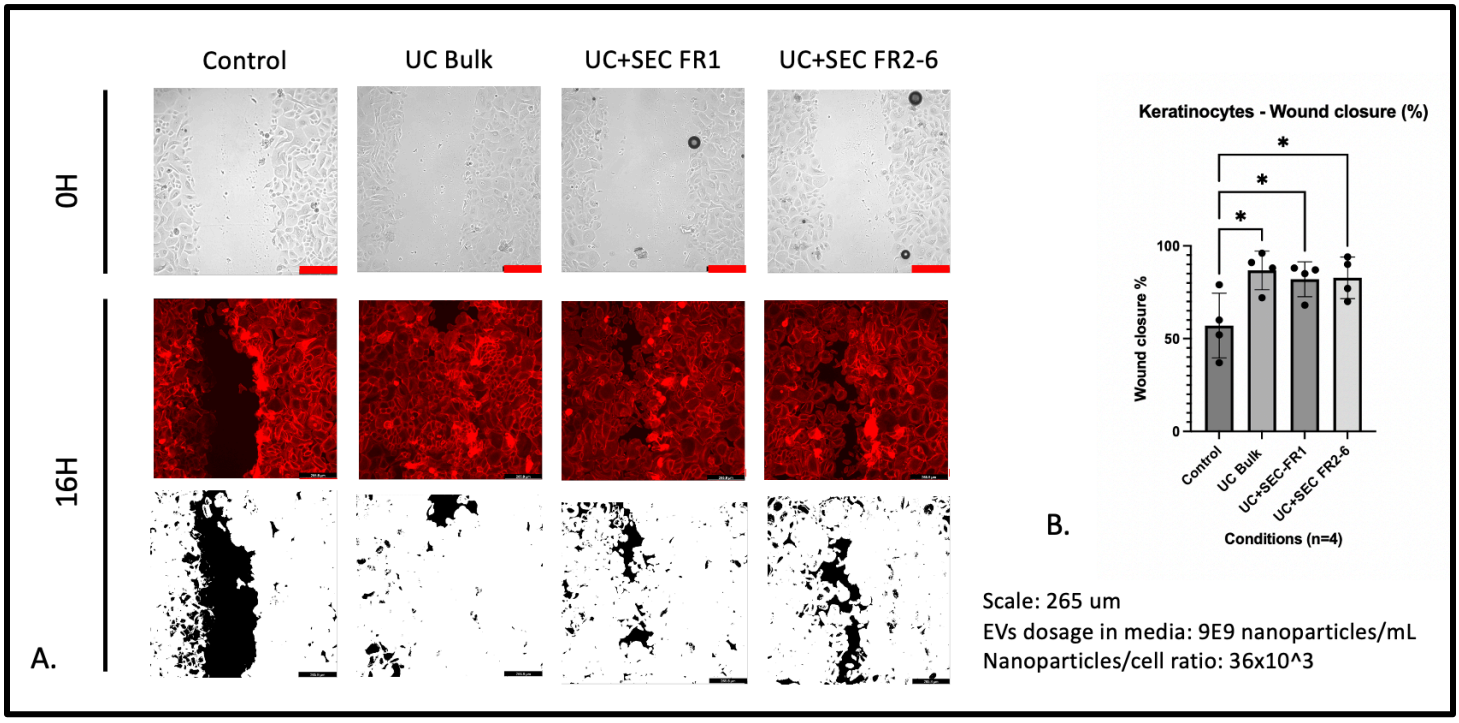

Figure 15: Dermal keratinocytes wound healing assay (A) Timeline imaging for the scratch 0H vs. 16H. Notice how the EVs preparation stimulated wound closure similar to the previous fibroblast assay (B) ANOVA quantification.

4.2 Endothelial cell activation and cell-cell adhesion

4.2.1 Inflamed model. Experimental design and rationale

Endothelial inflammatory activation and intercellular adhesion represent interconnected processes in vascular physiology [83, 84]. As illustrated in Figure 16, endothelial cells respond to inflammatory stimuli by upregulating adhesion molecules such as vascular cell adhesion molecule 1 (VCAM-1/CD106) to recruit circulating leukocytes. Concurrently, these cells undergo cadherin restructuring, loosening intercellular junctions to facilitate immune cell extravasation into damaged tissues.

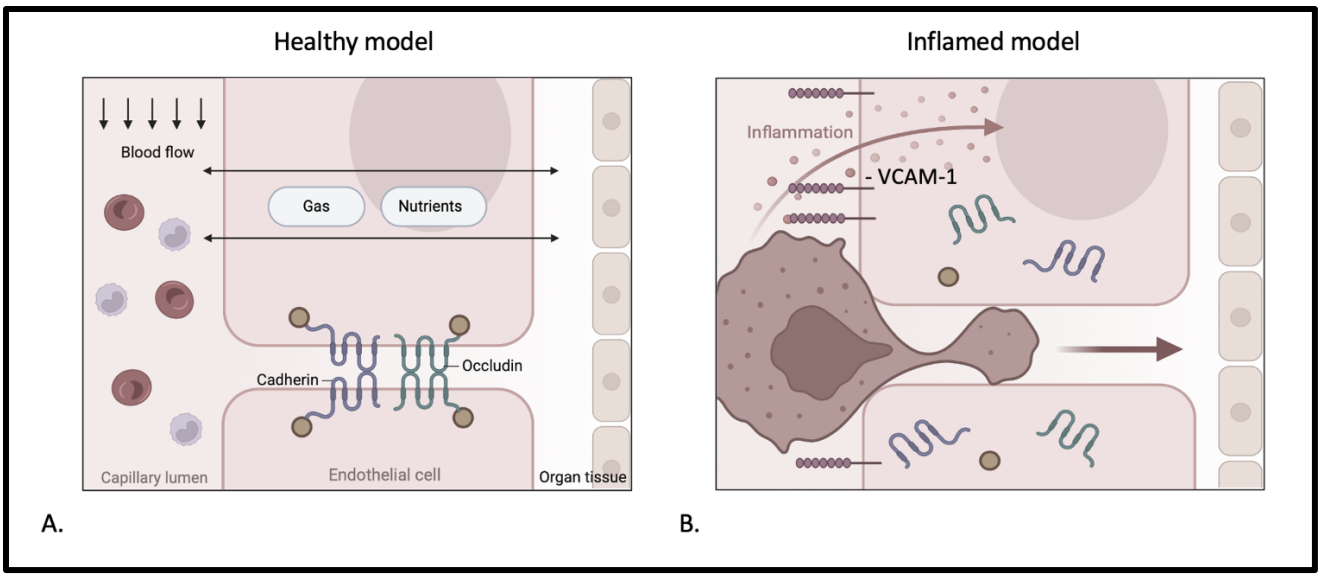

Figure 16: In vivo endothelial cell response to inflammation. (A) Healthy model where endothelial cells are tightly united by junctions that regulate the nutrient and gas exchange to the surrounding tissues (B) inflammatory response, endothelial cells upregulate VCAM-1 to attract blood leukocytes to the inflamed site and downregulate their inter junctions to allow immune cells to access the damaged tissue.

Although *in-vitro* models cannot fully recapitulate the complexity of in vivo inflammatory responses, cultured endothelial cells reliably respond to inflammatory cues by upregulating VCAM-1 and reorganizing intercellular junctions, particularly VE-cadherin (CD144) in microvascular endothelial cells. Our experimental design (Figure 17) was carefully constructed to simultaneously assess EV effects on both inflammatory activation and cell-cell adhesion.

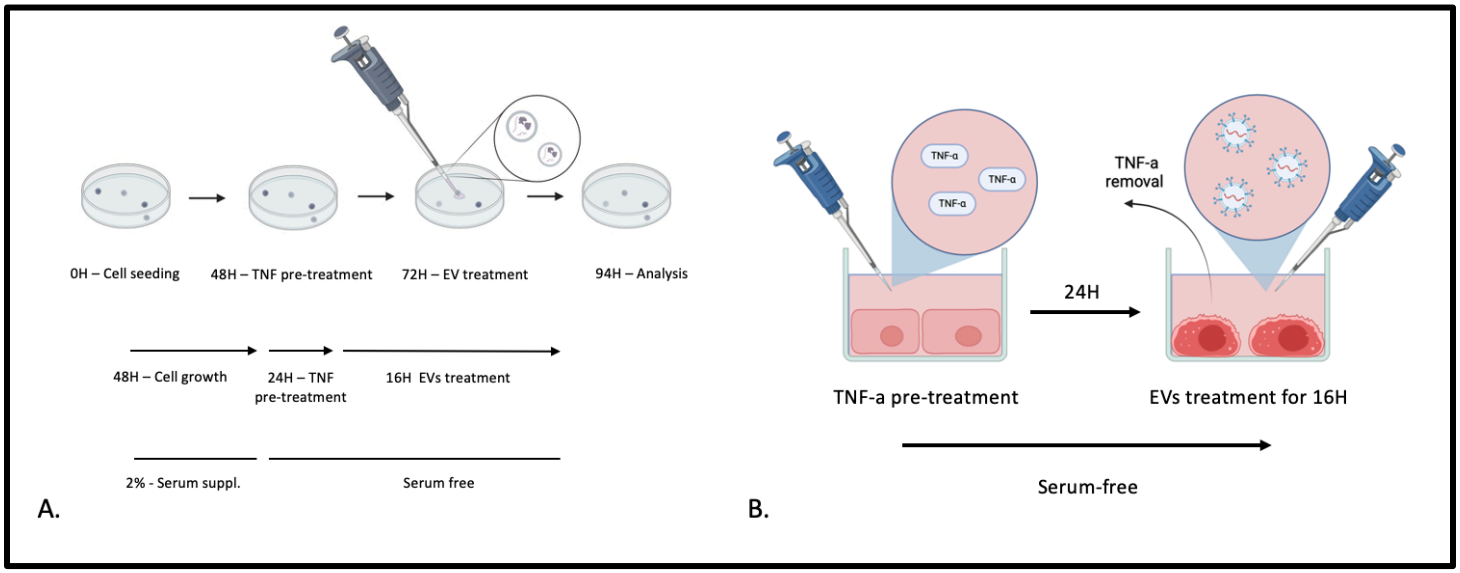

Figure 17: Experimental design testing endothelial cell activation and cell-cell adhesion recovery (A) Experimental timeline (B) Detailed timeline for the TNF-a pretreatment to the EVs co-culture with the cells. Notice that EVs are co-cultured with TNF inflamed cells but after TNF removal giving opportunity to the EVs to either to further stimulate inflammation and cadherin internalization or enhance and support cadherin formation.

This approach allowed us to test two contrasting functional protein populations identified in our proteomic analysis: (1) pro-inflammatory proteins potentially capable of upregulating VCAM-1 and

disrupting intercellular junctions, and (2) cell-cell adhesion proteins that might promote junctional integrity. To provide an opportunity for both protein populations to exert their effects, we developed the sequential treatment protocol illustrated in Figure 17.

The experimental groups were defined as follows:

1. Untreated control (no TNF-α or EV treatment)
2. TNF Control (TNF-α pre-treated, no EV treatment)
3. UC Bulk (TNF-α pre-treated and UC Bulk co-culture)
4. UC+SEC FR1 (TNF-α pre-treated and UC+SEC FR1 co-culture)
5. UC+SEC FR2-6 pool (TNF-α pre-treated and UC+SEC FR2-6 pool co-culture)

Primary juvenile human Dermal Microvascular Endothelial Cells (HDMEC) from PromoCell (Cat# C-12210) were seeded at 100,000 cells/well in 12-well plates and cultured for 48 hours until confluence. Cells were then incubated for 24 hours in serum-free medium containing 2.5 ng/mL TNF-α to induce inflammatory activation. Following this activation period, the TNF-α-containing medium was removed and replaced with fresh medium containing the respective EV preparations. After overnight incubation, cells were analyzed for markers of inflammatory activation and junctional integrity.

This experimental design specifically created a scenario where EVs could interact with already-inflamed endothelial cells in the absence of ongoing inflammatory stimulation. This approach allowed us to determine whether EV-associated proteins would:

1. **Exacerbate inflammation**: Further upregulate VCAM-1 and promote VE-cadherin internalization, essentially continuing the inflammatory program despite TNF-α removal; or
2. **Promote resolution**: Enhance cell-cell adhesion by restoring junctional integrity, potentially counteracting the prior TNF-α effects.

4.2.1 Inflamed model. Results and interpretation

The results of this experimental approach are presented in Figure 18. Immunocytochemistry analysis (Figure 18A) revealed upregulation of VCAM-1 in all EV-treated conditions compared to both untreated controls and TNF-α pre-treated controls. This finding was confirmed by immunoblotting and quantification of the VCAM-1/GAPDH ratio (Figures 18B and 18C), with UC+SEC FR1 treatment demonstrating the most pronounced effect.

Interestingly, while VE-cadherin expression levels did not show significant quantitative differences across treatment conditions, qualitative assessment of intercellular junctions revealed marked differences in junctional architecture. To quantify these differences, we measured the area of intercellular gaps in each condition (Figure 19). The TNF-α control exhibited substantial junctional disruption, with an average gap area of approximately 25 μm^2 per image field—significantly higher than the untreated control and all EV-treated conditions. Most notably, the UC Bulk condition reduced intercellular gap area to approximately 2 μm^2, comparable to the untreated control.

These results reveal an intriguing and somewhat paradoxical effect of microvascular endothelial cell-derived EVs: they simultaneously enhance VCAM-1 expression (a pro-inflammatory marker) while promoting junctional integrity (typically associated with reduced inflammation). This apparent contradiction warrants careful interpretation.

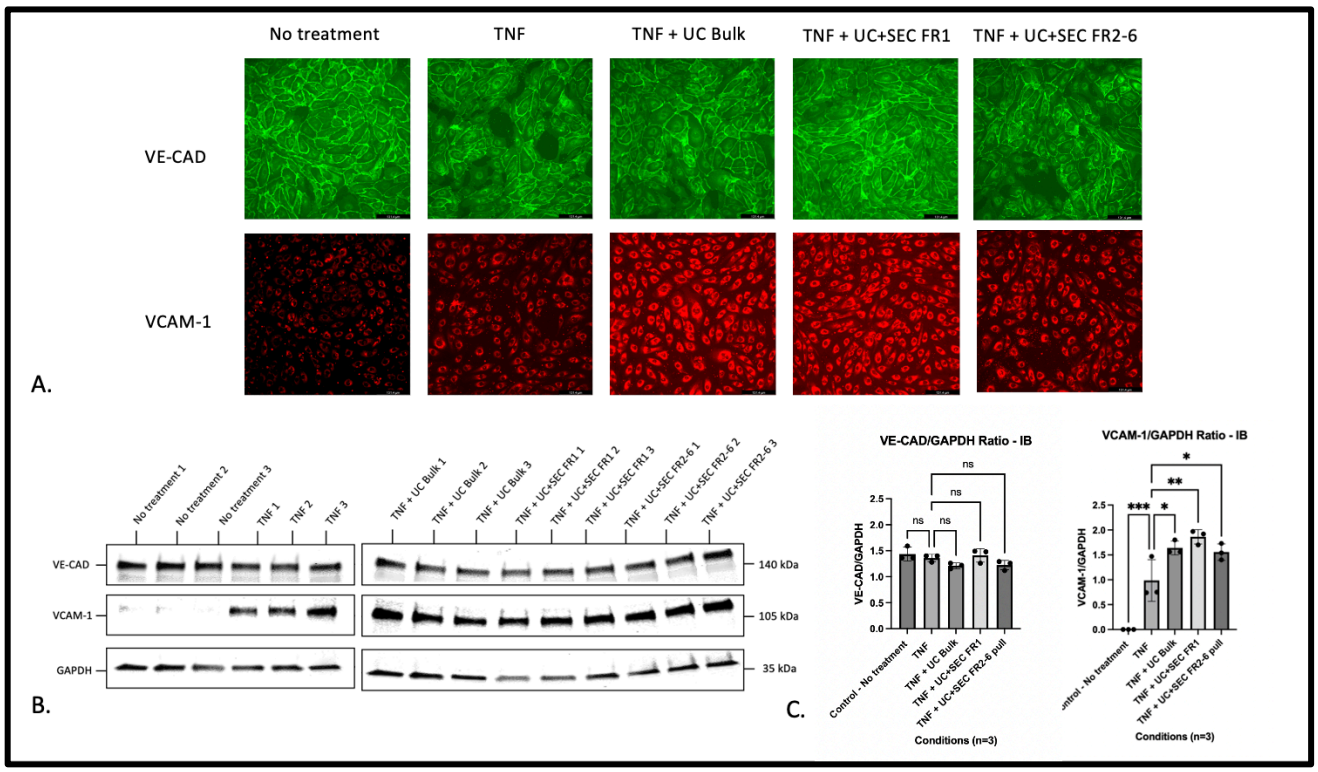

Figure 18: HMEC-1 microvascular endothelial cells-derived extracellular vesicles autocrine effect on inflamed primary dermal endothelial cells. (A) Immunocytochemistry of VE-cadherin (VE-CAD) and VCAM-1. Notice the upregulation on the UC Bulk and UC+SEC conditions. (B) Immunoblotting (C) GAPDH ration quantification for VE-CAD and VCAM-1. Notice the significant difference between all the EVs condition tested and the TNF control, in particular the UC+SEC FR1.

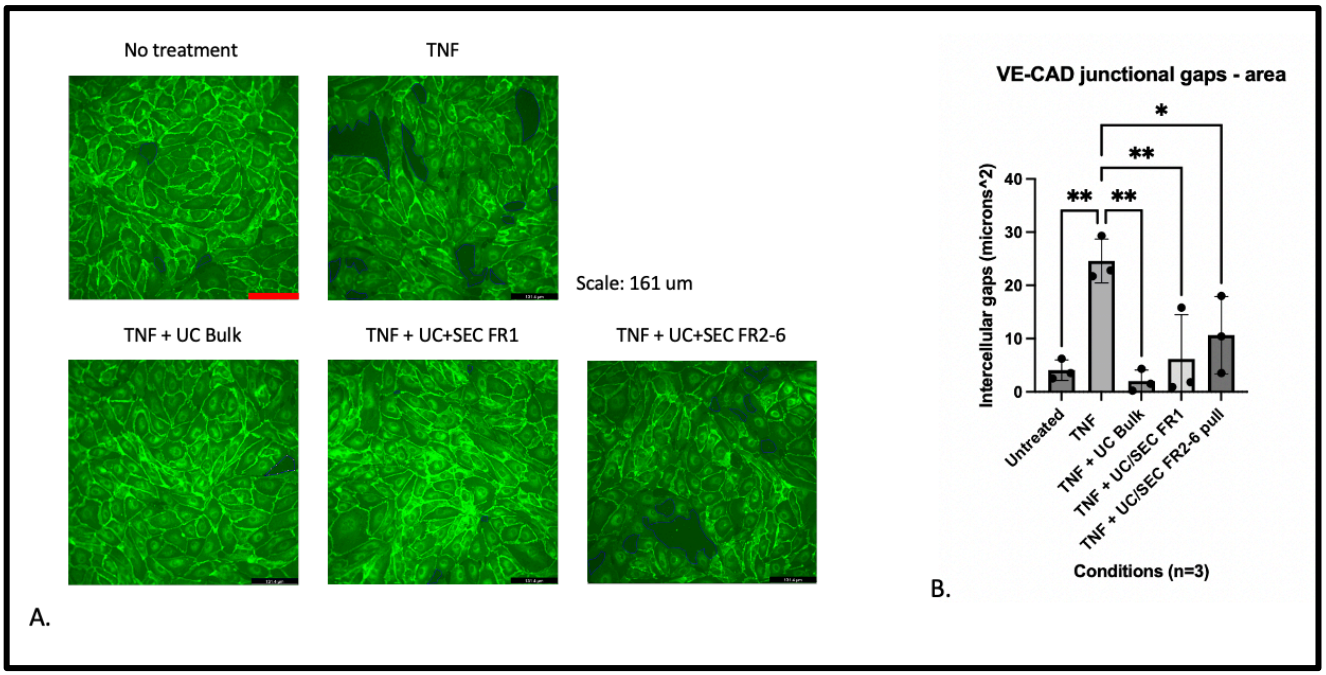

Figure 19: VE-CAD intercellular-gap junction. (A) Immunocytochemistry analysis of VE-CAD. Notice the intercellular gap junctions. (B) ANOVA analysis, Intercellular gaps total area quantification (microns^2).

We propose several potential explanations for these contrasting effects:

1. **Dual functional effect**: The diverse proteomic composition of EVs may simultaneously influence multiple cellular pathways. Pro-inflammatory proteins may activate pathways leading to VCAM-1 upregulation without necessarily affecting VE-cadherin organization, while cell-cell adhesion proteins independently promote junctional integrity. Several proteins identified in our proteomic analysis support this hypothesis:
    - **Annexins (ANXA1, ANXA2, ANXA5)**: Annexin A1 exhibits anti-inflammatory properties [85] while promoting wound repair [86], potentially explaining the maintenance of cell-cell contacts despite inflammatory marker expression.
    - **Thrombospondin-1 (THBS1)**: This novel protein detected in UC+SEC preparations can promote both inflammatory responses [87] and cell adhesion [88].
    - **Integrins (ITGB1, ITGAV)**: These mediate both inflammatory signaling and cell-cell adhesion [89].
2. **Essential nutrient provision**: EVs may deliver essential nutrients or protective factors to endothelial cells, enhancing their viability and morphological integrity under stress conditions. Given that this assay involved 48 hours of serum-free culture with initial TNF-α exposure, EV-associated proteins may have supported basic cellular homeostasis, enabling maintenance of normal junctional architecture despite inflammatory activation. Proteins supporting this hypothesis include:
    - **Heat shock proteins (HSPA8, HSPA1B)**: Identified in our inflammatory protein analysis, these promote cell survival under stress conditions [90].
    - **14-3-3 proteins**: These regulate multiple cellular processes including cell survival [91].
3. **Selective inflammatory programming**: EVs may contain proteins that specifically program endothelial cells to maintain certain inflammatory responses (VCAM-1 upregulation) while simultaneously protecting against barrier dysfunction. Proteins supporting this hypothesis include:
    - **FN1 (Fibronectin)**: Highly abundant in our samples and known to both promote inflammatory responses [92] and strengthen cell-cell adhesion [93].
    - **ANXA2 (Annexin A2)**: Mediates both inflammatory signaling [94] and junctional stability [95].
    - **CD9 and other tetraspanins**: These organize membrane microdomains and could segregate inflammatory signaling from junctional complexes.

These results highlight the complex functionality of EVs, which can modulate multiple cellular processes simultaneously. Unlike targeted pharmaceutical agents or recombinant cytokines, EVs contain diverse bioactive cargoes capable of influencing numerous cellular pathways concurrently. From a therapeutic perspective, our findings suggest a potentially beneficial effect of microvascular endothelial cell-derived EVs: they maintain VCAM-1 expression necessary for immune cell recruitment while preserving endothelial barrier integrity, which could protect against excessive vascular permeability during inflammation.

After the analysis of the presented results, we were keen to explore if the documented role of EVs stimulating VCAM-1 was also functional in a healthy model without pre-inflammation.

4.2.2 Healthy model. Experimental design and rationale

To further investigate the context-dependent effects of microvascular endothelial cell-derived EVs, we developed a parallel experimental paradigm examining EV effects under non-inflammatory conditions. This approach allowed us to determine whether the dual effects observed in our TNF-α model—simultaneous upregulation of VCAM-1 and enhancement of junctional integrity—represented a general property of these EVs or a context-specific response to inflammatory stimuli.

For healthy conditions, we replicated the timeline presented in Figure 17 but substituted PBS for TNF-α during the pre-treatment phase, maintaining serum-free conditions. Figure 20 illustrates the healthy model experimental timeline.

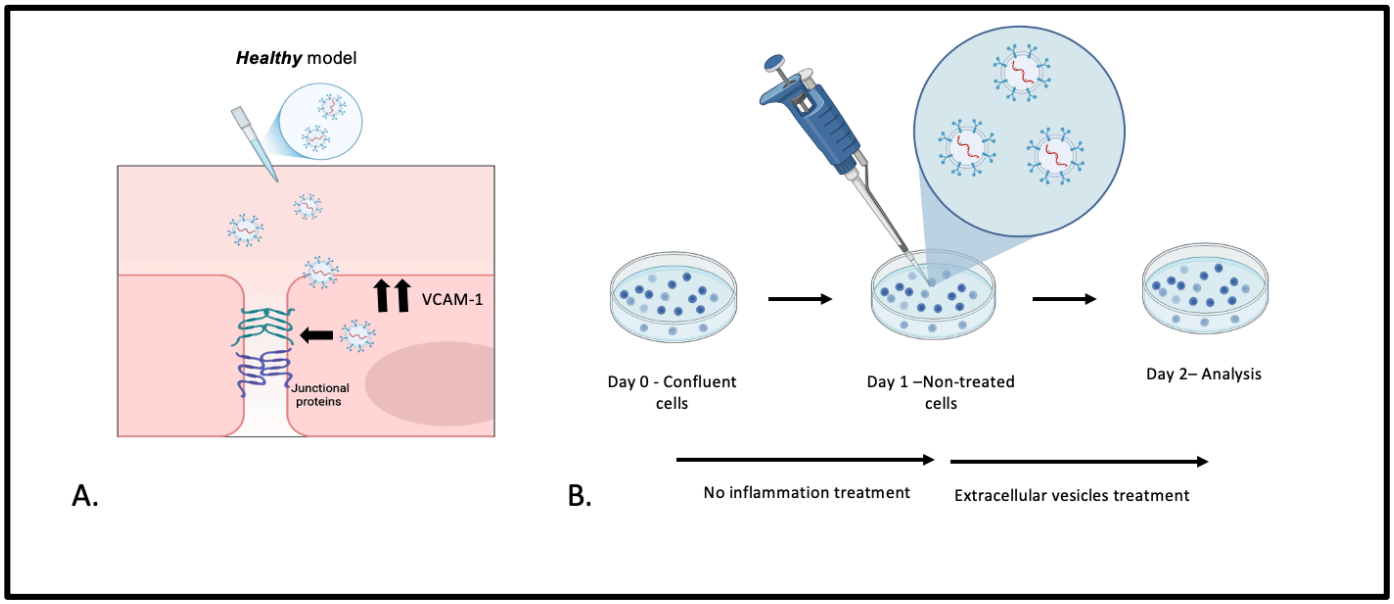

Figure 20: Experimental design testing endothelial cell activation and cell-cell adhesion recovery in a healthy model (A) Graphical representation of intended targets, EVs effect on the regulation of VCAM-1 and Junctional proteins (B) Experimental timeline. Compare with Figure 17A.

This parallel experimental design specifically targeted two key questions:

1. Do microvascular endothelial cell-derived EVs upregulate VCAM-1 expression in the absence of inflammatory priming?
2. Do these EVs modulate junctional protein organization under basal, non-inflammatory conditions?

In contrast to the *pre-inflamed* model, where our experimental design allowed EVs to potentially influence both ongoing inflammatory processes and recovery of junctional integrity, this healthy model isolated conditions to specifically test the pro-inflammatory capability of EVs without the confounding factor of pre-existing inflammation. This comparative approach enabled us to determine whether the effects observed in our TNF-α model represented a response to inflammatory cues or an intrinsic property of these vesicles regardless of cellular context.

4.2.3 Healthy model. Results and interpretation

The results from our healthy model experiments are presented in Figure 21. Immunocytochemistry analysis (Figure 21A) revealed no significant effect on VCAM-1 expression across all experimental conditions. This finding was confirmed by immunoblotting and quantification of the VCAM-1/GAPDH ratio (Figures 21B and 21C), which showed no statistically significant differences between control and EV-treated groups.

Similarly, as shown in Figure 22, we observed no substantial alterations in intercellular junctional organization in any of the EV-treated conditions compared to control. The maintenance of intact junctions was expected in this model, as healthy endothelial cells typically display well-organized VE-cadherin distribution at cell-cell borders.

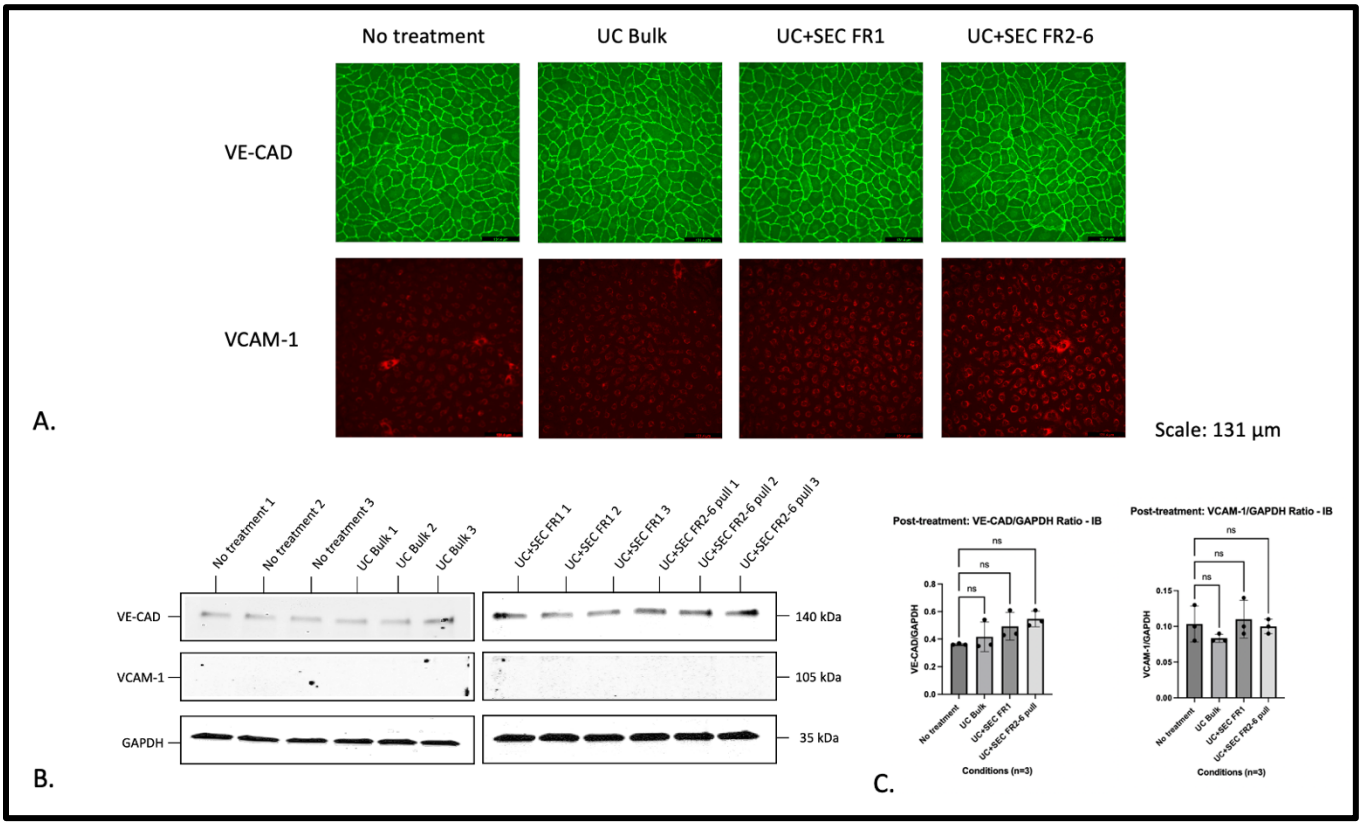

Figure 21: HMEC-1 microvascular endothelial cells-derived extracellular vesicles autocrine effect on healthy primary dermal endothelial cells. (A) Immunocytochemistry of VE-cadherin (VE-CAD) and VCAM-1. Notice the lack of effect on this model compared with Figure 19A(B) Immunoblotting (C) GAPDH ration quantification for VE-CAD and VCAM-1.

Although these results may appear straightforward, they provide crucial insights when contrasted with our findings from the inflammatory model:

1. **Context-dependent responsiveness**: Healthy microvascular endothelium appears insensitive to the regulatory effects of microvascular-derived EVs, as evidenced by the lack of change in VCAM-1 expression or junctional protein organization.
2. **Inflammation-specific signaling**: The inflammatory state of the recipient endothelial cells appears to be a critical determinant of their responsiveness to EV-mediated signaling, suggesting that inflammation may prime cells to respond to vesicle-associated regulatory factors.

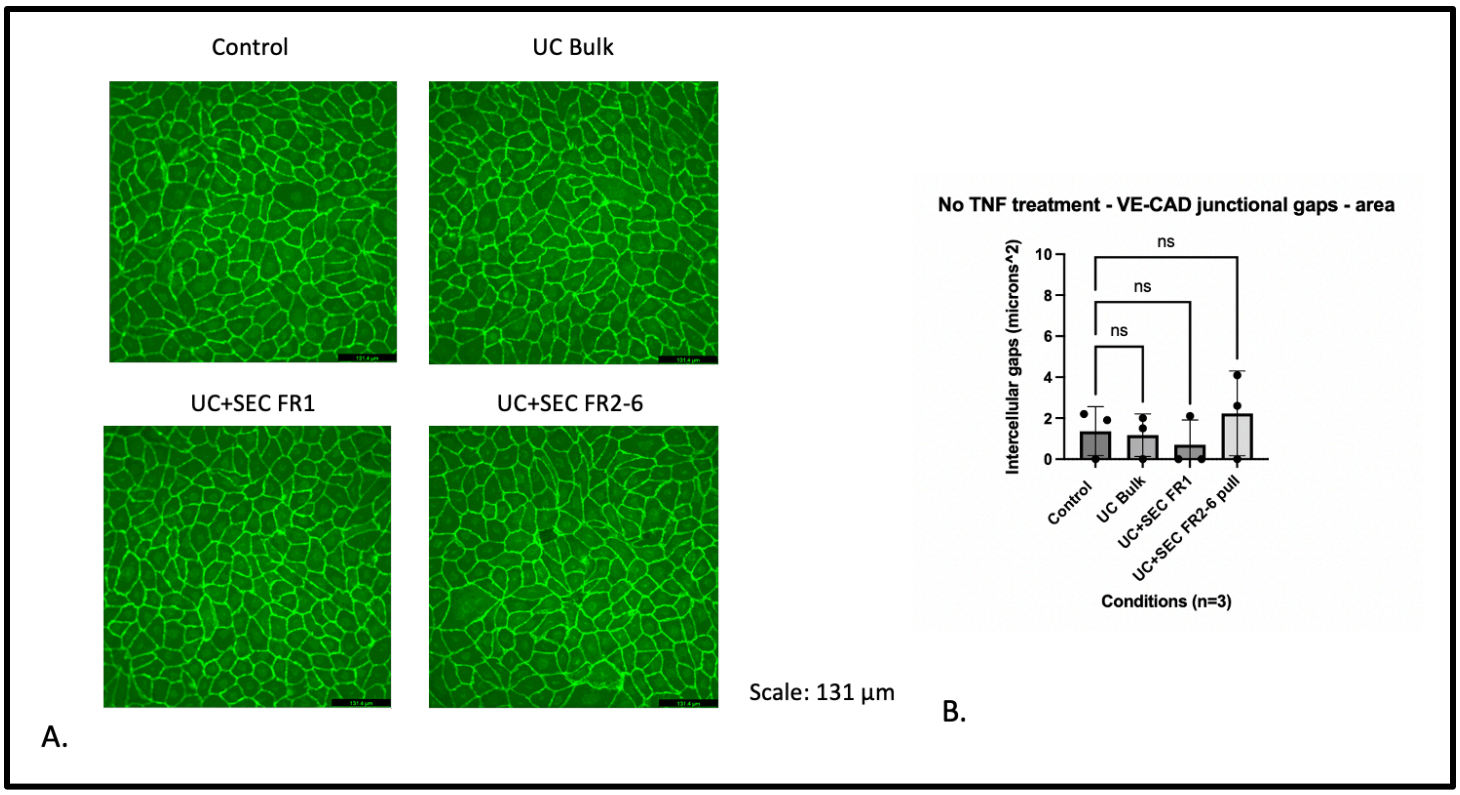

Figure 22: VE-CAD intercellular-gap junction in healthy model. (A) Immunocytochemistry analysis of VE-CAD. Notice the lack of gap junctions in comparison with figure 19A. (B) ANOVA analysis, Intercellular gaps total area quantification (microns^2).

These findings indicate that microvascular endothelial cell-derived EVs exert their effects in an inflammation-dependent manner. This context-specific function represents a previously unrecognized property of these vesicles and suggests a specialized role in modulating vascular responses during inflammatory states rather than under homeostatic conditions.

The physiological relevance of these observations extends beyond our experimental system. In vivo, microvascular endothelial cell-derived EVs are continuously released into the bloodstream and circulate throughout the vasculature. Our results suggest that these vesicles may serve as "surveillance signals" that remain functionally silent under normal physiological conditions but become activated during inflammatory stress, potentially serving as a feedback mechanism to prevent excessive inflammatory responses while maintaining essential barrier functions.

This inflammation-dependent effect aligns with emerging concepts in vascular biology regarding context-specific communication within the vascular microenvironment. During acute inflammatory events (such as tissue injury or infection) or chronic inflammatory conditions (such as diabetes, neurodegenerative disorders, or atherosclerosis), microvascular endothelial cells appear to release EVs that simultaneously support ongoing immune surveillance (through VCAM-1 maintenance) while protecting against excessive vascular permeability (through enhanced junctional integrity).

These results connect directly to our proteomic findings in Chapter 3, where we identified both pro-inflammatory mediators and cell-cell adhesion proteins within the same vesicle population. The differential cellular response to these vesicles based on inflammatory status suggests that

inflammation may trigger specific uptake mechanisms or signaling pathways that enable endothelial cells to selectively respond to this complex EV cargo.

Future studies should investigate whether the differential effects observed between inflammatory and healthy conditions result from distinct EV uptake mechanisms, altered intracellular processing of EV cargo, or inflammation-induced changes in downstream signaling pathways. Additionally, examining whether this inflammation-dependent response extends to other vascular cell types would further elucidate the specificity of this regulatory mechanism within the vascular microenvironment.

4.3 Regulation of angiogenesis assay

Our final functional assessment focused on examining the angiogenic regulatory potential of microvascular endothelial cell-derived EVs. The previous results documenting the effect of the EVs on the regulation of VE-cadherin was a positive indication that they may have an effect on angiogenesis as VE-cadherin-associated phosphorylation and internalization is increased during angiogenesis [96]. This investigation was also directly motivated by our proteomic findings, which identified several proteins with established roles in angiogenesis regulation (Figure 20A). Key proteins included VEGFA, a potent pro-angiogenic factor; thrombospondin-1 (THBS1), which has context-dependent pro- and anti-angiogenic properties; integrin subunits like ITGAV, which mediate endothelial cell adhesion during vessel formation; and angiopoietin-2 (ANGPT2), which regulates vascular remodeling and sprouting.

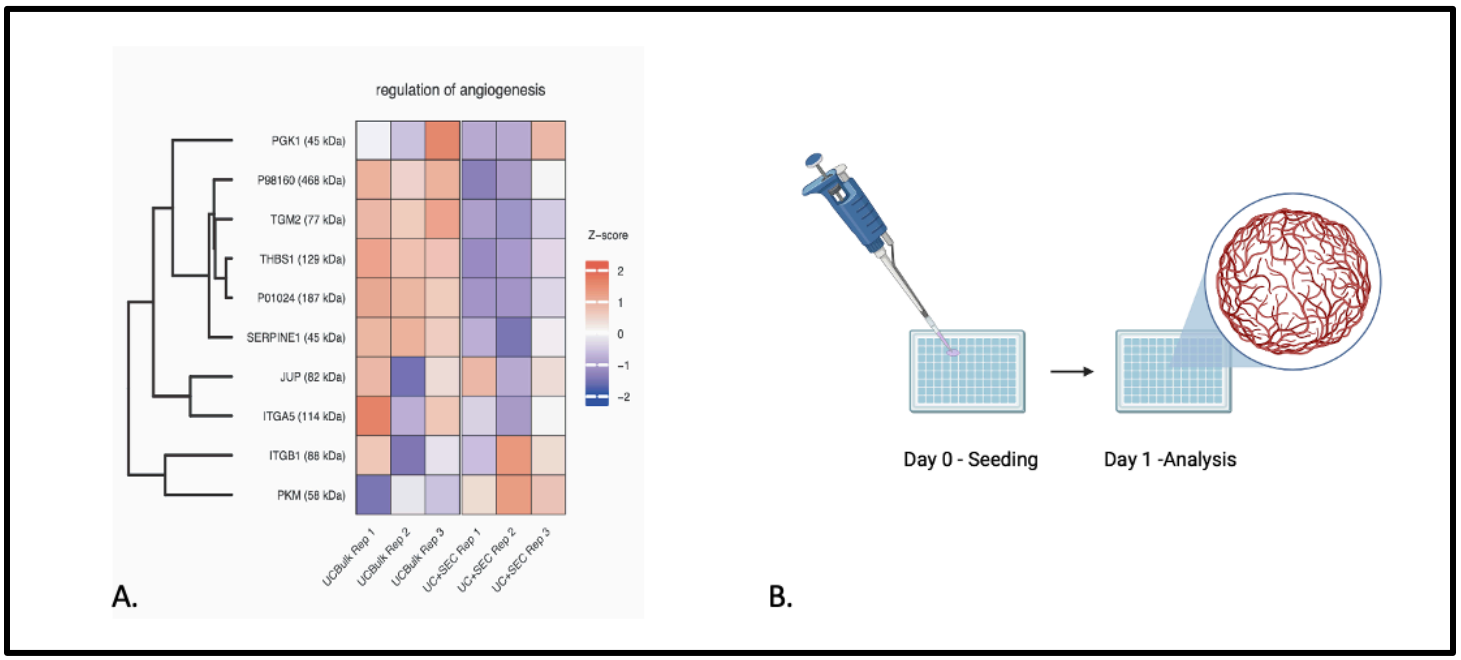

Figure 20: Experimental design for regulation of angiogenesis. (A) Proteomic population that stimulated the experimental design (B) Experimental timeline.

For this assay, we utilized a three-dimensional Matrigel-based approach to more closely recapitulate the complex spatial organization of angiogenesis in vivo. Primary HDMEC cells, previously used in our endothelial activation studies, served as our cellular model. The MCDB131 F15 medium with 2% serum supplementation, developed in Chapter 2, adequately supported 3D cell growth throughout the 16-hour experimental period.

As illustrated in Figure 20B, we pre-coated 96-well plates with 50 µL of pre-chilled Matrigel and allowed polymerization at 37°C for 45 minutes. Following gel formation, 15,000 cells/well were seeded in 100 µL of culture medium containing either PBS (control) or EV preparations at a 1:10 dilution. The experimental groups were:

1. Untreated control (no EV treatment)
2. UC Bulk (UC Bulk co-culture)
3. UC+SEC FR1 (UC+SEC FR1 co-culture)
4. UC+SEC FR2-6 pool (UC+SEC FR2-6 pool co-culture)

After overnight incubation, we captured brightfield images of the resulting tubular networks and quantified angiogenic parameters using an ImageJ macro adapted from Carpentier et al. 2020 [97]. This analytical approach provided over 15 quantitative variables describing network formation; however, for clarity and interpretability, we focused on two primary metrics: (1) Number of master junctions, representing connecting points between tubular structures, and (2) Number of meshes, quantifying complete network loops formed by the angiogenic sprouts.

Figure 21 presents the results of our angiogenesis assay. While qualitative assessment of brightfield images (Figure 21A) suggested modest enhancement of network formation in EV-treated conditions, quantitative analysis (Figure 21B) revealed that these differences did not reach statistical significance. We observed a trend toward increased master junctions and mesh formation in UC+SEC FR1-treated cultures compared to controls, but the variability between replicates prevented definitive conclusions regarding EV-mediated angiogenic regulation.

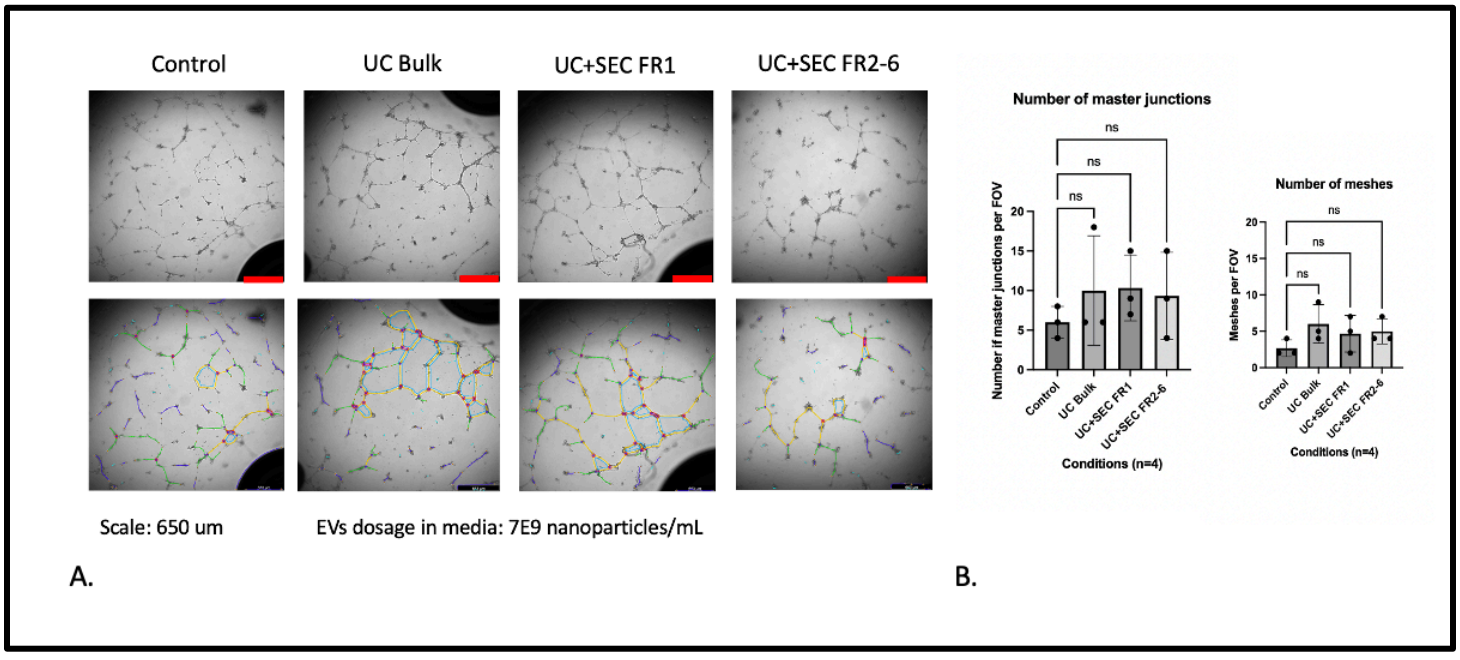

Figure 21: Angiogenesis assay. (A) Brightfield imaging of the cells in Matrigel (B) Angiogenesis quantification output, number of master junctions (Yellow on A) and number of meshes (Blue on A).

To further explore potential dose-dependent effects, we tested an increased EV concentration (1:5 dilution); however, this modification similarly failed to produce statistically significant enhancements in angiogenic parameters.

The discrepancy between our proteomic findings and functional results warrants careful consideration. Several methodological factors may explain the limited angiogenic response observed:

1. **Delivery challenges in 3D culture**: Unlike our wound healing and endothelial activation assays, where EVs were applied to pre-attached monolayer cultures, the 3D Matrigel system presents significant barriers to EV-cell interaction. When cells and EVs are co-seeded onto Matrigel, endothelial cells rapidly migrate and reorganize while EVs may remain predominantly at the gel surface, limiting cellular uptake and cargo delivery. This spatial separation likely reduces the effective EV dose reaching cells embedded within the forming tubular structures.
2. **Competition with media components**: Our optimized MCDB131 F15 medium, developed in Chapter 2, contains several growth factors and supplements that themselves promote angiogenesis, including bFGF (10 ng/mL), ANG1 (5 ng/mL), and ANG2 (2.5 ng/mL). These concentrations substantially exceed the amounts of corresponding proteins present in our EV preparations, potentially masking subtle EV-mediated effects. Indeed, our attempts to establish a positive control using recombinant ANG2 (1 ng/mL and 5 ng/mL) failed to demonstrate significant enhancement beyond the basal medium conditions, confirming this hypothesis.
3. **Temporal considerations**: The 16-hour timepoint, while standard for Matrigel angiogenesis assays, may not represent the optimal window to observe EV-mediated effects, which could require longer exposure for meaningful modulation of tubular network formation.
4. **EV stability in 3D matrix**: EVs may experience limited mobility within the Matrigel matrix, restricting their diffusion to cells not in immediate proximity to the vesicles.

Alternative approaches that might better capture EV-mediated angiogenic regulation include:

1. **Pre-conditioning protocol**: Treating endothelial cells with EVs prior to seeding on Matrigel could enhance cellular uptake of vesicles and their bioactive cargo before the spatial constraints of 3D culture are established.
2. **EV embedding within Matrigel**: Incorporating EVs directly into the Matrigel matrix before polymerization could improve vesicle distribution throughout the 3D environment. However, this approach risks compromising EV integrity due to the temperature shifts and potential denaturation during the polymerization process.
3. **Time-course analysis**: Extending the observation period or implementing multiple timepoints might reveal EV-mediated effects that emerge later in the angiogenic process.
4. **Alternative reduced-growth factor media**: Developing a minimal medium that supports basic endothelial survival but provides limited angiogenic stimulation could create a more sensitive background for detecting EV-mediated effects.

Despite the lack of statistical significance, our findings do not necessarily contradict the angiogenic regulatory potential suggested by our proteomic analysis. Rather, they highlight the methodological challenges inherent in demonstrating subtle biological modulation in complex 3D systems where multiple signaling pathways operate simultaneously. The trends observed, particularly with UC+SEC FR1 preparations, warrant further investigation using refined experimental approaches specifically designed to overcome the limitations identified here.

4.4 Final remarks on the *in-vitro* functional effects of microvascular endothelial cells EVs

This chapter has provided substantial experimental evidence validating the functional relevance of microvascular endothelial cell-derived EVs in several biological processes predicted by our proteomic analysis in Chapter 3. Our findings both confirm existing knowledge and reveal novel insights into the

complex roles these vesicles play in intercellular communication within the vascular microenvironment.

Our investigation into wound healing demonstrated a clear and consistent pro-migratory effect of microvascular endothelial cell-derived EVs on both dermal fibroblasts and keratinocytes—key cellular mediators of tissue repair. The significant enhancement of wound closure, with up to 45% improvement compared to control conditions, validates our proteomic identification of wound healing-associated proteins such as annexins, fibronectin, and integrins in these EVs. This finding suggests potential therapeutic applications for these vesicles in promoting tissue repair, particularly in conditions characterized by impaired wound healing.

Perhaps the most intriguing discovery emerged from our examination of EVs' effects on endothelial inflammatory activation and junction integrity. We observed a seemingly paradoxical response wherein EVs simultaneously upregulated inflammatory markers (VCAM-1) while enhancing junctional integrity—effectively maintaining the endothelium's immunological surveillance function without compromising barrier function. This previously undocumented dual effect highlights the complex multi-pathway signaling capacity of EVs and suggests they may play a nuanced role in vascular homeostasis during inflammatory responses. The ability to maintain robust cell-cell junctions despite ongoing inflammatory signaling could represent an adaptive mechanism that prevents excessive vascular permeability during inflammation.

Our angiogenesis assay, while not yielding statistically significant results, revealed trends suggesting potential pro-angiogenic effects of these EVs. The limitations encountered in this experimental approach—particularly the challenge of delivering EVs effectively in 3D culture conditions—highlight important methodological considerations for future studies. Alternative approaches, such as pre-conditioning cells with EVs before 3D culture or developing longer-duration assays, may better capture the angiogenic regulatory capacity of these vesicles.

Several significant technical advances were achieved through these functional studies:

1. **Development of standardized EV dosing protocols**: We established reproducible nanoparticle-to-cell ratios (21-36×10^3 nanoparticles/cell) that consistently elicited biological responses across different cell types.
2. **Optimization of image analysis methodologies**: Our adaptation of phalloidin staining for wound healing quantification and detailed analysis of intercellular gap areas for junction integrity assessment provide improved analytical approaches for these common assays.
3. **Comparative analysis of isolation methods**: By testing EVs isolated through different methods (UC Bulk vs. UC+SEC), we demonstrated that isolation methodology influences not only vesicle purity but also their functional properties, with purified fractions (UC+SEC FR1) showing enhanced activity in several assays.

Collectively, these findings address the third research question posed in Section 1.4: "How do microvascular endothelial cell-derived extracellular vesicles regulate vascular remodeling processes within the microvascular niche?" We have demonstrated that these EVs mediate multiple facets of vascular remodeling, including wound healing, inflammatory signaling, and barrier function regulation. The functional effects observed align with our proteomic characterization, confirming that the cargo proteins identified in Chapter 3 translate to meaningful biological activities.

These results establish a foundation for future investigations into the therapeutic potential of microvascular endothelial cell-derived EVs. Their ability to promote wound healing while preserving vascular barrier function suggests applications in conditions characterized by endothelial dysfunction, excessive inflammation, or impaired tissue repair. Moreover, the methodological approaches developed here provide a framework for further functional characterization of these complex biological mediators in both physiological and pathological contexts.

Chapter 5: Final Remarks and Conclusions

This dissertation has explored the isolation, characterization, and functional analysis of microvascular endothelial cell-derived EVs. Through a systematic approach encompassing methodological optimization, comprehensive proteomic profiling, and targeted functional assays, we have addressed significant knowledge gaps in our understanding of how these vesicles contribute to vascular homeostasis and remodeling. This final chapter synthesizes our key findings, discusses their implications within the broader scientific context, acknowledges methodological limitations, and outlines promising directions for future research.

5.1 Addressing Knowledge Gaps in Microvascular Endothelial Cell-Derived EVs

In Chapter 1, we identified several critical knowledge gaps regarding microvascular endothelial cell-derived EVs. Our research has made substantial progress in addressing these limitations:

5.1.1 Isolation Methodology

The first significant knowledge gap concerned the technical challenges associated with isolating and purifying microvascular endothelial cell-derived EVs. As documented in Chapter 1, previous studies [7, 10] faced substantial limitations due to serum contamination and non-standardized isolation protocols. Our research directly addressed this gap through the development of:

1. **Low-serum culture conditions:** We established the F15 media formulation that enables the culture of HMEC-1 cells with just 2% serum supplementation while maintaining endothelial phenotype (Chapter 2). This represents a critical advancement over conventional high-serum conditions, reducing potential serum-derived EV contamination—a major confounder in previous studies.
2. **Optimized combination methodology:** By systematically comparing isolation methods, we demonstrated that the combination of ultracentrifugation with size exclusion chromatography (UC+SEC) yields EV preparations with superior purity compared to ultracentrifugation alone. This was confirmed through multiple characterization approaches, including cryo-EM visualization (Chapter 3), which revealed substantially reduced non-vesicular debris in UC+SEC preparations.
3. **Scalable production protocol:** We established a reproducible methodology for generating highly purified EVs at yields exceeding 2×10^10 nanoparticles per isolation, addressing a critical technical barrier to comprehensive proteomic and functional analyses.

These methodological advancements constitute a significant contribution to the field, providing researchers with optimized protocols for obtaining microvascular endothelial cell-derived EVs with minimal contamination and sufficient yield for downstream applications.

5.1.2 Proteomic Characterization

The second major knowledge gap involved the incomplete proteomic characterization of microvascular endothelial cell-derived EVs. Previous studies [3, 5, 15, 98-101] had provided limited insight into the cargo composition of these vesicles, particularly those derived under physiologically relevant conditions. Our research has substantially expanded this knowledge base through:

1. **Comprehensive proteomic analysis:** Our shotgun proteomic approach identified 316 proteins in UC+SEC preparations, including 70 proteins not previously documented in microvascular endothelial cell-derived EVs (Chapter 3). This represents the most comprehensive characterization of these vesicles to date under low-serum conditions.
2. **Identification of functionally relevant cargo:** Gene Ontology analysis revealed significant enrichment for proteins involved in wound healing, cell-cell adhesion, angiogenesis regulation, and inflammatory responses. This functional mapping provides crucial insights into the potential biological roles of these EVs in vascular homeostasis and pathology.
3. **Method-dependent proteome differences:** By comparing the proteomes of EVs isolated through different methods, we demonstrated that isolation methodology significantly influences protein detection, with UC+SEC enabling identification of numerous proteins not detectable in UC Bulk preparations. This finding has important implications for interpreting previous studies that relied exclusively on ultracentrifugation [10, 86, 102].

Our proteomic characterization has transformed the understanding of microvascular endothelial cell-derived EV cargo, revealing a complex protein signature with direct relevance to vascular biology.

5.1.3 Functional Characterization

The third and perhaps most significant knowledge gap concerned the limited functional characterization of microvascular endothelial cell-derived EVs within the microvascular niche. Previous studies had provided minimal insight into how these vesicles influence neighboring cells and modulate vascular remodeling processes. Our research has substantially advanced this understanding through:

1. **Wound healing enhancement:** We demonstrated that microvascular endothelial cell-derived EVs significantly promote wound closure in both dermal fibroblasts and keratinocytes (Chapter 4), with up to 45% improvement compared to control conditions. This finding provides the first direct evidence that these vesicles actively contribute to tissue repair mechanisms.
2. **Context-dependent dual regulation of endothelial function**: Our comparative experiments with both inflamed and healthy endothelial models revealed a previously undocumented context-dependent effect wherein EVs simultaneously upregulate inflammatory markers (VCAM-1) while enhancing junctional integrity, but only in cells that have been previously exposed to inflammatory stimuli (Chapter 4). This inflammation-dependent response suggests a specialized role in maintaining vascular barrier function during inflammatory states without affecting healthy vasculature—a sophisticated regulatory mechanism not previously attributed to these vesicles.
3. **Inflammation-specific signaling:** The striking contrast between EV effects on TNF-α-stimulated versus healthy endothelial cells provides compelling evidence that the inflammatory state of recipient cells is a critical determinant of their responsiveness to EV-mediated signaling. This suggests that inflammation may prime cells to respond to vesicle-associated regulatory factors, effectively creating a "surveillance system" that becomes active only during inflammatory stress.
4. **Cell type-specific responses:** By examining EV effects on multiple cell types, we demonstrated that the functional impact of these vesicles varies depending on the recipient cell population, highlighting the context-dependent nature of EV-mediated intercellular communication.

These functional insights address a critical gap in our understanding of how microvascular endothelial cell-derived EVs contribute to vascular homeostasis and remodeling within the microvascular niche. The discovery of inflammation-dependent effects is particularly significant, suggesting a level of biological sophistication in EV-mediated signaling that allows for selective modulation of vascular responses based on microenvironmental context.

5.2 Integration with Current Literature and Novel Contributions

Our findings both confirm and extend current knowledge regarding microvascular endothelial cell-derived EVs, making several novel contributions to the field:

5.2.1 Methodological Advancements

Our systematic comparison of isolation methodologies builds upon previous work by Xu et al. [73] and others who have highlighted the limitations of ultracentrifugation-only approaches. However, our specific application to microvascular endothelial cells under low-serum conditions represents a novel contribution. The observation that SEC purification following ultracentrifugation enables detection of proteins not identified in UC Bulk preparations aligns with recent studies by Takov et al. [76], who demonstrated similar enhanced detection in plasma-derived EVs.

Particularly significant is our development of optimized low-serum culture conditions for HMEC-1 cells. While previous studies had suggested these cells could be cultured under reduced serum conditions [24], our systematic optimization of media components—particularly the identification of angiopoietins ANG1 and ANG2 as critical factors and the unexpected negative effect of hypoxanthine—provides novel insights into the nutritional requirements of microvascular endothelial cells for EV production.

5.2.2 Novel Proteomic Insights

Our proteomic analysis identified 70 proteins not previously documented in microvascular endothelial cell-derived EVs, including 30 proteins exclusively detected in UC+SEC preparations. The identification of Thrombospondin-1 (THBS1), Desmoplakin (DSP), and Galectin-3-binding protein (LGALS3BP) is particularly noteworthy given their established roles in vascular remodeling and wound healing.

These findings extend the previous work by de Jong et al. [9], who provided the first proteomic analysis of HMEC-1-derived EVs but focused primarily on comparing protein populations between EVs from cells cultured under different stress conditions. Our analysis complements this earlier work by providing a more comprehensive proteome under low-serum conditions and with enhanced purification methodology.

The identification of diverse functional protein clusters aligns with recent studies by Cantaluppi et al. [15] and others who have demonstrated that endothelial-derived EVs contain cargo capable of modulating multiple biological processes simultaneously. However, our specific mapping of microvascular endothelial cell-derived EV proteins to wound healing, inflammatory regulation, and cell-cell adhesion pathways represents a novel contribution to the field.

5.2.3 Functional Significance

I. Microvascular endothelial cells-derived EVs on microvascular inflammatory activation

Perhaps our most significant contribution lies in demonstrating the functional impact of microvascular endothelial cell-derived EVs on multiple cell types relevant to vascular biology. The observation that these vesicles substantially enhance wound closure in both fibroblasts and keratinocytes extends previous findings by Cantaluppi et al. [5], who demonstrated that endothelial progenitor cell-derived EVs enhance angiogenesis of pancreatic islets. Our work expands this concept to demonstrate that microvascular endothelial cell-derived EVs directly promote wound healing in non-endothelial cell populations.

The discovery of inflammation-dependent effects represents a groundbreaking contribution to our understanding of EV-mediated signaling. By conducting parallel experiments in both inflamed and healthy endothelial models, we uncovered a sophisticated context-specific response pattern that has not been previously documented in the literature. The dual effect of EVs on endothelial inflammatory activation and junction integrity—occurring exclusively in cells with prior inflammatory exposure—suggests that these vesicles function as specialized modulators of vascular responses during inflammatory states.

This contextual responsiveness aligns with recent work by by Boyer et al. [3], who demonstrated that endothelial cell-derived EVs alter vascular smooth muscle cell phenotype through high-mobility group box (HMGB) proteins. Their findings revealed that endothelial-derived EVs can stimulate VCAM-1 expression and enhance leukocyte adhesion in vascular smooth muscle cells while also inducing protein synthesis and senescence markers. This suggests a ***complex regulatory role*** of endothelial-derived EVs that extends beyond simple pro- or anti-inflammatory functions, potentially coordinating tissue responses across multiple cell types during vascular remodeling.

The inflammation-dependent nature of EV effects suggests an elegant biological mechanism whereby these vesicles serve as "surveillance signals" that remain functionally silent under normal physiological conditions but become activated during inflammatory stress. This provides a potential feedback mechanism to prevent excessive inflammatory responses while maintaining essential barrier functions. Such contextual responsiveness represents a previously unrecognized level of sophistication in EV-mediated intercellular communication within the vascular microenvironment.

The physiological significance of this context-dependent signaling extends to various inflammatory conditions affecting the microvasculature, including sepsis, acute respiratory distress syndrome, and chronic inflammatory disorders. Our findings suggest that endothelial-derived EVs may constitute an intrinsic regulatory mechanism that helps preserve vascular integrity during inflammatory challenges—a function of particular importance in organs with specialized vascular barriers such as the brain, lung, and kidney.

Furthermore, our identification of specific proteins within these EVs that could mediate their dual effects—including annexins (ANXA1, ANXA2, ANXA5), thrombospondin-1 (THBS1), and various integrins—provides molecular targets for further mechanistic studies and potential therapeutic interventions aimed at modulating vascular responses during inflammation.

Collectively, these findings establish microvascular endothelial cell-derived EVs as important mediators of cell-cell communication in the vascular microenvironment, with multifaceted roles in

coordinating tissue responses that extend well beyond the classical functions previously attributed to endothelial cells themselves. The context-dependent nature of their effects represents a novel paradigm in our understanding of EV-mediated signaling and has significant implications for both basic vascular biology and the development of EV-based therapeutics for inflammatory vascular disorders.

II. Microvascular endothelial cells-derived EVs on wound healing

Our identification of specific EV-mediated effects on wound healing processes is further supported by the growing body of evidence showing that microvascular communication via EVs is critical for maintaining tissue homeostasis. For instance, the LOXL2-containing EVs identified in our study complement findings by Boyer et al. regarding HMGB protein transfer, suggesting that endothelial-derived EVs may serve as carriers for multiple bioactive proteins that collectively regulate vascular cell phenotypes and functions.

The differential responses we observed among cell types treated with microvascular endothelial cell-derived EVs—particularly the cell type-specific enhancement of migration, proliferation, and ECM production—indicate a sophisticated level of intercellular communication. This selective modulation of recipient cell function is consistent with emerging evidence that EVs can deliver targeted signals to specific cell populations based on their surface receptor profiles and uptake mechanisms.

Furthermore, our findings regarding the pro-migratory effects of EVs on fibroblasts and keratinocytes have significant implications for wound healing applications. Recent studies have demonstrated that application of endothelial-derived EVs can accelerate cutaneous wound closure in vivo, and our mechanistic insights into how these vesicles specifically promote cell migration and ECM remodeling provide a molecular basis for these therapeutic effects.

The capacity of microvascular endothelial cell-derived EVs to transfer functional proteins and miRNAs, as evidenced in our proteomics analysis and functional assays, reveals a novel mechanism by which the endothelium may influence the behavior of surrounding tissue cells during both homeostatic maintenance and response to injury. The identification of specific signaling pathways activated by these EVs, including those related to inflammation, migration, and ECM production, opens new avenues for therapeutic intervention targeting microvascular dysfunction in various pathological conditions.

5.3 Limitations and Considerations

Despite the significant advancements described above, several limitations warrant consideration when interpreting our findings:

5.3.1 Methodological Limitations

1. **Cell line model:** Our use of the HMEC-1 cell line, while enabling reproducible experimentation, may not fully recapitulate the heterogeneity of microvascular endothelial cells across different tissue beds. Primary microvascular endothelial cells from diverse tissues may produce EVs with distinct cargo profiles and functional properties.
2. **Static culture conditions:** Our static endothelial cell culture model lacks physiological flow, a key regulator of endothelial phenotype and function. This absence of hemodynamic forces simulates low-flow conditions associated with atheroprone regions, potentially explaining the

pro-inflammatory profile of our isolated EVs. Future studies incorporating flow-based culture systems would provide more physiologically relevant insights into EV biogenesis and cargo selection under normal vascular conditions.

3. **Isolation efficiency:** Although our optimized UC+SEC methodology substantially improves EV purity; it inevitably results in some vesicle loss compared to UC Bulk preparations. This trade-off between purity and yield could potentially bias our functional assessments toward effects mediated by the most abundant EV populations.
4. ***In vitro* conditions:** Despite our efforts to minimize serum supplementation, the culture conditions used for EV isolation remain an artificial environment that may not precisely mirror in vivo conditions. The stress associated with low-serum culture could potentially alter EV cargo composition relative to physiological conditions.

5.3.2 Analytical Limitations

1. **Protein-centric approach:** Our proteomic analysis provides comprehensive insight into the protein cargo of microvascular endothelial cell-derived EVs but does not address other potentially important cargo components such as lipids, metabolites, and small RNAs. These non-protein components could contribute significantly to the observed functional effects.
2. **Static timepoint analysis:** Our proteomic characterization represents a snapshot of EV cargo at a specific timepoint under standard culture conditions. The dynamic changes in EV composition in response to different physiological or pathological stimuli remain to be fully elucidated.
3. **Correlative functional evidence:** While our functional assays demonstrate clear biological effects of microvascular endothelial cell-derived EVs, they do not definitively establish which specific cargo components mediate these effects. The complex and heterogeneous nature of EV cargo makes it challenging to attribute observed functions to individual molecular components.
4. **Lack of EV uptake studies:** We did not investigate the mechanisms and efficiency of EV uptake by different recipient cell types. This represents a significant analytical gap, as differential uptake rates could explain the observed variations in functional responses between cell types. For instance, the more pronounced wound healing enhancement in dermal fibroblasts compared to keratinocytes (45% versus 29% improvement over controls) might reflect differences in EV internalization efficiency rather than intrinsic differences in responsiveness to EV cargo. Understanding these uptake dynamics would provide crucial mechanistic insights and potentially enable optimization of EV dosing for specific target cell populations.

5.3.3 Technical Considerations in Functional Assays

1. **Angiogenesis assay limitations:** As discussed in Chapter 4, our inability to demonstrate statistically significant effects in the angiogenesis assay may reflect technical challenges in delivering EVs effectively in 3D culture systems rather than a true absence of angiogenic regulatory potential.
2. **Dose-response relationships:** While we established standardized nanoparticle-to-cell ratios that elicited consistent responses, comprehensive dose-response studies across a wider concentration range might reveal threshold effects or biphasic responses not captured in our experiments.
3. **Temporal dynamics:** Our functional assays typically examined EV effects at specific endpoints (e.g., 16 hours for wound healing, overnight incubation for endothelial activation).

The temporal dynamics of these responses, including potential early or delayed effects, remain to be fully characterized.

5.4 Future Directions

Building upon the foundation established in this dissertation, several promising avenues for future research emerge:

5.4.1 Comprehensive Multi-omics Characterization

While our proteomic analysis provides valuable insights into the protein cargo of microvascular endothelial cell-derived EVs, a comprehensive understanding of their regulatory potential requires analysis of additional cargo components:

1. **Small RNA profiling:** Characterizing the miRNA and other small RNA content of these EVs could reveal additional regulatory mechanisms. Particular attention should be given to miRNAs that regulate wound healing, angiogenesis, and inflammatory pathways.
2. **Lipidomic analysis:** The lipid composition of EVs contributes significantly to their biological properties, including cellular uptake and membrane fusion. Comprehensive lipidomic profiling would complement our proteomic data and could reveal additional functional mechanisms.
3. **Metabolomic profiling:** Metabolites transported within EVs can directly influence recipient cell metabolism. Identifying the metabolic cargo of microvascular endothelial cell-derived EVs could reveal novel regulatory mechanisms not evident from proteomic analysis alone.

5.4.2 Mechanistic Studies

Building on our functional observations, future research should aim to elucidate the specific molecular mechanisms underlying the observed effects:

1. **Cargo depletion studies:** Selective depletion of specific proteins (e.g., through antibody precipitation or enzymatic degradation) from EV preparations could help identify the key molecular mediators of observed functional effects. This approach could be particularly valuable for understanding the seemingly paradoxical effects on endothelial inflammatory activation and junction integrity.
2. **Recipient cell signaling:** Detailed analysis of signaling pathway activation in recipient cells following EV treatment would provide mechanistic insight into how these vesicles elicit their biological effects. Particular attention should be given to pathways implicated in wound healing, cell-cell adhesion, and inflammatory regulation.
3. **Single-vesicle analysis:** Emerging technologies enabling the characterization of individual EVs could help determine whether functional heterogeneity exists within the overall population. This approach could reveal whether specific subpopulations of EVs mediate distinct biological effects.
4. **EV uptake mechanisms:** Investigating how different cell types internalize these vesicles, particularly comparing uptake mechanisms between inflamed and healthy endothelial cells, would provide crucial insight into the basis of context-dependent responses. Determining whether inflammatory priming alters EV receptor expression, endocytosis pathways, or intracellular processing of EV cargo could explain the differential effects observed in our healthy versus inflamed model experiments.

5.4.3 Physiological and Pathological Contexts

Extending our in vitro findings to more complex physiological and pathological contexts represent a critical next step:

1. **In vivo wound healing models:** Evaluating the effects of microvascular endothelial cell-derived EVs in animal models of wound healing could validate our *in vitro* findings and provide insights into their therapeutic potential. Both acute wounds and chronic wound models (e.g., diabetic ulcers) should be considered [103, 104].
2. **Inflammatory disease models:** Given the dual effect of these EVs on endothelial inflammatory activation and junction integrity, their potential role in inflammatory vascular diseases warrants investigation. Models of sepsis [105], acute respiratory distress syndrome, or inflammatory bowel disease could be particularly informative [106-108].
3. **Tissue-specific effects:** Exploring the effects of these EVs on microvascular function in different tissue beds could reveal context-dependent variability in their biological impact [11, 12, 109]. This would address the heterogeneity of microvascular endothelial cells across different organs.
4. **Temporal dynamics of inflammation:** Investigating whether the effects of EVs vary depending on the stage of inflammation (acute versus chronic, early versus late phase) could provide important insights into their physiological role. Time-course studies examining EV effects at different points in the inflammatory cascade would help establish their role in the transition from inflammatory response to resolution.

5.4.4 Therapeutic Applications

The wound healing-promoting and barrier-preserving effects of microvascular endothelial cell-derived EVs suggest potential therapeutic applications:

1. **EV-based wound healing therapies:** The development of formulations containing these EVs for topical application to acute or chronic wounds represents a promising translational direction [104]. Optimization of EV delivery systems to enhance stability and tissue penetration would be essential for this application.
2. **Vascular barrier protection:** The ability of these EVs to enhance endothelial junction integrity while maintaining inflammatory surveillance could be valuable in conditions characterized by vascular hyperpermeability [12], such as sepsis or acute respiratory distress syndrome.
3. **Bioengineered EVs:** Leveraging our proteomic insights, it may be possible to engineer EVs with enhanced or targeted therapeutic properties [75, 77] for specific applications in vascular medicine.

5.5 Conclusion

This dissertation has significantly advanced our understanding of microvascular endothelial cell-derived EVs through the development of optimized isolation methodologies, comprehensive proteomic characterization, and functional validation in multiple cellular contexts. Our findings reveal these vesicles as complex mediators of intercellular communication within the vascular microenvironment, capable of influencing wound healing, inflammatory regulation, and barrier function in a context-dependent manner.

The discovery of inflammation-dependent effects represents a particularly significant contribution, revealing these EVs as sophisticated regulators that respond differently based on the inflammatory status of recipient cells. This context-specific functionality suggests an elegant biological mechanism whereby these vesicles serve as "surveillance signals" that remain functionally silent under normal physiological conditions but become activated during inflammatory stress to help maintain vascular integrity while supporting appropriate immune responses.

By addressing critical knowledge gaps identified at the outset of this work, we have established a foundation for future investigations into the physiological and pathological roles of these vesicles. The dual capacity of microvascular endothelial cell-derived EVs to promote wound healing while preserving vascular barrier function specifically during inflammation suggests promising therapeutic applications in conditions characterized by impaired tissue repair or endothelial dysfunction.

Future research building upon this work has the potential to further elucidate the molecular mechanisms underlying these effects, explore their relevance in diverse physiological and pathological contexts, and develop novel therapeutic approaches leveraging the unique properties of these vesicles. Through continued investigation in this field, we may ultimately harness the regulatory potential of microvascular endothelial cell-derived EVs to address significant unmet needs in vascular medicine.

References

1. Théry, C., L. Zitvogel, and S. Amigorena, *Exosomes: composition, biogenesis and function.* Nature reviews immunology, 2002. **2**(8): p. 569-579.
2. Raposo, G. and W. Stoorvogel, *Extracellular vesicles: exosomes, microvesicles, and friends.* Journal of Cell Biology, 2013. **200**(4): p. 373-383.
3. Boyer, M.J., et al., *Endothelial cell-derived extracellular vesicles alter vascular smooth muscle cell phenotype through high-mobility group box proteins.* Journal of extracellular vesicles, 2020. **9**(1): p. 1781427.
4. Sigdel, S., et al., *Perivascular adipose tissue and perivascular adipose tissue-derived extracellular vesicles: new insights in vascular disease.* Cells, 2024. **13**(16): p. 1309.
5. He, S., et al., *Endothelial extracellular vesicles modulate the macrophage phenotype: Potential implications in atherosclerosis.* Scandinavian journal of immunology, 2018. **87**(4): p. e12648.
6. Coly, P.-M., et al., *Atheroprone shear stress stimulates noxious endothelial extracellular vesicle uptake by MCAM and PECAM-1 cell adhesion molecules.* BioRxiv, 2023: p. 2022.12. 31.522373.
7. Comarița, I.K., et al., *Therapeutic potential of stem cell-derived extracellular vesicles on atherosclerosis-induced vascular dysfunction and its key molecular players.* Frontiers in cell and developmental biology, 2022. **10**: p. 817180.
8. Raju, S., et al., *Multiomics unveils extracellular vesicle-driven mechanisms of endothelial communication in human carotid atherosclerosis.* bioRxiv, 2024.
9. de Jong, O.G., et al., *Cellular stress conditions are reflected in the protein and RNA content of endothelial cell-derived exosomes.* Journal of extracellular vesicles, 2012. **1**(1): p. 18396.
10. Osawa, S., et al., *Fibronectin on extracellular vesicles from microvascular endothelial cells is involved in the vesicle uptake into oligodendrocyte precursor cells.* Biochemical and Biophysical Research Communications, 2017. **488**(1): p. 232-238.
11. Hosseini-Beheshti, E. and G.E. Grau, *Extracellular vesicles and microvascular pathology: Decoding the active dialogue.* Microcirculation, 2019. **26**(2): p. e12485.
12. Hosseinkhani, B., et al., *Cerebral microvascular endothelial cell-derived extracellular vesicles regulate blood− brain barrier function.* Fluids and Barriers of the CNS, 2023. **20**(1): p. 95.
13. Kurachi, M., M. Mikuni, and Y. Ishizaki, *Extracellular vesicles from vascular endothelial cells promote survival, proliferation and motility of oligodendrocyte precursor cells.* PLoS One, 2016. **11**(7): p. e0159158.
14. Yamamoto, S., et al., *Inflammation-induced endothelial cell-derived extracellular vesicles modulate the cellular status of pericytes.* Scientific reports, 2015. **5**(1): p. 8505.
15. Cantaluppi, V., et al., *Microvesicles derived from endothelial progenitor cells enhance neoangiogenesis of human pancreatic islets.* Cell transplantation, 2012. **21**(6): p. 1305-1320.
16. Zhang, M., et al., *Methods and technologies for exosome isolation and characterization.* Small Methods, 2018. **2**(9): p. 1800021.
17. Gupta, D., A.M. Zickler, and S. El Andaloussi, *Dosing extracellular vesicles.* Advanced drug delivery reviews, 2021. **178**: p. 113961.
18. King, J., et al., *Structural and functional characteristics of lung macro-and microvascular endothelial cell phenotypes.* Microvascular research, 2004. **67**(2): p. 139-151.
19. Witwer, K.W., et al., *Updating MISEV: Evolving the minimal requirements for studies of extracellular vesicles*. 2021, Wiley Online Library. p. e12182.
20. Wu, C.C. and M.J. MacCoss, *Shotgun proteomics: tools for the analysis of complex biological systems.* Curr Opin Mol Ther, 2002. **4**(3): p. 242-250.
21. Consortium, U., *UniProt: a hub for protein information.* Nucleic acids research, 2015. **43**(D1): p. D204-D212.

22. Lehrich, B.M., Y. Liang, and M.S. Fiandaca, *Foetal bovine serum influence on in vitro extracellular vesicle analyses.* Journal of extracellular vesicles, 2021. **10**(3): p. e12061.
23. Urzì, O., R.O. Bagge, and R. Crescitelli, *The dark side of foetal bovine serum in extracellular vesicle studies.* J Extracell Vesicles, 2022. **11**(10): p. e12271.
24. Ades, E.W., et al., *HMEC-1: establishment of an immortalized human microvascular endothelial cell line.* Journal of Investigative Dermatology, 1992. **99**(6): p. 683-690.
25. Muñoz-Vega, M., et al., *Characterization of immortalized human dermal microvascular endothelial cells (HMEC-1) for the study of HDL functionality.* Lipids in Health and Disease, 2018. **17**: p. 1-8.
26. Hahne, M., et al., *Unraveling the role of hypoxia-inducible factor (HIF)-1α and HIF-2α in the adaption process of human microvascular endothelial cells (HMEC-1) to hypoxia: Redundant HIF-dependent regulation of macrophage migration inhibitory factor.* Microvascular research, 2018. **116**: p. 34-44.
27. Budworth, R., et al., *Histamine-induced changes in the actin cytoskeleton of the human microvascular endothelial cell line HMEC-1.* Toxicology in vitro, 1999. **13**(4-5): p. 789-795.
28. Wei, Z., et al., *Fetal bovine serum RNA interferes with the cell culture derived extracellular RNA.* Scientific reports, 2016. **6**(1): p. 31175.
29. Labitzke, R. and P. Friedl, *A serum-free medium formulation supporting growth of human umbilical cord vein endothelial cells in long-term cultivation.* Cytotechnology, 2001. **35**: p. 87-92.
30. Karasek, M.A., *Microvascular endothelial cell culture.* Journal of Investigative Dermatology, 1989. **93**(2): p. S33-S38.
31. Boes, M., B.L. Dake, and R.S. Bar, *Interactions of cultured endothelial cells with TGF-β, bFGF, PDGF and IGF-I.* Life Sciences, 1991. **48**(8): p. 811-821.
32. Jih, Y.-J., et al., *Distinct regulation of genes by bFGF and VEGF-A in endothelial cells.* Angiogenesis, 2001. **4**: p. 313-321.
33. Gavard, J. and J.S. Gutkind, *VEGF controls endothelial-cell permeability by promoting the β-arrestin-dependent endocytosis of VE-cadherin.* Nature cell biology, 2006. **8**(11): p. 1223-1234.
34. Cho, C.-H., et al., *Designed angiopoietin-1 variant, COMP-Ang1, protects against radiation-induced endothelial cell apoptosis.* Proceedings of the National Academy of Sciences, 2004. **101**(15): p. 5553-5558.
35. Daly, C., et al., *Angiopoietin-2 functions as an autocrine protective factor in stressed endothelial cells.* Proceedings of the National Academy of Sciences, 2006. **103**(42): p. 15491-15496.
36. Harfouche, R. and S.N. Hussain, *Signaling and regulation of endothelial cell survival by angiopoietin-2.* American Journal of Physiology-Heart and Circulatory Physiology, 2006. **291**(4): p. H1635-H1645.
37. OH, C., *Get the most from your cell cultures with GlutaMAX™ media.*
38. Meininger, C.J. and G. Wu, *L-glutamine inhibits nitric oxide synthesis in bovine venular endothelial cells.* The Journal of pharmacology and experimental therapeutics, 1997. **281**(1): p. 448-453.
39. Wu, G., et al., *Glutamine metabolism in endothelial cells: ornithine synthesis from glutamine via pyrroline-5-carboxylate synthase.* Comparative Biochemistry and Physiology Part A: Molecular & Integrative Physiology, 2000. **126**(1): p. 115-123.
40. Maralani, M.N., A. Movahedian, and S.H. Javanmard, *Antioxidant and cytoprotective effects of L-Serine on human endothelial cells.* Research in Pharmaceutical Sciences, 2012. **7**(4): p. 209.
41. Masoud, N.M., M. Ahmad, and H.J. Shaghayegh, *Protective effects of L-serine on human endothelial cells mediated by heme oxygenase-1.* Clinical Biochemistry, 2011. **44**(13): p. S181-S182.
42. Furihata, T., et al., *Hydrocortisone enhances the barrier properties of HBMEC/ciβ, a brain microvascular endothelial cell line, through mesenchymal-to-endothelial transition-like effects.* Fluids and Barriers of the CNS, 2015. **12**: p. 1-15.
43. Xu, R., et al., *Hydrocortisone modulates the effect of estradiol on endothelial nitric oxide synthase expression in human endothelial cells.* Life Sciences, 2001. **69**(23): p. 2811-2817.

44. Heller, R., et al., *L-Ascorbic acid potentiates nitric oxide synthesis in endothelial cells.* Journal of Biological Chemistry, 1999. **274**(12): p. 8254-8260.
45. Smith, A.R., F. Visioli, and T.M. Hagen, *Vitamin C matters: increased oxidative stress in cultured human aortic endothelial cells without supplemental ascorbic acid.* The FASEB Journal, 2002. **16**(9): p. 1102-1104.
46. Utoguchi, N., et al., *Ascorbic acid stimulates barrier function of cultured endothelial cell monolayer.* Journal of Cellular Physiology, 1995. **163**(2): p. 393-399.
47. Francis, G.L., *Albumin and mammalian cell culture: implications for biotechnology applications.* Cytotechnology, 2010. **62**(1): p. 1-16.
48. Zoellner, H., et al., *Serum albumin is a specific inhibitor of apoptosis in human endothelial cells.* Journal of cell science, 1996. **109**(10): p. 2571-2580.
49. Srivastava, K., et al., *In vitro cultivation of Plasmodium falciparum: studies with modified medium supplemented with ALBUMAX II and various animal sera.* Experimental parasitology, 2007. **116**(2): p. 171-174.
50. Bowman, C.M., et al., *HEPES may stimulate cultured endothelial cells to make growth-retarding oxygen metabolites.* In Vitro Cellular & Developmental Biology, 1985. **21**: p. 140-142.
51. Itagaki, A. and G. Kimura, *TES and HEPES buffers in mammalian cell cultures and viral studies: problem of carbon dioxide requirement.* Experimental cell research, 1974. **83**(2): p. 351-361.
52. Kim, Y.-J., et al., *Hypoxanthine causes endothelial dysfunction through oxidative stress-induced apoptosis.* Biochemical and biophysical research communications, 2017. **482**(4): p. 821-827.
53. Robillard, K.R., D.B. Bone, and J.R. Hammond, *Hypoxanthine uptake and release by equilibrative nucleoside transporter 2 (ENT2) of rat microvascular endothelial cells.* Microvascular research, 2008. **75**(3): p. 351-357.
54. Cary, D. and F. Mendelsohn, *Effect of forskolin, isoproterenol and IBMX on angiotensin converting enzyme and cyclic AMP production by cultured bovine endothelial cells.* Molecular and cellular endocrinology, 1987. **53**(1-2): p. 103-109.
55. Dufourcq, P., et al., *Membrane thrombomodulin levels are decreased during hypoxia and restored by cAMP and IBMX.* Thrombosis research, 1995. **77**(3): p. 305-310.
56. Hasan, A.U., et al., *IBMX protects human proximal tubular epithelial cells from hypoxic stress through suppressing hypoxia-inducible factor-1α expression.* Experimental Cell Research, 2017. **358**(2): p. 343-351.
57. Toi, M., et al., *Thymidine phosphorylase (platelet-derived endothelial-cell growth factor) in cancer biology and treatment.* The lancet oncology, 2005. **6**(3): p. 158-166.
58. Usuki, K., et al., *Platelet-derived endothelial cell growth factor has thymidine phosphorylase activity.* Biochemical and biophysical research communications, 1992. **184**(3): p. 1311-1316.
59. Aljada, A. and P. Dandona, *Effect of insulin on human aortic endothelial nitric oxide synthase.* Metabolism, 2000. **49**(2): p. 147-150.
60. Wang, H., et al., *Insulin signaling stimulates insulin transport by bovine aortic endothelial cells.* Diabetes, 2008. **57**(3): p. 540-547.
61. Carlevaro, M.F., et al., *Transferrin promotes endothelial cell migration and invasion: implication in cartilage neovascularization.* The Journal of cell biology, 1997. **136**(6): p. 1375-1384.
62. Hemmaplardh, D. and E. Morgan, *Transferrin and iron uptake by human cells in culture.* Experimental Cell Research, 1974. **87**(1): p. 207-212.
63. Baker Jr, R.D., S.S. Baker, and R. Rao, *Selenium deficiency in tissue culture: implications for oxidative metabolism.* Journal of pediatric gastroenterology and nutrition, 1998. **27**(4): p. 387-392.
64. Karlenius, T.C., et al., *The selenium content of cell culture serum influences redox-regulated gene expression.* Biotechniques, 2011. **50**(5): p. 295-301.

65. Mandal, A.K., et al., *Effect of insulin and heparin on glucose-induced vascular damage in cell culture.* Kidney international, 2000. **57**(6): p. 2492-2501.
66. Terranova, V.P., et al., *Human endothelial cells are chemotactic to endothelial cell growth factor and heparin.* The Journal of cell biology, 1985. **101**(6): p. 2330-2334.
67. Jiang, B., M. Haverty, and P. Brecher, *N-Acetyl-l-cysteine enhances interleukin-1β–induced nitric oxide synthase expression.* Hypertension, 1999. **34**(4): p. 574-579.
68. Recchioni, R., et al., *Apoptosis in human aortic endothelial cells induced by hyperglycemic condition involves mitochondrial depolarization and is prevented by N-acetyl-L-cysteine.* Metabolism-Clinical and Experimental, 2002. **51**(11): p. 1384-1388.
69. Schröder, H., et al., *N-Acetyl-L-cysteine protects endothelial cells but not L929 tumor cells from tumor necrosis factor-α-mediated cytotoxicity.* Naunyn-Schmiedeberg's archives of pharmacology, 1993. **347**: p. 664-666.
70. Olander, M., N. Handin, and P. Artursson, *Image-based quantification of cell debris as a measure of apoptosis.* Analytical chemistry, 2019. **91**(9): p. 5548-5552.
71. Halliwell, B., *Oxidative stress in cell culture: an under-appreciated problem?* FEBS letters, 2003. **540**(1-3): p. 3-6.
72. Schneider, M., I.W. Marison, and U. Von Stockar, *The importance of ammonia in mammalian cell culture.* Journal of biotechnology, 1996. **46**(3): p. 161-185.
73. Xu, Z.-H., et al., *Brain microvascular endothelial cell exosome–mediated S100A16 up-regulation confers small-cell lung cancer cell survival in brain.* The FASEB Journal, 2019. **33**(2): p. 1742-1757.
74. Zhang, X., et al., *Exosomes secreted by endothelial progenitor cells improve the bioactivity of pulmonary microvascular endothelial cells exposed to hyperoxia in vitro.* Annals of translational medicine, 2019. **7**(12): p. 254.
75. Armstrong, J.P., M.N. Holme, and M.M. Stevens, *Re-Engineering Extracellular Vesicles as Smart Nanoscale Therapeutics.* ACS Nano, 2017. **11**(1): p. 69-83.
76. Wei, R., et al., *Combination of size-exclusion chromatography and ultracentrifugation improves the proteomic profiling of plasma-derived small extracellular vesicles.* Biological Procedures Online, 2020. **22**: p. 1-11.
77. Coelho, C., et al., *Study of microbial extracellular vesicles: separation by density gradients, protection assays and labelling for live tracking.* Bio-protocol, 2020. **10**(2): p. e3502-e3502.
78. Dhondt, B., et al., *Unravelling the proteomic landscape of extracellular vesicles in prostate cancer by density-based fractionation of urine.* Journal of extracellular vesicles, 2020. **9**(1): p. 1736935.
79. Duong, P., et al., *Cushioned-Density Gradient Ultracentrifugation (C-DGUC) improves the isolation efficiency of extracellular vesicles.* PloS one, 2019. **14**(4): p. e0215324.
80. Bunkenborg, J., et al., *The minotaur proteome: Avoiding cross-species identifications deriving from bovine serum in cell culture models.* Proteomics, 2010. **10**(16): p. 3040-3044.
81. Keller, A., et al., *Empirical statistical model to estimate the accuracy of peptide identifications made by MS/MS and database search.* Analytical chemistry, 2002. **74**(20): p. 5383-5392.
82. Spiekstra, S.W., et al., *Wound-healing factors secreted by epidermal keratinocytes and dermal fibroblasts in skin substitutes.* Wound Repair and Regeneration, 2007. **15**(5): p. 708-717.
83. Dejana, E., F. Orsenigo, and M.G. Lampugnani, *The role of adherens junctions and VE-cadherin in the control of vascular permeability.* Journal of cell science, 2008. **121**(13): p. 2115-2122.
84. Giannotta, M., M. Trani, and E. Dejana, *VE-cadherin and endothelial adherens junctions: active guardians of vascular integrity.* Developmental cell, 2013. **26**(5): p. 441-454.
85. Perretti, M. and F.N. Gavins, *Annexin 1: an endogenous anti-inflammatory protein.* Physiology, 2003. **18**(2): p. 60-64.
86. Leoni, G., et al., *Annexin A1–containing extracellular vesicles and polymeric nanoparticles promote epithelial wound repair.* The Journal of clinical investigation, 2015. **125**(3): p. 1215-1227.

87. Lin, Q., et al. *Bioinformatic prediction revealed the potential effects of THBS1 mutation on liver fibrosis and inflammation*. in *American Society for Cell Biology 2022 Annual Meeting (03/12/2022-07/12/2022, Washington DC, USA)*. 2022.
88. Corbella, E., et al., *THBS1 and THBS2 enhance the in vitro proliferation, adhesion, migration and invasion of intrahepatic cholangiocarcinoma cells.* International Journal of Molecular Sciences, 2024. **25**(3): p. 1782.
89. Xie, L., et al., *ITGB1 alleviates osteoarthritis by inhibiting cartilage inflammation and apoptosis via activating cAMP pathway.* Journal of Orthopaedic Surgery and Research, 2023. **18**(1): p. 849.
90. Wu, E., et al., *HSPA8 acts as an amyloidase to suppress necroptosis by inhibiting and reversing functional amyloid formation.* Cell Research, 2023. **33**(11): p. 851-866.
91. Darling, D.L., J. Yingling, and A. Wynshaw-Boris, *Role of 14–3–3 proteins in eukaryotic signaling and development.* Current topics in developmental biology, 2005. **68**: p. 281-315.
92. Ouchi, K., et al., *FN1: a novel fusion partner of ALK in an inflammatory myofibroblastic tumor.* Pediatric Blood & Cancer, 2015. **62**(5): p. 909-911.
93. Soikkeli, J., et al., *Metastatic outgrowth encompasses COL-I, FN1, and POSTN up-regulation and assembly to fibrillar networks regulating cell adhesion, migration, and growth.* The American journal of pathology, 2010. **177**(1): p. 387-403.
94. Bećarević, M., *TNF-alpha and annexin A2: inflammation in thrombotic primary antiphospholipid syndrome.* Rheumatology international, 2016. **36**(12): p. 1649-1656.
95. Sveeggen, T., *Annexin A2 Controls Lipid Composition Necessary for Junctional Stability in Response to Sphingosine 1-Phosphate*. 2022.
96. Wallez, Y., I. Vilgrain, and P. Huber, *Angiogenesis: the VE-cadherin switch.* Trends in cardiovascular medicine, 2006. **16**(2): p. 55-59.
97. Carpentier, G., et al., *Angiogenesis analyzer for ImageJ—A comparative morphometric analysis of "endothelial tube formation assay" and "fibrin bead assay".* Scientific reports, 2020. **10**(1): p. 11568.
98. Deng, Z.-b., et al., *Adipose tissue exosome-like vesicles mediate activation of macrophage-induced insulin resistance.* Diabetes, 2009. **58**(11): p. 2498-2505.
99. Dougherty, J.A., et al., *Extracellular vesicles released by human induced-pluripotent stem cell-derived cardiomyocytes promote angiogenesis.* Frontiers in physiology, 2018. **9**: p. 1794.
100. Merino-González, C., et al., *Mesenchymal stem cell-derived extracellular vesicles promote angiogenesis: potencial clinical application.* Frontiers in physiology, 2016. **7**: p. 24.
101. Yin, G.N., et al., *Pericyte-derived extracellular vesicles-mimetic nanovesicles improves peripheral nerve regeneration in mouse models of sciatic nerve transection.* International Journal of Molecular Medicine, 2022. **49**(2): p. 1-12.
102. Tokarz, A., et al., *Extracellular vesicles participate in the transport of cytokines and angiogenic factors in diabetic patients with ocular complications.* Folia Medica Cracoviensia, 2015. **55**(4).
103. Ahmadpour, F., et al., *Effects of exosomes derived from fibroblast cells on skin wound healing in Wistar rats.* Burns, 2023.
104. Narauskaitė, D., et al., *Extracellular vesicles in skin wound healing.* Pharmaceuticals, 2021. **14**(8): p. 811.
105. Słomka, A., et al., *Large extracellular vesicles: have we found the holy grail of inflammation?* Frontiers in immunology, 2018. **9**: p. 2723.
106. Eirin, A., et al., *Mesenchymal stem cell–derived extracellular vesicles attenuate kidney inflammation.* Kidney international, 2017. **92**(1): p. 114-124.
107. Ren, Z., et al., *Mesenchymal Stem Cell-Derived Exosomes: Hope for Spinal Cord Injury Repair.* Stem Cells Dev, 2020. **29**(23): p. 1467-1478.
108. Njock, M.-S., et al., *Endothelial cells suppress monocyte activation through secretion of extracellular vesicles containing antiinflammatory microRNAs.* Blood, The Journal of the American Society of Hematology, 2015. **125**(20): p. 3202-3212.

109. Chen, G., et al., *Cardiomyocyte-derived small extracellular vesicles can signal eNOS activation in cardiac microvascular endothelial cells to protect against Ischemia/Reperfusion injury.* Theranostics, 2020. **10**(25): p. 11754.